Russian Chemical Reviews **68** (10) 821 – 857 (1999) © 1999 Russian Academy of Sciences and Turpion Ltd

UDC 541(15-64) : 537.5

Ferroelectricity of polymers based on vinylidene fluoride

V V Kochervinskii

Contents

I. Introduction
II. General characteristics
III. Characteristic features of the polarisation switching processes
IV. Curie transition
V. The mechanism of the generation of ferroelectricity based on NMR studies
VI. The influence of pressure on the characteristics of the ferroelectric transition
VII. The influence of the structural features of polymers on their ferroelectric characteristics
VIII. Ferroelectricity of ultrathin films
IX. Conclusion

Abstract. Characteristics of the ferroelectricity in polyvinylidene fluoride (PVDF) and copolymers based on vinylidene fluoride (VDF) with different previous thermomechanical histories are analysed. Switching of polarisation and the fluctuation mechanism of formation of new nuclei upon the appearance of conformation defects such as kink bonds are considered. The role of the space charge, which stabilises the new polarisation position, is noted. It is shown that the Curie transition can be either a first- or second-order phase transition depending on the copolymer composition. The influence of the morphology of PVDF on some ferroelectric characteristics is found. In particular, the morphology of thick lamellar crystals is favourable for enhanced spontaneous polarisation. It is shown that a ferroelectric structure approaching the texture of an ideal single crystal can be created in Langmuir – Blodgett films. As the number of unimolecular layers decreases, the concentration of conformational defects in these films increases and the crystallographic order in the lattice is violated. This intensifies the low-temperature Curie transition. The bibliography includes 247 references.

I. Introduction

Poly(vinylidene fluoride) (PVDF) and copolymers based on vinylidene fluoride (VDF) present interest for both fundamental science and applied research. This is due to the fact that these materials were found to exhibit ferroelectric properties normally atypical of polymers. Owing to the high piezo- and pyro-electric activities found in PVDF films,[1] this polymer has been recommended in some cases as a competitive material for energy converters of various types.[2,3] The results of experimental and theoretical studies in this field need to be surveyed at intervals for two reasons. Firstly, this could prompt the ways for optimisation of characteristics of the materials studied, which is significant for the solution of applied problems. Secondly, this would help to elucidate the influence of the polymeric state of substance on its electrophysical characteristics and would thus provide the understanding of the fundamental features of the formation of ferroelectricity and piezo- and pyroelectric properties in other polymers, for example, in poly(vinylidene cyanide),[4–13] odd nylons,[4–16] polyacrylonitrile,[17,18] polyurethanes,[19,20] liquid-crystal polymers[21–26] and biopolymers.[27]

PVDF is known to exhibit clear-cut polymorphism.[28] Three of the four crystallographic modifications of PVDF usually have non-zero cell dipole moments; therefore, there are prerequisites for the formation of a ferroelectric structure. Crystallites (or their sections) can be compared with domains characterised by a particular value of spontaneous polarisation.

II. General characteristics

The ferroelectric character of PVDF and VDF copolymers is confirmed, among other facts, by the occurrence of dielectric hysteresis for these materials. Figure 1 presents the variation of the electric displacement (D) as a function of the electric field strength E for a uniaxially stretched PVDF film.[29] It can be seen that hysteresis is displayed only in fields with a strength greater

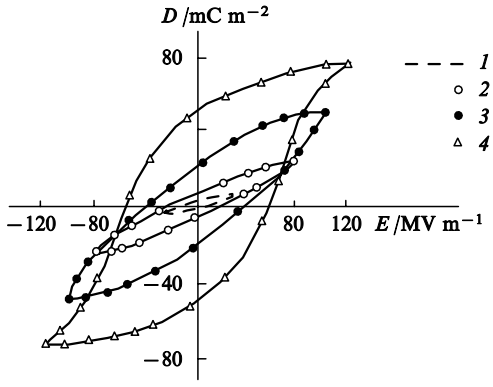


Figure 1. Electric displacement in a uniaxially stretched PVDF film at 20 °C *vs* strength of the external electric field.[29]
Frequency of the electric field 10^{-3} Hz; strength /MV m^{-1}: (*1*) 40, (*2*) 80, (*3*) 100, (*4*) 120.

V V Kochervinskii Troitsk Institute for Innovation and Fusion Research, 142092 Troitsk, Moscow Region, Russian Federation.
Fax (7-095) 334 57 76. Tel. (7-095) 165 14 74

Received 23 November 1998
Uspekhi Khimii **68** (10) 904 – 943 (1999); translated by Z P Bobkova

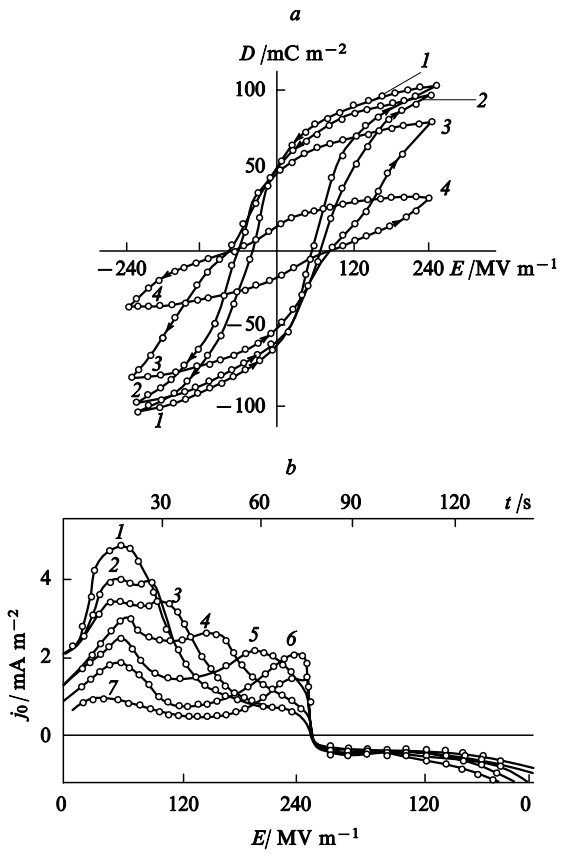


Figure 2. Temperature dependences of the electric displacement (*a*) and the polarisation current density (*b*) *vs* the electric field strength in the initial non-polarised PVDF film.[29]
T /°C: 20 (*1*), −20 (*2*), −60 (*3*), −100 (*4*) (*a*); 20 (*1*), 0 (*2*), −20 (*3*), −40 (*4*), −60 (*5*), −80 (*6*), −100 (*7*) (*b*); t is the current time.

than 40 MV m^{-1} and that an increase in the field strength results in an increase in both the remanent (for $E = 0$) and spontaneous polarisation, P_r and P_s, respectively. In relatively low fields (80 MV m^{-1}), the curve shows double hysteresis. This can be seen in more detail in Fig. 2, which shows the variation of properties of a non-polarised film placed in a 240 MV m^{-1} field for temperatures varying over wide limits.

Temperature plays an important role for the manifestation of ferroelectricity in PVDF and in crystallisable VDF copolymers. Only a fraction of the sample bulk is occupied by crystals; the rest (which makes 50% to 60% in PVDF) is filled by a disordered phase. The role of this phase in the formation of ferroelectricity is not entirely clear. The dynamics of chains in the disordered phase can have a substantial influence on the characteristics of the electric hysteresis (see Fig. 2). In temperature regions below the glass transition temperature of PVDF ($T_g \simeq -40$ °C), large-amplitude motions of chain sections are frozen. Some researchers (*e.g.*, Tamura *et al.*[30]) have observed even the disappearance of the hysteresis in low fields. However, in high fields, disappearance was not noted but the $D-E$ dependences were characterised by double hysteresis (see Fig. 2*a*). This can be seen more clearly in the field dependences of the polarisation current density (see Fig. 2*b*), which have two peaks at low temperatures. The position of one (lower-field) peak remains virtually unchanged, while the other peak shifts to lower fields as the temperature rises. The low-field peak may be related to the response of polar crystals to the application of the field and the peak at higher fields may be due to the response of dipoles in the disordered phase. Evidently, an increase in the temperature is favourable for the activation of the latter process because the second peak markedly shifts to lower fields. In the region below −40 °C, this shift can occur due to a decrease in the relaxation times of the local forms of mobility upon an increase in temperature; above −40 °C, this can be due to the generation of cooperative forms of mobility with high amplitudes.[28]

Thus, the amorphous phase makes a certain contribution to the formation of ferroelectricity and cannot be regarded as an 'inert matrix'. This conclusion appears sufficiently justified because the double hysteresis has been noted both for PVDF[31] and for VDF copolymers with tetrafluoroethylene (TFE)[32,33] or trifluoroethylene (TrFE).[34] It has been shown for the latter copolymer[34] that the probability of double hysteresis depends on the method used to prepare the sample. In particular, double hysteresis in the VDF copolymer with TrFE of the 52.8/47.2 composition is manifested only for samples crystallised by slow cooling of the melt. In the several initial polarisation cycles, these samples exhibit a typical double hysteresis, which is transformed into a single hysteresis in the subsequent cycles (Fig. 3). A similar result has been obtained for uniaxially stretched PVDF samples (Fig. 4*a*); no double hysteresis is observed for polarised samples at any temperature. This transformation in the pattern of the $D-E$ hysteresis should point to fundamental changes in the material structure after the generation of non-zero remanent polarisation.

One process which might result in structural changes is the irreversible increase in the degree of crystallinity after polarisation.[35] The kinetics of transition of the film subjected to polarisation into a new structural state depends on the frequency of the electric field applied. Thus at room temperature and a frequency of $\sim 10^{-3}$ Hz, this requires several poling cycles;[29,34] when the frequency is 50 Hz, the double hysteresis passes into single hysteresis in one cycle of the increase in the intensity of the polarising field.[31,32] Analysis of the time dependences of the polarisation current and thermodepolarisation curves for the 75/25 VDF/TrFE copolymer suggests that polarisation involves two types of dipoles (in the crystal and in the amorphous phase).[36]

It can be seen from comparison of Figs. 2 and 4 that the structural changes in the film induced by poling have a substantial effect on the temperature dependences of both the coercive field and the remanent polarisation. Whereas in the initial sample, E_c changes slightly with the temperature, in the polarised state, this value markedly increases as the temperature diminishes. The state of chain dynamics in the disordered phase affects precisely the magnitude of the coercive field; it can be seen that the $E_c - T$ plot is broken at about the glass transition temperature (see Fig. 4*b*). The sharper growth in the E_c in the region of T_g indicates that freezing of the high-amplitude cooperative motion of chain segments retards substantially the processes of polarisation switching. The remanent polarisation depends on the temperature to a lesser extent, although an increase in P_r has been noted below 50 °C.

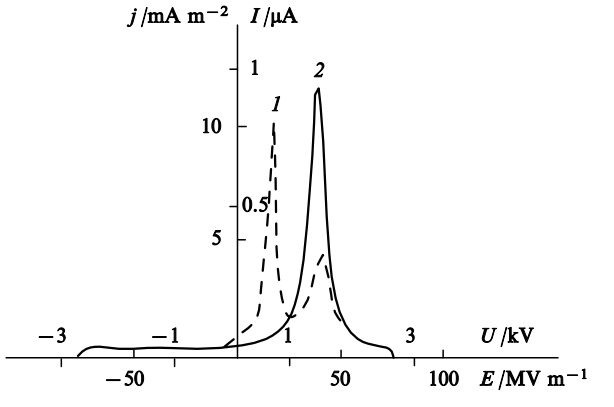


Figure 3. Reversible polarisation current *vs* the intensity and voltage (U) of the electric field (5×10^{-3} Hz/ 27 °C) in the several initial (*1*) and subsequent (*2*) cycles of poling of VDF/TrFE samples.[34]

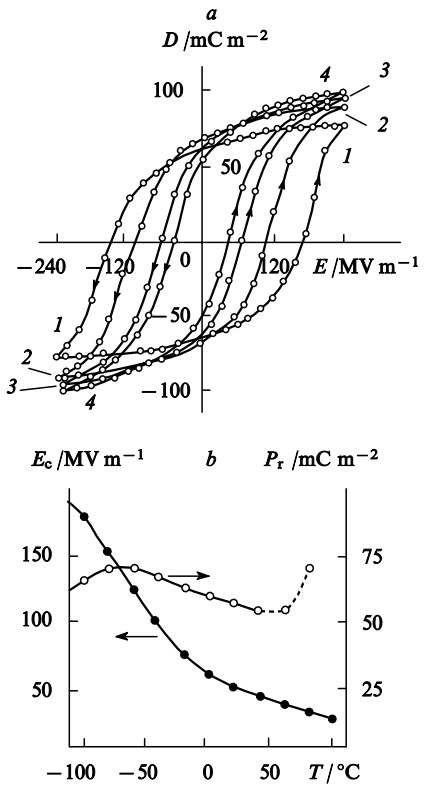


Figure 4. Influence of the temperature on the $D-E$ hysteresis curves (*a*) and on the hysteresis parameters (coercive field E_c and the remanent polarisation P_r) (*b*) in uniaxially stretched polarised PVDF films.[29]
T / °C: −100 (*1*), −60 (2), −20 (*3*), 20 (*4*).

Measurements of the hysteresis during the variation of the polarising field frequency from 10^{-2} to 10^{-4} Hz demonstrated that neither P_r nor the piezoelectric constant e_{31} depend on the frequency. This finding permitted the conclusion[29] that the ferroelectricity in PVDF has a purely dipole origin. A similar conclusion has been drawn for the 73/27 VDF/TFE copolymer, for which experimental P_r and P_s values are in good agreement with those calculated using a simple dipole model.[37]

It has been assumed [38] that free charge carriers in the polymer get frozen in deep traps and this compensates to an extent the intrinsic polarisation of crystals. This hypothesis was confirmed[38] by the data on the influence of annealing of a polarised PVDF film on the shape of the $D-E$ hysteresis curve. The curve obtained in the first cycle of measurements after annealing was distorted. This was explained by assuming that immediately after the annealing, the charge carriers are characterised by a non-equilibrium distribution, which changes during the subsequent poling cycles.

The dipole nature of the ferroelectricity is also confirmed by the hysteresis type of variation of the intensities of some absorption bands in the IR spectra.[28, 39, 40] This conclusion is also supported by the qualitatively consistent results of studies [41, 42] devoted to X-ray recording of the change in the distribution of the *b* axes (direction of the dipole moment) of the β-phase lattice after polarisation. It was shown that the intensity of the 110, 200 reflections of the crystalline β-phase changes by more than 20% following polarisation along particular directions. When developing the model of polarisation switching, Kepler and Andersen [42] proceeded from the fact that the orthorhombic cell of the β-phase can be transformed into a hexagonal cell upon 1% distortion. The chains in the planar zigzag conformation can occupy one of six equivalent positions (Fig. 5). When a field E is applied, the *b* axis of the cell occupies one of these positions with the probability [42]

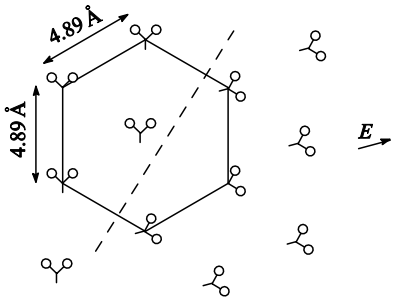


Figure 5. Packing of the PVDF chains in the crystal lattice of the β-phase. The dashed line denotes the boundary between the domains.[43]

$$f(\psi) = \exp(a\cos\psi)\left[\sum_{i=1}^{6}\exp(a\cos\psi_i)\right]^{-1}, \quad (1)$$

where ψ is the angle between the domain dipole moment (μ) and the direction of the field (E); in addition, $\psi_i = \psi + (1/3)(i-1)\pi$; $a = \mu E/kT$.

After polarisation, the orientation of the dipole moments can be described by the normalised distribution function

$$\frac{n(\psi)}{n_0} = f(\psi)\left[\int_0^{2\pi} f(\psi)d\psi\right]^{-1} = \quad (2)$$
$$= \frac{3}{\pi}\left[\exp(a\cos\psi)\right]\left[\sum_{i=1}^{6}\exp(a\cos\psi_i)\right]^{-1}$$

(n is the number of oriented axes, n_0 is the total number of axes), and polarisation is described by the equation

$$P = \frac{3P_0}{\pi}\int_0^{2\pi}\left[\exp(a\cos\psi)\cos\psi\right]\left[\sum_{i=1}^{6}\exp(a\cos\psi_i)^{-1}\right]d\psi, \quad (3)$$

where P_0 is the overall polarisation under the assumption that all dipoles are completely oriented.

The intensity of X-ray diffraction for the case of variation of the angle between the direction of incidence of the beam and the perpendicular to the film surface has been calculated.[42] The intensity curves for various values of the parameter $\exp(2\mu E/kT)$ were constructed. The experimental points obtained by averaging over seven samples are in the best agreement with the calculation based on the assumption that $\exp(2\mu E/kT) \simeq 10^3$.

Similar experiments have been carried out in another study. [44] The researchers monitored the variation in the intensity of the 110, 200 reflections after poling of a PVDF film shaped like a cylinder rotating around its axis, which coincided with the stretching direction. These experiments also confirmed the hypothesis that the dipole orientation can change by 60 ° steps during polarisation (see Fig. 5). This polarisation model is also confirmed by calculations of the potential energy for the chain rotation, which show that two neighbouring equilibrium positions of the CF_2 group are separated by 60 °.[42] Finally, the data on the hysteresis of the IR bands upon application of a field also point to 60-degree reorientations. Indeed, in terms of the model assuming 180-degree steps of rotation, no changes in the IR absorption intensity should be expected because the intensity is proportional to $\cos^2\theta$ (see Ref. 40).

The values of polarisation calculated from Eqn (3) are presented in Table 1. The most probable $\exp(2\mu E/kT)$ value for PVDF amounts to 10^3; it is matched by $P \simeq 111$ mC m^{-2}. The crystallinity of the sample is normally ~50%; hence, polarisation should be 50 mC m^{-2}, which is consistent with the PVDF remanent polarisation found experimentally. The known $\exp(2\mu E/kT)$ value can be used to determine the dipole moment of the domain. [42] For the field $E = 600$ kV cm^{-1} at 100 °C, it amounts to 3×10^{-28} C m. If the dipole moment of a monomer

Table 1. Polarisation of crystalline PVDF calculated for various magnitudes of the $\mu E/kT$ parameter. [42]

$\mu E/kT$	$\exp(2\mu E/kT)$	P /mC m^{-2}
0.00	1	0
1.15	10	66
2.30	10^2	98
3.45	10^3	111
4.61	10^4	116
5.76	10^5	120
6.91	10^6	121

unit in a planar zigzag chain is taken to be $\mu_0 = 7 \times 10^{-30}$ C m, then a domain should comprise ~ 40 monomer units. The polar β-phase crystals with normal sizes (~ 100 Å) contain many more monomer units. This means that field-induced orientation occurs in an area the size of which is much smaller than the size of the β-phase crystal. This conclusion is probably confirmed by the data of analysis of the ferroelectric and pyroelectric characteristics of thin films of the 70/30 VDF/TrFE copolymer prepared by the Langmuir–Blodgett method.[45] In the films containing several monolayers, the formation of a domain structure was noted; hysteresis of the pyroelectric current and a first-order Curie transition of the ferroelectric–paraelectric type was clearly observed for these films.

The regions of spontaneous polarisation, typical of ferroelectrics, can be probed using the electrochromism of optical labels. The optical labels used are normally azo dyes that efficiently absorb in the visible region. For instance, 4-dimethylamino-4′-nitrostilbene (DANS), for which the dipole moment in the ground state and the difference between the dipole moments in the ground and excited states are known, has been used as the optical label for PVDF and systems based on it.[46, 47] To estimate the strength of the local (internal) field E_l which had appeared in the sample after polarisation, the researchers made use of the fact that the absorption spectra of DANS in the perturbed ($E \neq 0$) and non-perturbed ($E = 0$) states differ in the absorbance and in the frequency of the main absorption band.[48]

The local field strength in polarised samples of a blend of PVDF and poly(methyl methacrylate) (PMMA) proved to be more than twice as high as the strength of the external field during poling.[47] A similar result has been obtained for the VDF/TrFE copolymer.[46] Apparently, for these polymers, the influence of the charge carriers injected from the electrode material should be taken into account. This hypothesis is supported by the results of analysis of the polarisation profile in these samples by the thermal pulse method.[49, 50] The polarisation profile is formed not only by dipoles but also by the space charge. The role of the latter is to stabilise the areas of oriented dipoles, which ensures the invariability of E_l in the temperature range of annealing (60–90 °C).[47] Some decrease in E_l near 60 °C (glass transition region) implies, apparently, that the fields of the disordered phase areas should also make a contribution to E_l. This contribution is relatively low because the most pronounced decrease in E_l occurs at about ~ 120 °C, where annealing is accompanied by depolarisation processes due to disorientation of the β-phase crystals.

Jimbo *et al.*[51] have attempted to determine the above-noted substantial changes in the coercive field observed in the polarised PVDF upon the temperature variation (see Fig. 4) using a simple phenomenological relaxation theory. In accordance with this theory, they calculated the E_c values, which corresponded to the experimental data in the temperature range chosen.

As noted above, PVDF and VDF-based copolymers contain at least two phases (ordered crystalline phase and disordered amorphous phase) having substantially different electric parameters, in particular, dielectric permittivity. This is attributable to the fact that the disordered phase occurs at room temperature in the liquid-like state and its chains execute cooperative motion with large amplitudes.[28] Therefore, depolarisation field E_d, the direction of which is opposite to that of the applied field E, can arise at the boundaries of ferroelectric crystals.

The field E_l which really acts on the crystal can be described by the equation [52]

$$E_l = E - E_d = f\left[\left(E - \frac{L}{\varepsilon\varepsilon_0}\right)(P_c - P)\right] = f\left[\left(E - \frac{L}{\varepsilon\varepsilon_0}\right)\left(\frac{1}{\alpha f} - 1\right)P\right], \quad (4)$$

where f is a parameter related to the depolarisation factor L and to the difference between the dielectric constant of the sample as a whole ε and that of the crystalline region ε_c (their polarisations are P and P_c, respectively), ε_0 is the vacuum dielectric constant and α is the degree of crystallinity.

The fact that E_l is lower than E means that the experimental hysteresis curves do not reflect characteristics of polar crystals. By processing experimental $P-E$ curves, Ikeda *et al.*[52] elucidated the dependences for the crystallites, *i.e.*, those in the P_c-E_l coordinates. The theoretical P_c-E_l curves were constructed for $L = 0.04$ and 0.08; provided that $\varepsilon = 12$ and $\varepsilon_c = 3$, this is matched by $f = 1.031$ and 1.064 and the draw ratios for an ellipsoidal crystal are 6.5 and 3.8. Since f differs insignificantly from unity, then, taking into account that $E_l = fE_c$ (see Ref. 51), the coercive field values for the calculated and experimental curves are virtually identical.

Spontaneous polarisation of the crystal P_{sc} and that for a sample with the degree of crystallinity α are related as follows:[51]

$$P_{sc} = \frac{P}{f\alpha}.$$

When $\alpha = 0.45$, spontaneous polarisation is substantially higher than the overall polarisation. The value $P_{sc} \simeq 170$ mC m^{-2} obtained by Ikeda *et al.*[52] is consistent in order of magnitude with the spontaneous polarisation (130 mC m^{-2}) calculated for a perfect crystal of the β-phase.

III. Characteristic features of the polarisation switching processes

The analysis of the features of polarisation switching processes is conveniently started with the data on PVDF; this homopolymer has been studied in the uniaxially stretched state, in which the crystalline phase occurred in the ferroelectric β-modification. Switching experiments usually consist in the application to the film of a stepwise field and recording of the time dependence of the electric displacement or polarisation current. The latter operation is often replaced by differentiation of the $D(t)$ curve (t is the current time) with respect to time. These curves are shown in Fig. 6. It can be seen that, as the electric field strength increases, the inflection point in the $D(t)$ curve and, correspondingly, the

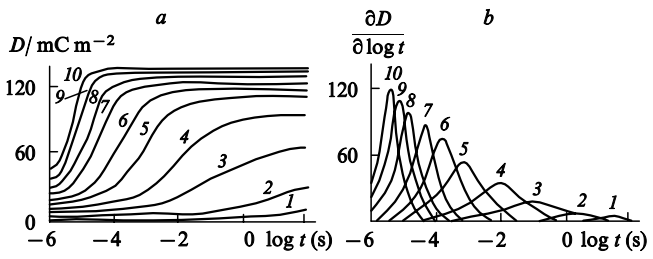


Figure 6. Time dependences of the electric displacement (*a*) and its derivative with respect to time (*b*) for the ferroelectric switching in a polarised PVDF film at 20 °C and at various external electric field strengths.[53]
E/ MV m^{-1}: 20 (*1*), 40 (*2*), 60 (*3*), 80 (*4*), 100 (*5*), 120 (*6*), 140 (*7*), 160 (*8*), 180 (*9*), 200 (*10*).

maximum of the derivative shift to shorter times. This type of behaviour has also been noted for classical inorganic ferroelectrics and is usually described by the relations

$$\tau_s = \tau_0 \exp\left(\frac{E_a}{E}\right) \quad (5)$$

or

$$\tau_s = \tau_0 \left(\frac{E}{E_0}\right)^{-n}, \quad (6)$$

where τ_s is the time of polarisation switching [corresponding to the maximum of the derivative of $D(t)$ or to the switching point], τ_0 is the pre-exponential factor, E_a is the activation field, and E_0 and n are constants. The $D(t)$ function can be represented as follows

$$D = D_0 + 2P_s\left[1 - \exp\left(\frac{t}{\tau_s}\right)\right]^n, \quad (7)$$

where D_0 is the instant electric displacement and $2P_s$ is the reversible polarisation. The exponent n corresponds approximately to the half-width of the $\partial D/\partial \log t$ peak. When the field strength is 60 MV m^{-1}, the exponent n for the 65/35 VDF/TrFE copolymer is greater than 5.

It has been noted above that the specific character of the polymeric state is due, on the one hand, to the strong anisotropy of bonds along and across the chain and, on the other hand, to the presence of an amorphous phase in addition to the crystalline phase. The chain dynamics of the amorphous phase below and above glass transition temperature are substantially different;[28] therefore, to understand the mechanism of generation of ferroelectricity in polymers, it is important to find out how this can influence the switching characteristics. Furukawa *et al.*[53] have studied the processes of switching in a polarised PVDF film in which the amorphous phase occurred in the liquid-like or vitrified state (Fig. 7). It can be seen that, when the field is so high (200 MV m^{-1}), switching can also take place below T_g (−40 °C). Below the glass transition temperature, the equilibrium electric displacement regularly decreases, the maximum switching rate D diminishes, and the peaks themselves become markedly broader as the temperature decreases. Figure 8 presents the field dependences of the switching times in a polarised PVDF film at various temperatures. These plots are linear both above and below the glass transition temperature, indicating that relations (5) and (6) hold. Transition of the amorphous phase into the glassy state noticeably changes the switching parameters (Table 2). In fact, as the temperature diminishes from room temperature to T_g, the exponent n and the constant τ_0 in Eqn (6) substantially increase (see Table 2). If the field dependences are represented as Eqn (5), then, in accordance with the results obtained by Furukawa and Johnson,[54] the transition of the disordered phase in the glassy state is also accompanied by a substantial increase in the activation field; E_a is 1.1 GV m^{-1} at 20 °C and 1.9 GV m^{-1} at −60 °C.

PVDF is characterised by higher activation fields and by higher exponents n in relations (6) or (7) than inorganic ferroelectrics. This fact was explained[53] in terms of the model of nucleation and growth of domains. Within the framework of this model, the switching curve $D(t)$ is described by the expression

$$D = 2P_s\left\{1 - \exp\left[-\int_0^t N_0 R e^{-Rs} F(v(t-s)^m)\,ds\right]\right\}, \quad (8)$$

where N_0 is the number of nucleation sites, R is the probability of nucleation, s is the current time, F is a factor depending on the shape of the growing domain, v is the growth rate, t is the total time, and m is the growth dimensionality. If switching is assumed to occur in very thin lamellae, consideration can be restricted to two-dimensional growth, *i.e.* $m = 2$. In this case, it follows from Eqn (8) that

$$D = 2P_s\left\{1 - \exp\left[-\frac{2FN_0v^2}{R^2}\left(\frac{R^2t^2}{2} - RT + 1 - e^{-Rt}\right)\right]\right\}. \quad (9)$$

If $Rt \gg 1$, then

$$D = 2P_s[1 - \exp(FN_0v^2t^2)], \quad (10)$$

if $Rt \ll 1$, then

$$D = 2P_s\left[1 - \exp\left(-\frac{FN_0v^2R}{3}t^3\right)\right]. \quad (11)$$

In both cases, the n values found by the calculations are smaller than those found experimentally. Agreement with experimental results can be attained by assuming that the domain growth is self-accelerated.

The influence of the state of the disordered phase on the switching parameters has also been studied by Matsushige *et al.*,[55] who derived switching characteristics from the time variation of the transpolarisation current at the same field strength

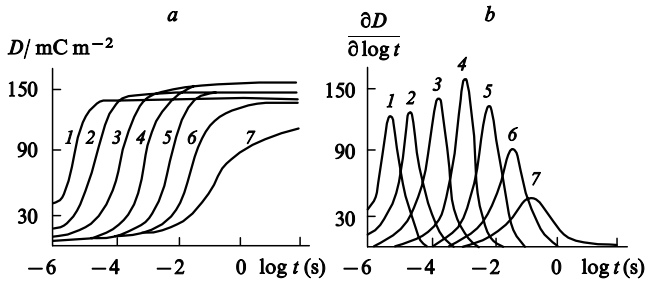


Figure 7. Time dependences of the electric displacement (*a*) and its derivative with respect to time (*b*) for the ferroelectric switching in a polarised PVDF film at $E = 200$ MV m^{-1} and various temperatures.[53]
T/°C: 20 (*1*), 0 (*2*), −20 (*3*), −40 (*4*), −60 (*5*), −80 (*6*), −100 (*7*).

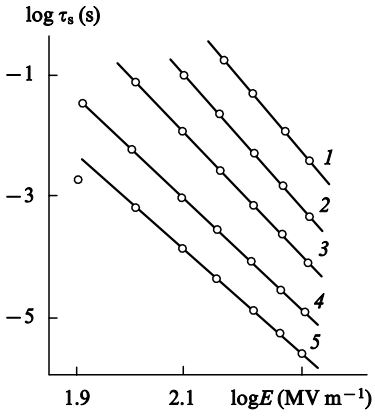


Figure 8. Field dependences of the switching times in a polarised PVDF film at various temperatures.[53]
T/ °C: −60 (*1*), −40 (*2*), −20 (*3*), 0 (*4*), 20 (*5*).

Table 2. Values n and τ_0 for PVDF and the 73/27 VDF/TrFE copolymer determined in the switching experiments.

T/ °C	n	log τ_0 (s)
PVDF [53, 54]		
20	7.6	12.02
0	8.0	13.63
−20	9.7	18.35
−40	10.7	21.19
−60	10.6	22.15
VDF/TrFE [51]		
20	10.2	16.48

(200 MV m^{-1}). Three temperature regions of variation of τ_s characterised by different activation energies of the switching process can be distinguished. The first region lies below T_g and has an activation energy of 2.3 kcal mol^{-1}. Here, the dynamics of molecular motion is characterised by only local types of motion, which can occur in both the amorphous and crystalline phases.[28] The activation energy of switching increases somewhat when cooperative forms of motion are excited in the amorphous phase (60 °C > T > T_g). Finally, the third region falls to temperatures above 60 °C, when motion in crystalline lamellae begins.[28] This motion decreases the activation barrier to switching.

Thus, switching is sensitive not only to crystalline domains but also to the surrounding disordered areas.

A complex pattern of the curves of reversible polarisation has also been found for the VDF/TrFE copolymer. Specific features of switching near the Curie point, in which a ferroelectric–paraelectric transition occurs, have been studied.[56] In the vicinity of this point (68 °C), the plot for D at low fields has two steps (Fig. 9).

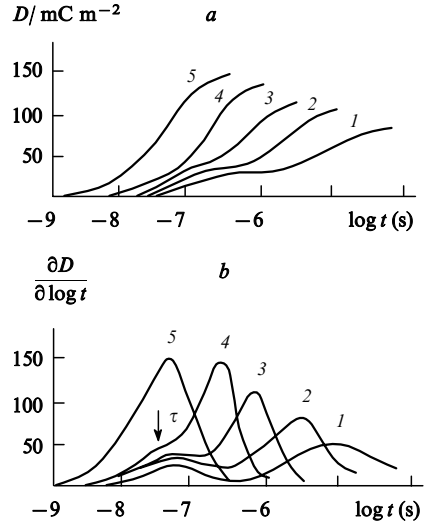


Figure 9. Time dependences of the electric displacement (*a*) and its derivative with respect to time (*b*) for polarsation switching in 65/35 VDF/TrFE at 63 °C and various field strengths.[56]
E /MV m^{-1}: 75 (*1*), 90 (*2*), 135 (*3*), 200 (*4*), 300 (*5*).

The shape of experimental curves is described adequately by an equation with two switching times, one (τ) being independent on the field intensity and the other (τ_s) depending on it according to the law normal for ferroelectrics (Fig. 10). The switching time (τ) varies in the same way as that for an ordinary relaxation process; therefore, the expression for D can be written as follows:[56]

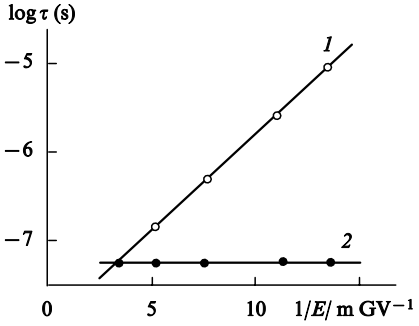


Figure 10. Field dependences of the switching times τ_s (*1*) and τ (*2*) in the 65/35 VDF/TrFE copolymers at 63 °C.[56]

$$D = \varepsilon_0 E + \Delta\varepsilon E\left[1 - \exp\left(-\frac{t}{\tau}\right)^{\beta}\right] + 2P_r\left[1 - \exp\left(-\frac{t}{\tau_s}\right)^{n}\right], \quad (12)$$

where $\Delta\varepsilon$ is the relaxation force, β is a parameter determining the distribution of the relaxation time, and n is a parameter determining the shape of the switching curve. This expression is suitable (provided that τ does not depend on E) for describing the experimental switching curves shown in Fig. 9. In particular, it also accounts for the shape of the curve at high fields. The straight lines shown in Fig. 10 intersect at a certain field strength. At the point of intersection, $\tau = \tau_s$; therefore, switching curves for such field strength attest to a one-step process.

The changes in the field dependence of τ_s with an increase in the temperature in the copolymer considered and in PVDF are similar. However, as the Curie point is approached, the slope of this plot markedly decreases. According to Eqn (5), this is equivalent to the decrease in the activation field E_a. Taking into account the probable generation of great fluctuations of the motion near the Curie point, a hypothetical mechanism for the nucleation of domains during polarisation switching was proposed.[56] The scheme of this mechanism is presented in Fig. 11. The authors proceeded from the real conformational structure found in the chains of PVDF and VDF copolymers.

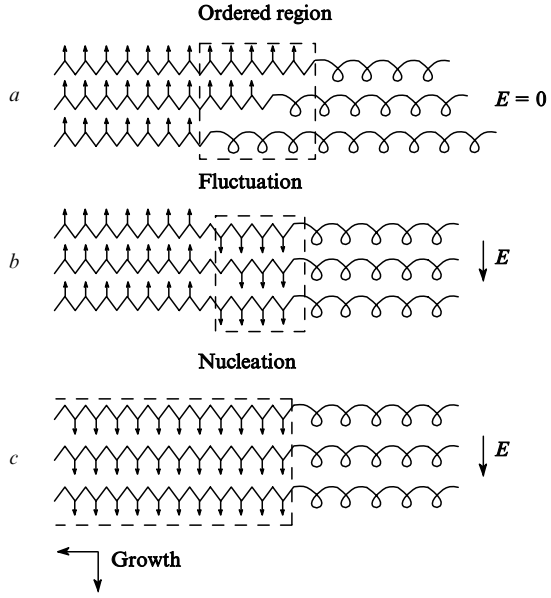


Figure 11. Scheme for the fluctuation motion (*a*), nucleation (*b*) and the growth of the nucleus (*c*) in the switching processes in 65/35 VDF/TrFE.[56]

The ordered areas in the VDF copolymers with TrFE or TFE are known to crystallise as the ferroelectric β-phase with the planar zigzag conformation. The polarisation of a domain in a polarised film is stipulated by the external field. The results of X-ray and IR-spectroscopy studies demonstrate that, in addition to the planar zigzag conformation, chain sections occurring in a mixed conformation, TT, TG, or TG$^-$, are also present.[28] They should be located either in the amorphous phase or in the crystals of the paraelectric phase, which can coexist with the ferroelectric phase. These sections should be the first to respond to a field because the relaxation times τ for them are shorter than τ_s (if the fields are not extremely high) (see Fig. 10). If the chains are mainly located in the film plane (this is the case for the uniaxially oriented state), a chain section having, for example, the TGTG$^-$ conformation should pass into a different position upon the interaction of the field with the transverse component of the dipole moment. In a high field, a conformational transition of the TGTG$^-$ → TTTT type is possible;[28] therefore, the second stage in the nucleation process is the appearance of chain sections in the

planar zigzag conformation with a new orientation of the dipole moment. Evidently, these processes involve simultaneously a certain rearranging region rather than individual sections of the chain because above T_g, the micro-Brownian motion in the amorphous phase is to some extent cooperative.[28] After a nucleus has formed by the above mechanism, it starts to grow in both the longitudinal and transverse directions.

Certainly, the mechanism described above merits attention because it is underlain by the real structure of the chains in PVDF and VDF copolymers. The validity of this mechanism is confirmed by the presence of tie chains, characteristic only of crystallisable polymers, in the compounds considered. As a result of spontaneous nucleation during crystallisation, the same chain can be incorporated in both the crystal and the neighbouring disordered phase. If the chain section adjacent to the crystal occurs in the $TGTG^-$ conformation, the orientation and conformational changes described above would create internal stresses in the section of the same chain contained in the crystal because the direction of its dipole moment would be opposite to the new direction of the field. This fact as well as the influence of an external electric field are additional factors inducing transpolarisation of a region of the crystalline phase. The time τ (like the normal relaxation time) decreases as the temperature increases, which can also affect the temperature dependence of the switching time τ_s.[55]

The above mechanism for the generation and development of domains in the switching processes does not take into account the effect of the space charge formed by both the inherent charge carriers and those injected from the electrodes during poling. However, experimental results imply that this effect cannot be neglected. For example, in a study [57] dealing with switching in the 73/27 VDF/TrFE copolymer on exposure to 1-second rectangular pulses, an unusual phenomenon was discovered, which can be described as follows. As the delay period t_ω between the preceding and the subsequent pulses (having opposite polarities) increases, the switching curves regularly shift to longer switching times. The same trend is observed if the strength of the external field decreases (see, for example, Figs. 6, 8). This correlation led the researchers to the conclusion that the decrease in the switching time following an increase in the duration of leaving the sample after a high-voltage pulse has been applied is due to field effects. Since the external field strength was maintained constant (80 MV m^{-1}), all the foregoing was explained by variation of the local field acting on the domain. The period the sample is left and the final concentration of charge carriers in the sample bulk create real prerequisites for the processes described above.

Free charge carriers are present both in non-polarised (remaining catalyst, ionic side products of the synthesis, *etc.*) and polarised PVDF. In the latter case, there are also charge carriers injected from the electrode. It is assumed that charge carriers are captured into deep traps located along the boundaries between the ordered and amorphous regions. If these regions occur in the liquid-like state, in which the segments execute cooperative motion with large amplitudes,[28] there are conditions for the charge to be liberated and re-captured by another trap. From energy reasons, it is more favourable for these carriers to be located on polar surfaces of crystallites, which should result in partial compensation of their polarisation. The local polarisation P_l would differ from the macroscopic value P; in accordance with Eqn (4), this should change the field E_l acting on the crystal. These effects have been considered quantitatively.[58] The expression proposed for E_l has the form

$$E_l = -\frac{n'(1-\alpha)P_0}{\varepsilon_a - (\varepsilon_a - \varepsilon_c)n'(1-\alpha)} \exp\left(-\frac{t_\omega}{\tau}\right), \tag{13}$$

where n' is the depolarisation factor for ellipsoidal crystals with dielectric constant ε_c immersed in an amorphous matrix with dielectric constant ε_a, and α is the volume fraction of these crystals. The exponential term (kinetic factor) includes the characteristic relaxation time of the space charge τ, which is related to the conductivity of the amorphous phase g by the equation

$$\tau = \frac{\varepsilon_a - (\varepsilon_a - \varepsilon_c)(1-\alpha)n'}{g[1-(1-\alpha)n']}. \tag{14}$$

The overall expression for the polarisation switching time with allowance for the foregoing has the following form:

$$\log \tau_s = \log \tau_0 + \frac{0.4343 E_a}{E + A\exp(-t_\omega/\tau) - E_l}, \tag{15}$$

where E_a and A are constants for a given polymer, E_l reflects the correction of the external field E due to the effect of the depolarising field.

Figure 12*a* shows experimental points for τ_s at various t_ω for samples of the 73/27 VDF/TrFE copolymer obtained by quenching and by slow cooling. It can be seen that τ_s increases with an increase in t_ω in accordance with Eqn (15). The τ_s value is always greater for a quenched sample, all other factors being the same. This can be explained qualitatively by the following fact, which has been confirmed experimentally. The volume fraction of the ferroelectric phase is always lower in a quenched sample; therefore, the conductivity of the amorphous phase g should be greater. In conformity with Eqn (14), this results in a lower τ and, according to relation (15), this increases τ_s. Yet another way for increasing the conductivity in the copolymer considered is an increase in the concentration of charge carriers by doping with, for example, iodine.[59] For a doped sample, the τ_s values are greater and the shape of the curves calculated from Eqn (15) is described adequately by experimental data (Fig. 12*b*).

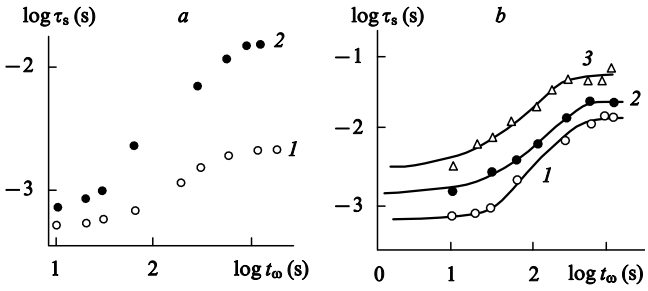


Figure 12. Plots for the polarisation switching time in 73/27 VDF/TrFE films prepared either by slow cooling or by quenching (*a*) and either non-doped or doped with iodine (*b*) in a 80 MV m^{-1} field (see Refs 57–59); (*a*): (*1*) cooling, (*2*) quenching; (*b*): (*1*) without doping, (*2*) doping for a week, (*3*) doping for a month; the solid line corresponds to the calculation by Eqn (15).

The experiments carried out by Bihler *et al.*[60, 61] were devoted to the non-trivial role of the space charge in the polarisation switching in PVDF and VDF copolymers. In the study of polarisation of the initial films and transpolarisation of polarised films in pulsed electric fields, the attention was concentrated on the comparison of the time dependences of the electric displacement D and the resulting remanent polarisation P_r. The D value was measured using a capacity divider circuit and P_r was measured by generation of a pressure pulse in the short circuit mode. The investigation objects were PVDF films crystallised as mixtures of α- and β-phases [60] and 75/25 VDF/TrFE copolymer films.[61] Figure 13 presents the time dependences of D and P_r for isotropic films of 75/25 VDF/TrFE to which a primary high-voltage pulse has been applied. Both characteristics vary according to similar patterns but the positions of the characteristic points on the $D(t)$ and $P_r(t)$ curves are substantially different. For example, the time it takes for P_r to reach half its equilibrium value (this is marked by the vertical line) in a 160 MV m^{-1} field amounts to ~100 μs, whereas the electric displacement virtually reaches its maximum over this period. More detailed data for this

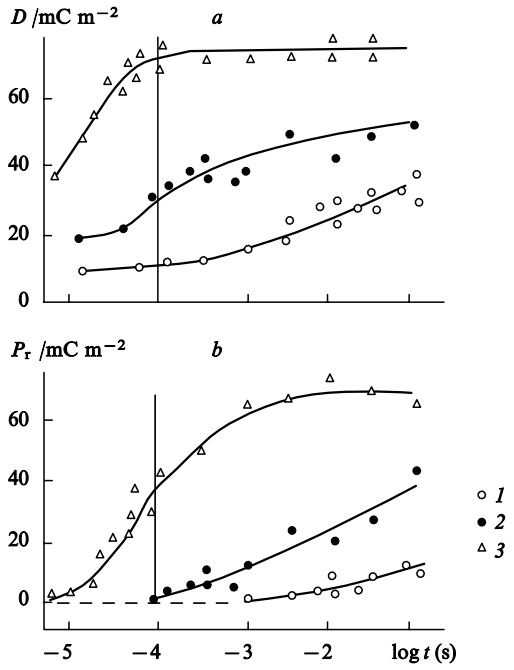


Figure 13. Time dependences of the electric displacement (*a*) and the remanent polarisation (*b*) upon application of a pulse electric field with various strengths in the initial non-polasrised films of the 75/25 VDF/TrFE copolymer.[61]
E /MV m^{-1}: 80 (*1*), 120 (*2*), 160 (*3*).

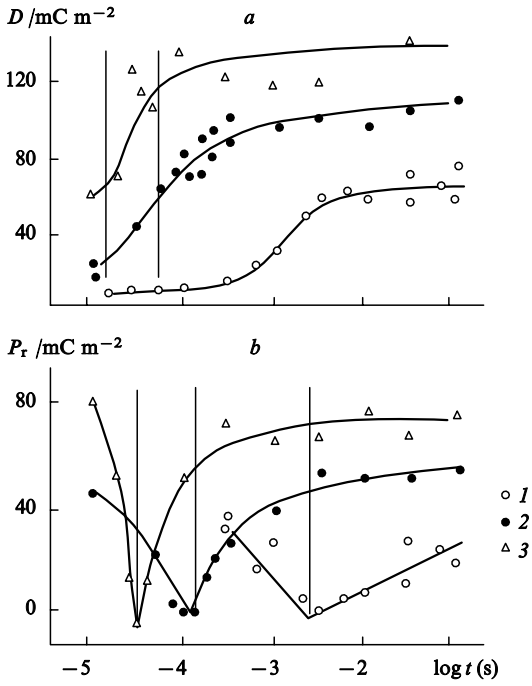


Figure 14. Time dependences of D (*a*) and P_r (*b*) for pulse transpolarisation in various fields of preliminarily polarised films of the 75/25 VDF/TrFE.[61]
E /MV m^{-1}: 80 (*1*), 120 (*2*), 160 (*3*).

copolymer and also for PVDF are presented in Table 3. It can be seen that for both compounds, the points where the slope begins and when half the equilibrium P_r value is attained on the $P_r(t)$ curve are substantially displaced to longer times with respect to the corresponding points on the $D(t)$ curves. Qualitatively similar data have also been obtained for preliminarily polarised films upon application of a high-voltage pulse with the opposite polarity (Fig. 14). The $D(t)$ curves follow the same pattern as those for initial (non-polarised) films but the $P_r(t)$ plots have a minimum which separates two branches reflecting antiparallel variation. The descending branch of P_r evidently corresponds to the removal of the polarisation which had existed before the pulse with the opposite polarity was applied. The increase in P_r is apparently due to the formation of a remanent polarisation in the new direction. As in the previous case, the time it takes for D to reach half its equilibrium value (marked by vertical lines) proves even shorter than the time required for the initial polarisation to diminish to zero (a vertical line is also drawn through the minimum point). This led the researchers[60, 61] to the conclusion that the processes responsible for the increase in D and P_r are not equivalent. It is believed that an increase in D reflects the rotation of dipoles, which respond to a high field almost instantaneously. The delay of the formation of the remanent polarisation is due to the fact that this process involves the carriers forming the space charge. If dipoles of the ferroelectric β-phase have occupied a new position in the field, then, due to the finite mobility of charge carriers, the space charge would occupy a new equilibrium position within some period after the dipoles have rotated, which is actually observed in the experiment. The influence of the space charge is not limited to the retarded kinetics of equilibration of P_r with respect to D. The space charge also plays an important role in the stabilisation of the remanent polarisation, resulting in the retention of piezo- and pyro-electric properties in polarised films of PVDF and VDF copolymers over long periods of time.

Table 3. Parameters of the characteristic points in the time dependences for 75/25 VDF/TrFE and PVDF recorded during poling of films by high-voltage pulses of various durations.

E/ MV m^{-1}	Beginning of the slope /μs		The time it takes to reach half the maximum value /μs	
	I	II	I	II
VDF/TrFE[61]				
80	400	3 000	1 000	17 000
120	30	100	50	2 000
200	1	10	< 10	80
PVDF[60]				
120	200	2 000	20 000	40 000
200	< 10	80	10	3 000

Note. I are characteristic points on the $D(t)$ curves; II are characteristic points on the $P_r(t)$ curves.

Thus, polarisation switching in PVDF films and films of VDF copolymers with a ferroelectric β-phase occurs most likely in two stages. The first (fast) stage involves reorientation of domains due to the rotation of dipoles *via* 60-degree rotations of the chains (see Fig. 5). This conclusion is confirmed by numerous structural data and also by calculations of the activation energy of switching in terms of this model.[62] According to these calculations, the activation barrier should not exceed several tens of kilocalories per mole, which agrees with the experimental values. For example, it has been reported[55] that the activation barrier does not exceed 10 kcal mol^{-1} and, according to another publication,[63] it is not higher than 18 kcal mol^{-1}. The latter value is much lower than would be required by the model which implies 180-degree rotations of the chain.[62] The stage of formation (nucleation) of new domains is apparently a fluctuation type process.[56, 64] For this stage, it is necessary to take into account the possibility that the same chain can be incorporated both in the crystal and in the disordered phase adjacent to it. If the relaxation processes in the latter are taken into account in the nucleation of a new domain,

the chains in the crystal acquire an additional rotational moment, which facilitates the growth of new domains.[62]

The structural heterogeneity of PVDF creates prerequisites for the influence of fine features of the phase boundary; the disordered phase is characterised by a higher dielectric constant, which may result in the appearance of a depolarising field.[57, 59, 65] When free charge carriers are present, the structural heterogeneity induces the second stage of the resultant switching process. In this stage, due to the migration of the carriers over the disordered interfacial regions, the space charge relaxes to a state matching the newly formed domains.

IV. Curie transition

The ferroelectricity of the polymer systems in question should be described by general phenomenological relations. For example, in the absence of mechanical stress ($X = 0$), the variation of free energy G as a function of polarisation P is described by the expression

$$G = \frac{1}{2}\beta(T-T_0)P^2 + \frac{1}{4}\gamma P^4 + \frac{1}{6}\delta P^6, \tag{16}$$

where T_0 is the characteristic temperature; the β and δ constants are positive, and the sign of constant γ depends on the type of transition (it is negative for first-order transitions and positive for second-order transitions). The first derivative of G with respect to polarisation gives an equation which describes the electric field

$$E = \beta(T-T_0)P + \gamma P^3 + \delta P^5. \tag{17}$$

For a second-order phase transition, $\beta > 0$, $\gamma > 0$, and δ can be regarded as being equal to zero. In this case, the equation for the dielectric susceptibility χ has the form

$$\chi = [\beta(T-T_0) + 3\gamma P_s^2] - 1. \tag{18}$$

By differentiating this expression, one finds the second- (ε_2) and third-order (ε_3) dielectric constants[65]

$$\varepsilon_2 = -3\gamma P_s \chi^3, \tag{19}$$

$$\varepsilon_3 = (-\gamma + 18\gamma^2 P_s^2 \chi)\chi^4. \tag{20}$$

At temperatures below the Curie point T_C,

$$P_s^2 = \frac{\beta(T_0 - T)}{\gamma} \tag{21}$$

and

$$\varepsilon_3 = 8\gamma\chi^4. \tag{22}$$

Since $\gamma > 0$, the ε_3 value is positive and ε_2 is negative. Above the Curie point, $P_s = 0$; hence, $\varepsilon_2 = 0$. With allowance for Eqn (20), we have

$$\varepsilon_3 = -\gamma\chi^4.$$

Thus, for a second-order phase transition, the second-order dielectric constant ε_2 is always negative below the Curie point and at T_C, it becomes equal to zero. The sign of the third-order dielectric constant ε_3 changes from positive to negative at the Curie point.

As noted above, for a first-order phase transition, $\gamma < 0$, and $\delta > 0$. In this case,

$$\chi = [\beta(T-T_0) + 3\gamma P_s^2 + 5\delta P_s^4]^{-1}, \tag{23}$$

$$\varepsilon_2 = -(3\gamma + 10\delta P_s^2)P_s\chi^3, \tag{24}$$

$$\varepsilon_3 = -[\gamma P_s^2(10\delta - 18\chi\gamma^2 - 120\chi\gamma\delta P_s^2 - 200\chi\delta^2 P_s^4)]\chi^4. \tag{25}$$

The Curie point is determined by the temperature at which the energies of the polar and nonpolar phases become identical. This means [with allowance for Eqn (16)] that

$$T_C = T_0 + \frac{3\gamma^2}{16\beta\delta}. \tag{26}$$

During heating, the first-order phase transition ($\gamma < 0$) will be observed above T_C, whereas during cooling, it will occur below T_C. Thus, in practice, to determine the type of Curie transition, one should record the temperature dependences of ε_2 and ε_3 or establish the presence (or the absence) of a hysteresis of one or another characteristics during heating or cooling.

Strong piezoelectricity was first detected in a textured PVDF film;[1] therefore, it is this homopolymer that was used to verify the hypothesis about the ferroelectric nature of this phenomenon. However, the homopolymer is an inconvenient object for the study of the temperature anomalies which accompany the hypothetical ferroelectric–paraelectric transition. The temperature region of the Curie transition coincides in this case with the melting region; therefore, it is difficult to separate them in the experiment.

The presence of piezo- and pyro-electric properties in PVDF has stimulated the search for ways of modifying the chemical structure of this polymer. Copolymerisation of VDF with TFE and TrFE proved to be the most suitable method. The introduction of even small amounts of these co-monomers results in the formation of the polar (ferroelectric) β-phase directly during crystallisation from the melt, which is not characteristic of the homopolymer.[28] This type of chemical modification of PVDF also influences the parameters of the unit cell being formed. The tendency of variation of the interplanar spacings in VDF/TFE copolymers upon the variation of the proportion of TFE can be followed by looking at Table 4. It can be seen that an increase in the TFE proportion is accompanied by an increase in the interplanar spacing corresponding to the intermolecular 200, 110 reflections. Hence, the cell packing becomes less dense along the direction perpendicular to the c axis.

Table 4. Interplanar spacings (Å) in oriented VDF/TFE copolymers with various co-monomer ratios.[66]

[VDF] (mol.%)	Reflections		
	200, 110	001	201, 111
100	4.28	2.56	2.22
89	4.38	2.55	2.21
79	4.48	2.56	2.23
71	4.61	2.56	2.24
64	4.75 [a]	2.57	2.26
54	4.82 [a]	2.58	2.27

[a] Non-resolved doublet.

This fact is, apparently, the main reason why the Curie transition and the melting point in these copolymers occur in different temperature ranges, which permits recording of the pure Curie transition by, for example, the X-ray diffraction method.[66] The influence of the temperature on the interplanar spacing and on the unit cell dimension along the a axis in the 76/24 VDF/TFE copolymer is illustrated by Fig. 15. It can be seen that hysteresis phenomena are observed not only for the refletion intensities but also for the interplanar spacings. The transition to the paraelectric phase is accompanied by a discontinuous increase in the unit cell parameter a. The temperature range in which both reflections coexist is attributed to the presence of both the ferroelectric and paraelectric phases. Yet another interpretation of this fact assumes the formation of some single phase with a symmetry lower than the hexagonal symmetry.[67, 68]

The changes in the 200 and 110 reflections for VDF/TFE copolymers with compositions 76/24 and 75/25 are qualitatively similar,[68] although the hysteresis phenomena are less pronounced

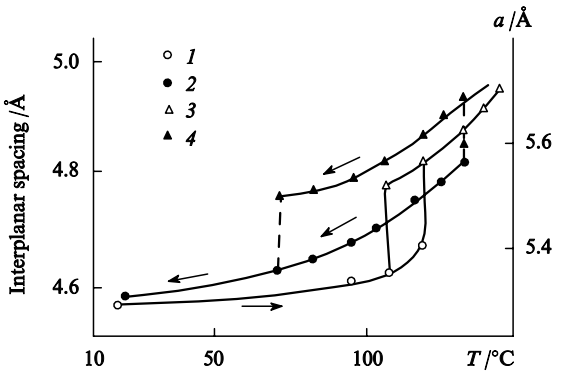


Figure 15. Temperature dependences of the interplanar spacings and the unit cell parameter *a* for the ferroelectric (*1*, *2*) and paraelectric (*3*, *4*) phases of the 76/24 VDF/TFE prepared in the heating (*1*, *3*) and cooling (*2*, *4*) regimes.[66]

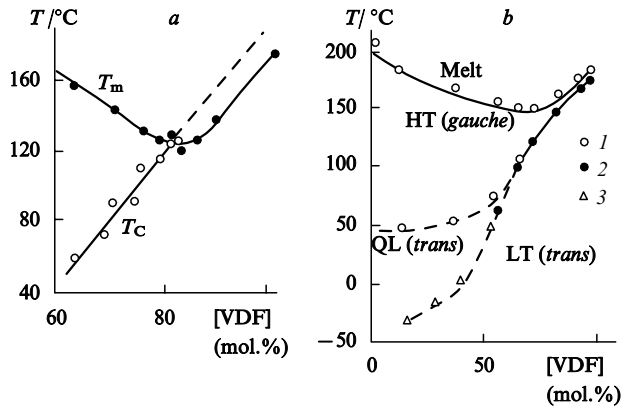


Figure 17. Melting and Curie points as functions of the VDF content in VDF/TFE copolymers [70] (*a*) and phase diagram of VDF/TrFE (*b*).[67] HT is the paraelectric phase, LT and QL are the ferroelectric phases; (*1*–*3*) are boundaries between the phases.

in the latter case. In view of the high information content of IR spectroscopy, it would be of interest to follow the variation of the conformational state of PVDF chains in the vicinity of the Curie transition by this method. These data are presented in Fig. 16 for the 75/25 VDF/TFE copolymer.[68] It can be seen that the bands at 842 and 1325 cm^{-1}, arising from the planar zigzag conformation in the chains of the VDF copolymer, become much less intense in the temperature region of this transition. Simultaneously, the proportion of chain units occurring in the helical *gauche*-conformation increases in the same temperature range. It is significant that the sharp decrease in the content of *trans*-conformers observed in the vicinity of the Curie transition involves not only VDF sections in the copolymer but also TFE sequences (a band at 620 cm^{-1}), a certain fraction of which (*e.g.*, for the 71/29 composition) can occur as dyads.[69]

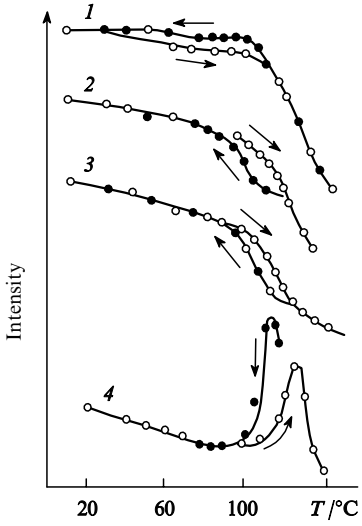


Figure 16. Temperature dependences of the relative variation of the intensities of the bands and 620 (*1*), 842 (*2*), 1325 (*3*), and 926 cm^{-1} (*4*) in the IR spectra of the ferroelectric 75/25 VDF/TFE copolymer.[68] (*1*) TFE groups in the *trans*-conformation, (*2*, *3*) VDF groups in the *trans*-conformation, (*4*) VDF groups in the *gauche*-conformation.

Thus, the ferroelectric–paraelectric transition in VDF/TFE copolymers is accompanied, apart from the change in the lattice parameters, by the substantial change in the conformational state of the chains, the equilibrium of the *trans*- and *gauche*-isomers being displaced towards the latter.

As the proportion of TFE in the copolymer increases, a regular decrease in the Curie point should be expected in addition to the monotonic 'loosening' of the crystal along the *a* axis of the unit cell. This is confirmed by the results of X-ray diffraction [67, 70] and spectroscopic [68] studies. According to X-ray diffraction data,[70] an increase in the fraction of TFE to 40 mol.% is accompanied by a linear decrease in the Curie point (Fig. 17*a*). The dependence of the melting point on the monomer ratio has a minimum; when the VDF fraction in the copolymer is below 80 mol.%, the Curie transition and melting temperatures are different, and these processes can be observed separately. With the assumption that the linear dependence of T_C on the VDF fraction still holds when this fractrion is above 80 mol.% (dashed line in Fig. 17*a*), the Curie point for pure PVDF (in the β-phase) should be 198 °C, which is higher than the melting point (175 °C).

Copolymers of VDF with TrFE, which possess higher piezoelectric characteristics, have been studied more comprehensively in this respect. In several studies of the thermal properties of these copolymers by differential scanning calorimetry (DSC), in addition to the melting endotherm, typical of crystallisable polymers, one more peak, attributed to the Curie transition, was observed at lower temperatures (Table 5).[67, 71–73] As the proportion of TrFE in the copolymer increases, the Curie point is displaced to lower temperatures. The enthalpy of this transition in the heating regime is always greater than that in the cooling regime. When the content of VDF is more than 70 mol.%, the Curie point exhibits a clear-cut hysteresis, pointing to a first-order phase transition. However, for the copolymer with 52.8 mol.% of VDF, the temperature hysteresis is hardly visible, which indicates the possibility of a second-order phase transition. In this case, the enthalpy is much lower.

Structural studies of VDF/TrFE copolymers showed [67] that their unit cell parameters, like those of VDF/TFE copolymers (see Fig. 15), change in the region of the Curie transition, which is due to the rearrangement of the polar cell into a nonpolar one. However, this transition is not so unambiguous, as was first suggested. Detailed analysis of the line contour of the intermolecular reflection near the Curie transition showed that two types of ferroelectric phases, QL and LT, can, in principle, exist.[28, 67] This conclusion has also been drawn in several other studies. For example, the presence of two heat evolution peaks below the melting region on the DSC curves has been explained [74] by the presence of two types of lattice of the ferroelectric phase differing in their degree of defectiveness. These peaks are matched by two maxima on thermal depolarisation curve for 75/25 and 70/30 VDF/TrFE copolymers. Experiments on the observance of dielectric hysteresis in these copolymers showed two peaks for the transpolarisation current, the characteristics of which depend on

Table 5. Temperatures and enthalpies of the Curie transition, melting and crystallisation for VDF/TrFE copolymers with various component ratios.[73]

[VDF] (mol.%)	Heating				Cooling			
	T_C / °C	ΔH_C / J g^{-1}	T_m / °C	ΔH_m / J g^{-1}	T_C / °C	ΔH_C / J g^{-1}	T_{cr} / °C	ΔH_{cr} / J g^{-1}
0	–	–	190	19	–	–	173	20
52.8	60	5.9	125	29	62	3.0	142	27
64.6	70	14	150	28	64	11	137	25
73	116	20	145	24	75	13	133	23
75	120	24	143	24	77	13	132	24
78	129	29	149	23	85	18	133	24
100 (PVDF)	–	–	153	41	–	–	139	32

the previous thermal history[34] and poling conditions of the samples.[75]

The appearance of dielectric anomalies points to the ferroelectric – paraelectric transition. Therefore, if there exist two types of ferroelectric phases with different degrees of crystallographic order, the temperature dependences for the real (ε') and imaginary (ε'') components of the complex dielectric constant should have two maxima. This is actually the case for the 65/35 VDF/TrFE copolymer (Fig. 18). The phase diagrams of VDF/TrFE copolymers show these two ferroelectric phases (see Fig. 17*b*, QL and LT

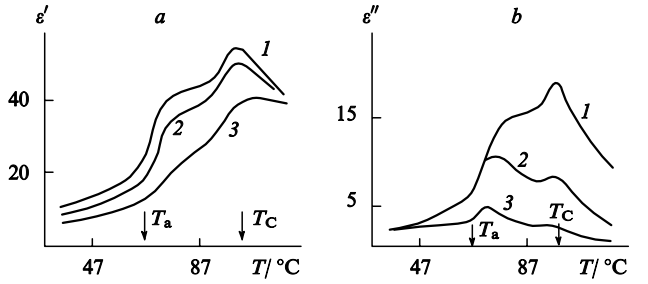


Figure 18. Temperature dependences of the real (*a*) and imaginary (*b*) components of the complex dielectric constant recorded during heating of the 65/35 VDF/TrFE copolymers.[76]
Frequency /MHz: 0.5 (*1*), 2.5 (*2*), 10 (*3*).

phases). According to the diagram, the more defective ferroelectric phase QL is formed only in copolymers with low concentrations of VDF, whereas in copolymers enriched in VDF, the ferroelectric transition follows the LT → HT pattern. Having agreed with the qualitative character of this diagram, Ogura *et al.*[76] reported data that made it more precise. Figure 19 shows the diffraction curves in the region of the principal intermolecular reflection for the 65/35 VDF/TrFE copolymer. At room temperature (below the Curie point), the copolymer with this composition should contain only the LT type ferroelectric phase (see

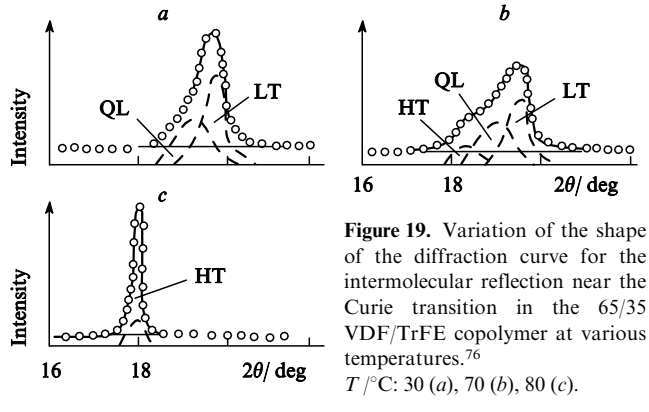


Figure 19. Variation of the shape of the diffraction curve for the intermolecular reflection near the Curie transition in the 65/35 VDF/TrFE copolymer at various temperatures.[76]
T /°C: 30 (*a*), 70 (*b*), 80 (*c*).

Fig. 17*b*). However, two components of the reflection (see Fig. 19*a*, *b*) point to the presence of both phases, QL and LT. In addition, as the temperature is raised, the LT → HT transition and then the HT → melt transition should occur. However, the paraelectric phase HT starts to appear in the presence of both the QL and LT phases (Fig. 20). In the vicinity of a certain temperature T_a, the proportions of the ferroelectric phases QL and LT start to decrease and the pattern of the temperature dependences of the corresponding interplanar spacings changes. In the same region, the paraelectric phase HT appears; in the range between T_a and T_C it coexists with the ferroelectric phases.

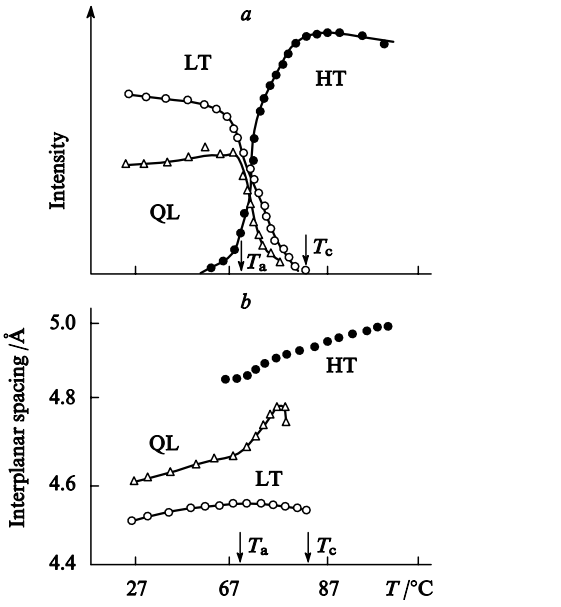


Figure 20. Temperature dependences of the reflection intensities (*a*) and interplanar spacings (*b*) for the paraelectric and ferroelectric phases in the region of the Curie transition for the 65/35 VDF/TrFE copolymer.[76]

The QL phase has greater interplanar spacings than LT. According to Tashiro *et al.*,[67] the less dense packing of the QL phase can be described by two structure models (Fig. 21). The first model implies the formation of crystals in which chains with planar zigzag conformations arranged in the (130) planes are bent with respect to *c* axis through an angle of 18 ° (Fig. 21*a*). Bends of this type can also arise in the crystals of the LT phase but in this case, the angle is ~3 °. The other model assumes the occurrence of 60° domains (Fig. 21*b*). These defects preclude the possibility of a denser packing, as in the LT phase. For example, the LT phase is characterised by the following monoclinic unit cell parameters: a = 9.12 Å, b = 5.25 Å, c (chain axis) = 2.55 Å, β = 93 °. The QL phase has the same lattice symmetry but contains a portion (~30%) of crystals with the above-noted defects. The crystal parameters are as follows: a = 9.16 Å, b = 5.43 Å, c (chain

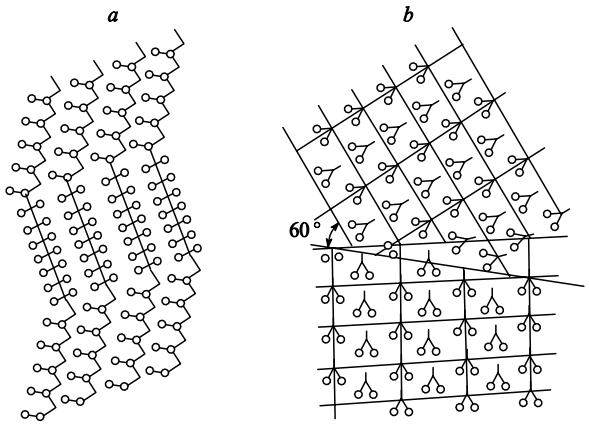


Figure 21. Schematic pattern of the disordered structure of the QL phase in the model of bent chains with the planar zigzag conformation (*a*) and in the model of the 60-degree domains (*b*).[67]

axis) = 2.53 Å, $\beta = 93°$. It can be seen that the lattice distortions arising on passing from the LT phase to the QL phase are accompanied by a noticeable decrease in the packing density in the polar direction (*b* axis).

As the Curie point is approached (in the rising temperature regime), conformational changes start to occur in the chains of the copolymers considered, as in the VDF/TFE copolymer (see Fig. 16). This is illustrated by Fig. 22 for 72/28 VDF/TrFE. It can be seen that near T_C, the intensity of the band at 1290 cm^{-1}, corresponding to the long sequences of VDF chains in the planar zigzag conformation (*trans*), sharply decreases.[28] Conversely, the intensity of the band at 612 cm^{-1}, due to the $TGTG^-$ conformation (*gauche*),[28] starts to increase substantially. Apparently, this is due to the fact that, as the Curie point is approached, bonds with 'defective' conformations, TG, T_3G, TG^- and T_3G^-, begin to appear in the the VDF chains in the planar zigzag conformation. This fact may account for the decrease in the intensities of reflections of the LT and QL phases and the increase in the intensity of the reflection due to the paraelectric HT phase (see Fig. 20*a*). The same assumption can explain the change in the interplanar spacing and the decrease in the intensity of the 001 reflection of the β-phase (see Fig. 22*a*,*b*). The pronounced hysterxesis of the above-mentioned characteristics indicates that the Curie transition in this copolymer is a first-order phase transition.

In view of the appearance of conformations corresponding to the α- and γ-modifications in the PVDF chains,[28] a dense packing of chains in the paraelectric HT phase should not be expected. In fact, this phase is characterised by the following unit cell parameters: $a = 9.75$ Å, $b = 5.63$ Å, c (chain axis) = 4.60 Å and $a/b = \sqrt{3}$. Several questions concerning the structure of paraelectric phase remain to be solved because calculation of the statistical chain packing does not provide agreement with experimental results.[67] This was attributed to the intense thermal motion in the HT phase, which can be recorded by dielectric measurements [77,78] and NMR.[79,80]

It should be noted that the presence of the QL and LT phases can account for the appearance of the 'anomalous' double hysteresis patterns in VDF/TrFE copolymers with high contents of a second co-monomer.[75,81,82]

The type of Curie transition in VDF copolymers is usually identified based on the presence or absence of hysteresis on the temperature dependence of one or another parameter sensitive to phase transformations. These parameters are found in the studies of thermal, electric and spectroscopic properties of objects. The NMR method and measurements of ultrasound [83] and crystal microhardness [84] are used more rarely for this purpose. Analysis of the temperature dependences of structural and spectroscopic characteristics of both VDF/TFE and VDF/TrFE containing more than 65 mol.% of VDF shows that temperature hysteresis is always observed in heating – cooling cycles (see Figs. 15, 16, 22). However, for VDF/TrFE copolymers of the compositions 60/40 and 52/48, this hysteresis becomes slightly visible.[85] This behaviour is typical of a second-order phase transition.

This conclusion was confirmed in another study [65] using a more appropriate method based on the measurement of nonlinear dielectric properties, in particular, second- (ε_2) and third-order (ε_3) dielectric constants. These characteristics behave in different ways in first- and second-order phase transitions. Figure 23 shows the temperature variation of ε_2 and ε_3 for 52/48 and 73/27 VDF/TrFE copolymers. It can be seen that these characteristics behave differently for the two copolymers. Indeed, ε_2 and ε_3 of the 73/27 copolymer remain finite and positive over the whole temperature range up to the Curie point, whereas for 52/48 copolymer, ε_2 drops to zero, and ε_3 changes its sign at the Curie point. In accordance with relations (20) and (25), the criterion for a second-order phase transition is clearly fulfilled for the 52/48 copolymer (see Fig. 23*a*,*c*). Conversely, for the 73/27 composition (and for 65/35, which is not shown in the Figure), the condition for a first-order phase transition is complied with. Thus, the hypothesis that the character of phase transition in

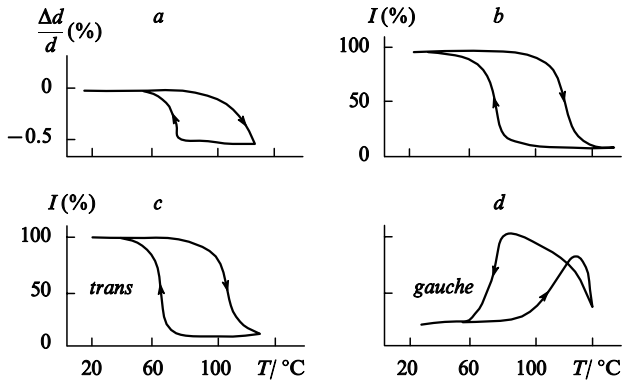


Figure 22. Temperature variations of the relative change in the interplanar spacing (*a*), the intensity of the 001 reflection (*b*), the intensity of the bands at 1290 (*c*) and 612 cm^{-1} (*d*) in the IR spectra of the 72/28 VDF/TrFE copolymer.[86]

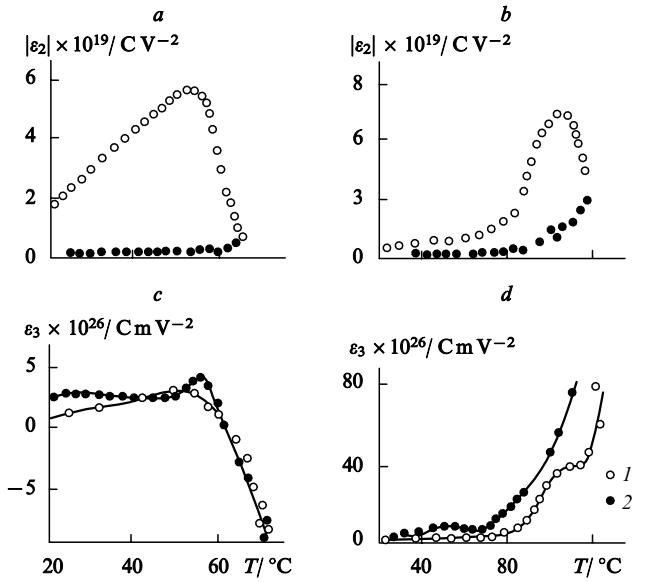


Figure 23. Temperature dependences of the second- and third-order dielectric constants in VDF/TrFE copolymers with compositions 52/48 (*a*, *c*), 73/27 (*b*, *d*) obtained in the heating (*1*) and cooling (*2*) regimes.[65]

VDF/TrFE copolymers changes at a composition of 52/48 (or near it) is confirmed not only by the specific features of the temperature hysteresis.

The VDF/TrFE copolymers are convenient as model compounds for predicting the behaviour of the LT–HT phase boundary. If the copolymer is considered to be ideally statistical, *i.e.* containing no composition fluctuations, the T_C value should be proportional to the concentration of ferroelectric groups in VDF.[88] This, however, is not confirmed by experiments (see Fig. 17*b*). This inconsistency can be due to the following reasons. Firstly, the appearance of ferroelectricity in the blocks of TrFE chains cannot be ruled out.[81,87] Secondly, the real copolymers cannot be regarded as ideally statistical. In fact, VDF/TrFE copolymers (as well as PVDF) contain a certain number of defects caused by the 'head-to-head' attachment.[28,69] In addition, for instance, in VDF/TFE copolymers, about 5% of TFE units occur as dyads even when the TFE proportion is 29 mol.%.[69]

Both reasons can, on the one hand, be responsible for the nonlinear course for the LT–HT phase boundary (see Fig. 17*b*) and, on the other hand, account for the formation of two ferroelectric phase modifications, LT and QL. The question why the Curie point in VDF/TrFE copolymers corresponds to a first-order phase transition for VDF contents of more than 60 mol.% and to a second-order phase transition for lower VDF concentrations has been tackled by Odajima [87] from the viewpoint of statistical theory. For this purpose, the investigator analysed the dielectric anomalies near the transition, characterised by the inverted dielectric absorption $\Delta\varepsilon$. Finite (non-zero) $1/\Delta\varepsilon$ values at the Curie point are inconsistent with the classical views [see, for example, relation (18)]. Evidently, this is due to the specific character of crystallisable polymeric systems, namely, to the presence of disordered areas, which are taken into account by using a constant in the theoretical description of the temperature dependence of $1/\Delta\varepsilon$ near the Curie transition.[77] The structural heterogeneity of VDF/TrFE copolymers and the possibility of composition fluctuations in their chains are responsible for the fact that the region of dielectric anomaly covers a fairly broad temperature range; the Curie transition can thus be attributed to diffuse phase transitions.[87] This is also confirmed by the fact that the Curie points found by DSC and NMR are lower than those found from dielectric measurements.[89–91]

The types of the phase transition at the Curie point have been predicted using the temperature dependences of the absorbances at two wavelengths (850 and 610 cm^{-1}) in the paraelectric phase of the copolymers considered. The former band corresponds to the bonds in the *trans*-conformation and the latter corresponds to the bonds in the *gauche*-conformation.[28] The D_{850}/D_{610} ratio was regarded as being equivalent to the ratio of populations of these states. In the case of the 72/28 VDF/TrFE copolymer, the D_{850}/D_{610} ratio for the paraelectric phase was found to increase on raising the temperature, while for the composition 52/48 it was found to decrease.[92] If the energies of the *trans*- and *gauche*-isomers are denoted by U_t and U_g, respectively, then for the 72/28 VDF/TrFE,

$$J = U_t - U_g < 0,$$

and for the composition 52/48,

$$J = U_t - U_g > 0.$$

In other words, *gauche*-isomers are found to be more stable in the former copolymer, and *trans*-isomers are more stable in the latter copolymer.

Resorting to these experimental facts, Odajima [87] developed a statistical theory of ferroelectric transitions in the copolymers in question for two models of pair interactions in the linear lattice formed by bonds in *trans*- and *gauche*-conformations with invoking combinatorial formulae.[93] The calculated reduced spontaneous polarisation as a function of reduced temperature in the region of ferroelectric transition is presented in Fig. 24*a*. According to both models, a first-order phase transition is manifested only for $J < 0$ because only in this case, do metastable states arise at temperatures $T > T_0$ (T_0 is the characteristic temperature). In the case where $J > 0$, a second-order phase transition occurs and no hysteresis is displayed. The latter situation ($J > 0$) occurs in 52/48 VDF/TrFE, for which almost no temperature hysteresis is observed in the region of transition.[92]

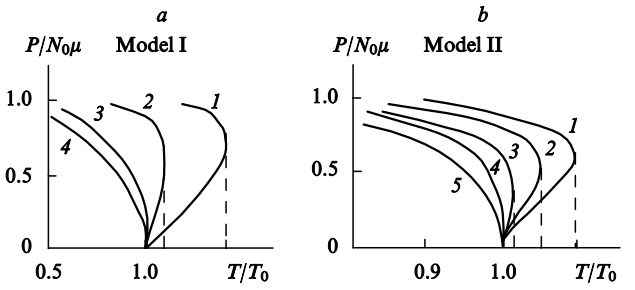


Figure 24. Temperature dependences of the reduced spontaneous polarisation in the region of the Curie transition for two models characterised by the parameter $B = J/kT_0$.[87]
B: −2.0 (*1*), −1.0 (*2*), 0 (*3*), 2.0 (*4*) (*a*); −0.3 (*1*), −0.2 (*2*), 0 (*3*), 0.5 (*4*), 2.0 (*5*) (*b*). N_0 is the concentration of dipoles, μ is the dipole moment of the CF_2 group.

Thus, the theory developed in the study cited [87] provides results which coincide qualitatively with experimental data. If a copolymer with a composition of 72/28 has $J < 0$,[92] then $P \neq 0$ can also be fulfilled at $T > T_C$ (see Fig. 24), *i.e.* prerequisites for temperature hysteresis appear, which is consistent with the data of Table 5. For the 65/35 VDF/TrFE copolymer, hysteresis is also observed but the situation is more complicated. For this copolymer, $J \approx 0$ (see Ref. 92) and temperature hysteresis is possible only in terms of model II (Fig. 24*b*), which uses more complex combinatorics of bonds in the linear lattice than model I. It remains to be seen whether the calculated character of phase transition in 52/48 VDF/TrFE copolymer coincides with that observed in the experiment. The calculation [87] was based on the fact that free energy does not depend on lattice parameters. Practically, this could be the case only if the measurements are carried out in the 'constricted' state. The majority of experiments are carried out under free conditions under which the sample lattice should deform under the action of polarisation. Thus, the electrostriction effect can influence the free energy and, as a consequence, a second-order phase transition should be transformed into a first-order transition.[94]

The 52/48 VDF/TrFE copolymer has a low Curie point; therefore, it can be used to monitor the influence of an external static field on the position of the Curie point. This task has been accomplished by Date. [95] The Curie transition was detected in the temperature dependences of the pyroelectric coefficient p_y based on the point where $p_y = 0$. This is exemplified in Fig. 25, which presents the experimental temperature dependences of the pyroelectric coefficient for this copolymer under the action of fields with various polarities. If the external field coincides in direction with the remanent polarisation, it shifts the Curie point to higher temperatures. If the field has the opposite sign, the Curie point shifts to lower temperatures. This shift is linear and has the slope

$$\frac{dT_C}{dE} = \Delta P \frac{T_C}{L}. \qquad (27)$$

Here ΔP is the change in the polarisation near the Curie transition and L is the latent heat. By increasing the amplitude of the negative bias field, the Curie point can be appreciably decreased; in this particular copolymer, it can be brought close to room temperature. If the temperature in some region is raised (*e.g.*, by use of a laser), the direction of spontaneous polarisation in this region will be reversed due to the bias field. This enables optical

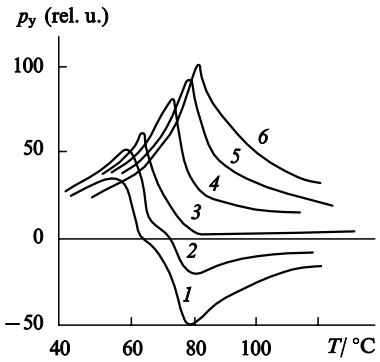


Figure 25. Temperature dependences of the pyroelectric constant in the 52/48 VDF/TrFE copolymer upon the application of electric fields with various strengths.[95]
E /MV m^{-1}: −10 (*1*), −5 (*2*), 0 (*3*), 5 (*4*), 10 (*5*), 15 (*6*).

recording of information with the aid of ferroelectric polymer films, which was actually demonstrated in practice.[95]

For recording, it is important to ensure efficient transfer of a thermal pulse to the ferroelectric matrix. Evidently, this can be attained by introduction into the films of dye molecules with an absorption band in the range of laser radiation. In this respect, studies of the behaviour of dyes carried out by Verkhovskaya *et al.*[96–98] appear significant. In particular, it was found that doping of 70/30 VDF/TrFE copolymer by merocyanines makes it possible to observe photoelectric sensitivity in the visible and UV regions of the spectrum. Analysis of the fluorescence[98] and absorption[96] spectra showed intense interaction of the rhodamine 6G molecule with the ferroelectric phase of the copolymer. The appearance of temperature hysteresis in the region of the Curie transition indicates that it is a first-order phase transition. The so-called structure-chromic effect was established; this means that spectral characteristics of the dye molecules change depending on whether the crystalline phase occurs in the ferroelectric or in the paraelectric state. Thus, the principal band of merocyanines shifts to the blue region and becomes less intense above the Curie point.[96,97] The optical recording in doped copolymers was performed using the dye spiropyran, which exhibits a photochromic effect. The possibility of observing the photorefractive effect using these systems has been demonstrated.[97]

V. The mechanism of the generation of ferroelectricity based on NMR studies

The nature of ferroelectricity in the polymers in question can be elucidated more precisely on the basis of the molecular dynamics characteristics. Quasielastic neutron scattering is sometimes used for this purpose;[99] various modifications of NMR are employed more often. VDF/TrFE copolymers with various ratios of the components have served as the objects of NMR studies. For example, copolymer with the composition 70/30 has been studied.[100] The researchers attempted to answer a number of fundamental questions. In particular, they tried to find out whether or not passing from the low-temperature ferroelectric phase to the high-temperature paraelectric phase gives rise to specific mobility. If this mobility does appear, whether it results in a higher symmetry in the disordered phase. The point group of symmetry in this phase, which can vary from 6/*mmm* (centrosymmetrical lattice) to 6/2*m* (non-centrosymmetrical lattice), also presents interest.

The signal of free induction at temperatures above 80 °C can be represented as a superposition of two components.[101] One component (for short times t) refers to the ^{19}F nuclei in the crystal and is described by the Gaussian function [100]

$$\mathrm{M}(t) = \Delta M(0)\exp\left(-\frac{M_{2c}t^2}{2}\right), \qquad (28)$$

where M_{2c} is the second moment of the line for the crystalline phase.

The second component is associated with the amorphous phase: at $T > 80$ °C, this component is described by a Lorentzian dependence, typical of viscous liquids. The temperature dependence of the free induction signal from the NMR data can be used to estimate the change in the dynamic degree of crystallinity (in addition to the static degree of crystallinity, which can be estimated, for example, based on X-ray data). Figure 26 shows the temperature dependences of the dynamic degree of crystallinity and the rate of transverse relaxation as well as the DSC curves for 70/30 VDF/TrFE copolymer. In the region of the Curie transition, the dynamic degree of crystallinity markedly changes and hysteresis in the heating and cooling regimes is observed. The temperature plots for the transverse relaxation rate for the crystal also change markedly in the transition region and exhibit a clear-cut hysteresis. The chain dynamics in the amorphous phase also proves to be sensitive to the phase transition because the corresponding line in this region does not vary monotonically, although hysteresis is barely visible in this case.

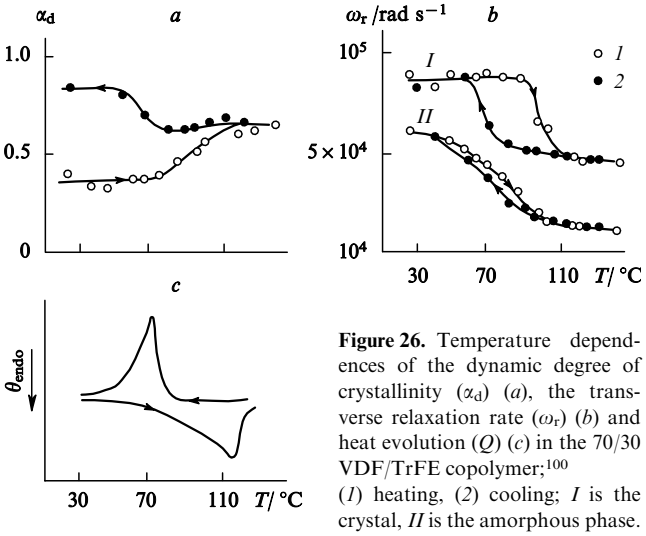


Figure 26. Temperature dependences of the dynamic degree of crystallinity (α_d) (*a*), the transverse relaxation rate (ω_r) (*b*) and heat evolution (Q) (*c*) in the 70/30 VDF/TrFE copolymer;[100]
(*1*) heating, (*2*) cooling; *I* is the crystal, *II* is the amorphous phase.

Thus, the Curie transition in this copolymer is of dynamic origin and can be likened to the plastic phase transitions observed in some low-molecular-mass crystals.[100]

By using different modulation frequencies (9.14 and 20 MHz), the researchers separated the contributions of the amorphous and crystalline phases to the spin–lattice relaxation times (T_1). The contribution of the amorphous phase (T_{1a}) varies nearly monotonically exhibiting no hysteresis in the transition region, whereas the contribution of the crystalline phase (T_{1c}) passes through a minimum in this region and exhibits a typical hysteresis in the heating–cooling cycles. Below the Curie point, the absolute values of T_{1a} and T_{1c} differ by more than an order of magnitude, whereas above the Curie point, they differ only by a factor of 2. Thus the parameters characterising the dynamics in the paraelectric phase are similar to those for the disordered phase. The chains forming the paraelectric phase can have several equilibrium positions, which should result in a higher symmetry compared to that in the ferroelectric phase.[102]

The character of the Curie transitions in VDF/TrFE copolymers of various compositions can be judged from the data that are given in Table 6 and include results obtained by the NMR method. It can be seen that the Curie transition temperatures determined by different methods are somewhat different; however, in some cases, the tendency for hysteresis in the cooling and

Table 6. Temperatures T_C (°C) found by various methods for VDF/TrFE copolymers of various compositions in the heating (*I*) and cooling (*II*) regimes.[104, 106]

Composition	NMR [a]		NMR [b]		DSC		DM [c]	
	I	II	I	II	I	II	I	II
52/48	63	63	65	65	60	62	79	73
65/35	89	70	90	75	70	64	103	69
72/28	116	75	115	79	114	75	134	84

[a] Based on the variation of the line width; [b] based on the variation of T_1; [c] dielectric method (measurement of $\Delta\varepsilon^{-1}$).

heating regimes can be followed. It is confirmed once again that in 52/48 copolymers, a second-order phase transition occurs, which is replaced by a first-order phase transition for higher VDF concentrations.

Ishii and Odajima [103] used the Ising model[104, 105] to calculate some parameters of the fluctuation transition, in particular, the effective distance (d) between the fluctuating ordered units connected by short-range forces and the correlation length of the fluctuation region of polarisation (ξ). The d and ξ values were found to be somewhat greater for 52/48 and 65/35 copolymers than for copolymers with other compositions. Apparently, the ferroelectric – paraelectric transformation in these copolymers is better interpreted as a second-order phase transition.

Later, the same researchers studied the molecular dynamics in the region of the Curie transition using a different NMR technique, namely, analysis of the shape of the absorption peaks.[106–109] Textured films of the copolymers were used as the samples; the angle between the external field and the stretching direction was varied. At room temperature, the absorption line consists of three components, which are interpreted in terms of nonequivalence of the local fields for the fluorine nuclei occurring in the bulk of the ferroelectric phase, at its boundaries, and in the amorphous phase. For 52/48 copolymer, the absorption line at 30 °C contains only two components.[106, 109] The temperatures of transition to the paraelectric phase, found from the narrowing of the widest component of the signal for various copolymers, are listed in Table 6. These temperatures are very close to the spin – lattice relaxation temperatures (T_1), their variation fitting in the general regularity of hysteresis in these copolymers. In fact, hysteresis is not displayed in the 52/48 copolymer but appears at higher VDF proportions.

Lovinger *et al.*[110] used ^{1}H and ^{19}F NMR spectroscopy to analyse the molecular dynamics in the VDF/TrFE copolymers containing 10 mol.% to 70 mol.% of VDF. When the composition was 70/30, the ^{1}H NMR free induction signal in the 15 – 60 °C temperature range consisted of three components. The narrowest and the medium components were attributed to the motion in the normal and 'stressed' amorphous phase, respectively. In the temperature range 60 °C < T < T_C, the medium component becomes more intense; this was interpreted as being due to the ferroelectric – paraelectric transition. The calculation of the second moment ΔH_2^2 for the medium and broad components, which are assigned to the paraelectric and ferroelectric phases, respectively, shows that these phases coexist in a broad temperature range, from 60 to 120 °C. The data on the second moment for the crystals of the paraelectric phase in the 70/30 VDF/TrFE copolymer indicate the possibility of substantial dynamic disorder in this phase. In fact, the ΔH_2^2 value for the rigid lattice of the paraelectric phase calculated based on the X-ray diffraction data should be 11.6 G^2, while the experimental value is only 2.5 G^2. This appreciable difference cannot be explained only by the changes in the type of packing in the crystal and in the chain conformations upon the Curie transition. Evidently, vigorous molecular motion, whose type is yet unknown, should be expected in the paraelectric phase. In particular, if the chains in the paraelectric phase are assumed to rotate about the macromolecule axes, the calculated ΔH_2^2 value decreases to 3.5 G^2 (see Ref. 110).

The difference in the dynamic degree of crystallinity found from ^{1}H and ^{19}F experiments for copolymers with VDF contents not higher than 70 mol.% is attributed to the difference in the compound compositions in the regions with slow and fast dynamics. The difference may be due to the segregation of phases enriched in VDF and TrFE groups; this is not at variance with the conclusion about the existence of two crystalline modifications in these copolymers [111] or with the conclusion concerning the presence of LT and QL phases. If segregation does occur, it should also influence characteristics of the disordered phase. Indeed, since the glass transition temperatures of PVDF and polytrifluoroethylene (PTrFE) are appreciably different (−40 and +40 °C, respectively), the regions enriched in VDF and TrFE should also be characterised by different glass transition temperatures. This can account for the specific features of the dynamics of these copolymers near 40 °C [71, 112] and for the data of ultrasonic [113] and NMR studies.[114]

A fairly unusual conclusion has been drawn [114] in a study of copolymers with various previous thermal histories. In particular, samples obtained by quenching and isothermal crystallisation were studied, the perfection and the volume fraction of crystals being higher in the latter case. The Curie point for samples obtained by quenching was found to be higher than that for isothermally crystallised ones. Similar results were obtained by the DSC method.[115] The second moment of the absorption line, ΔH_2^2, scarcely changes above the Curie point.[114] The interplanar spacing behaves in a similar way, while the intensities of the absorption bands corresponding to the planar zigzag conformation continue to change in the $T > T_C$ region.[116, 117] This means that the conformational changes in the vicinity of the Curie transition 'lag behind' the changes in the lattice type.

Unlike ΔH_2^2, the correlation time τ_c is determined by the movement of domain boundaries and, hence, the pattern of its temperature variation near T_C should be symmetrical. In reality, experiments showed slight asymmetry of this dependence.[114] Rigamonti [118] has attributed this asymmetry to the order – disorder transition.

Comparison of the anomalies in the temperature dependences of spin – lattice relaxation times in an ordinary and in a rotating system of coordinates near the Curie transition [114] shows that they resemble most closely the dielectric anomalies considered, for example, by Davis *et al.*[119] When comparing the spin – lattice relaxation times in copolymer samples obtained by quenching and isothermal crystallisation above the Curie point, the researchers noted that the samples are more perfect in the former case. This contradicts the known properties of crystallisable polymers. This contradiction can be explained by the presence in the copolymers of two crystalline phases, ferro- and paraelectric phases, which differ in both the lattice parameters and chain conformations. Crystallisation at $T > T_C$ should be accompanied by an increase in the proportion of chains in the helical conformations in the crystal; after cooling the sample to room temperature (*i.e.* below T_C), these chains will be perceived as conformational defects. This may be the reason for the lower Curie temperature observed for these samples. This hypothesis is confirmed by NMR data for samples of the 70/30 VDF/TrFE copolymer annealed above the Curie point.[120] Local mobility in the ferroelectric crystals was found; this can be attributed to the presence of the conformational defects mentioned above. These defects are 'weak points' in the ferroelectric phase (with chains in the planar zigzag conformation) but they can play an important role in the initiation of the Curie transition; specifically, they shift the transition to lower temperatures, which has been observed in a study.[114]

The chain dynamics in the disordered phase also influence the Curie transition. This phase has been reported [120] to have high-frequency mobility modes similar to those in the paraelectric phase. The parameters of these modes can also have an influence

on the characteristics of the ferroelectric transition because crystallisable polymers have no clear-cut phase boundaries.

At the crystal boundary, regions with tie-tough chains (TTC) are located, in which the same chains can be incorporated simultaneously in the disordered (in the strict crystallographic sense) phase and in the adjacent crystal. Since the neighbouring monomer units in a chain are linked by covalent bonds, the high-frequency motion modes in the disordered phase should at certain amplitudes generate conformational defects in the ferroelectric phase through the TTC sections. Evidently, this stage precedes the Curie transition. This is confirmed by the correlation between the variation of the interplanar spacing in the ferroelectric phase lattice and the intensity of the absorption band corresponding to the planar zigzag conformation. The change in the packing density of chains in the crystal is, apparently, the main reason for the generation of the high-frequency motion mode because high-frequency motions of the same nature were noted[120] in the amorphous phase below the Curie point and in the paraelectric crystal.

The views on the chain dynamics in the paraelectric phase have been detailed to a degree by varying the field frequency for resonance at the ^{1}H and ^{19}F nuclei and analysing the data on the anisotropy of the second moment for textured samples.[121] The researchers admit that rotation of the chain in the TGTG$^-$ conformation as a whole, which they proposed previously,[110] appears unlikely, because a similar ΔH_2^2 value is found for this type of motion for chains in a planar zigzag conformation.[121] The hypothesis of motion through propagation of kink bonds along the chain was also verified. For example, motion of the flip-flop type (a 180-degree kink) should result in the minimum of ΔH_2^2 being observed at an angle of 45° between the axis of tension and the direction of the magnetic field but this is not confirmed experimentally. This fact together with the fact that the calculated ΔH_2^2 value is several times greater than the experimental one prompted the researchers[121] to conclude that this motion is impossible in the paraelectric phase. Motions as 120- or 60-degree kinks (between three or six symmetrical positions) are more probable because they provide reasonable agreement with experimental results. The possibility of the 'crankshaft' type motion involving three neighbouring bonds was also considered in the study cited.

VI. The influence of pressure on the characteristics of the ferroelectric transition

The mechanism of the formation of ferroelectricity in polymers can be elucidated more precisely by investigating the specific influence of various external factors, in particular, pressure and uniaxial stretching, on the ferroelectric–paraelectric transition parameters. The results of a study,[122] dealing with the influence of pressure (up to ~1 GPa) on the components of the complex dielectric constant of PVDF and 70/30 VDF/TrFE can be considered as an example. The character of variation of the real dielectric constant ε' in the region of transitions upon variation of the external pressure can be followed from the temperature dependences shown in Fig. 27*a*. It can be seen that the $\varepsilon'(T)$ curve for atmospheric pressure has two characteristic points. The low-temperature maximum is attributed to the dielectric anomalies in the vicinity of the Curie transition (T_C) and the inflection at higher temperatures is ascribed to the dynamic melting process (T_m). At higher pressures, both transitions are displaced to higher temperatures. This shift is non-linear (Fig. 27*b*). If the relative change in the volume ($\Delta V/V_0$) is taken as the variable, the temperature dependences for the Curie transition and for melting become straight lines (Fig. 27*c*). The slope regularly increases as the transition temperature rises; this also applies to the region of the transition associated with freezing of the micro-Brownian motion in the disordered phase.[122]

In the case of the 52.8/47.2 VDF/TrFE copolymer, in which, as noted above, the Curie transition is a second-order phase

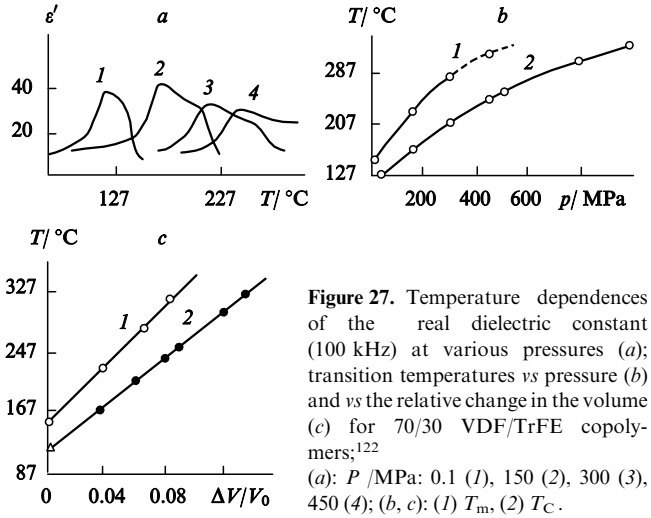


Figure 27. Temperature dependences of the real dielectric constant (100 kHz) at various pressures (*a*); transition temperatures *vs* pressure (*b*) and *vs* the relative change in the volume (*c*) for 70/30 VDF/TrFE copolymers;[122]
(*a*): *P* /MPa: 0.1 (*1*), 150 (*2*), 300 (*3*), 450 (*4*); (*b*, *c*): (*1*) T_m, (*2*) T_C.

transition, an increase in pressure influences the Curie transition temperature in a similar way.[73] If the Curie point is characterised by a maximum of ε', the Curie–Weiss equations for this copolymer have the following form:
for $T < T_C$,

$$\frac{1}{\varepsilon'} \simeq \frac{T_C - T}{C_1}, \tag{29}$$

and for $T > T_C$,

$$\frac{1}{\varepsilon'} \simeq \frac{T - T_C}{C_2}. \tag{30}$$

The C_1 and C_2 constants for the standard pressure are 123 and 140 °C and T_C = 67 °C.

Similar relations have been obtained for the dependence of ε' on the pressure p
for $p < p_C$,

$$\frac{1}{\varepsilon'} \simeq \frac{p_C - p}{C_3}, \tag{31}$$

and for $p > p_C$,

$$\frac{1}{\varepsilon'} \simeq \frac{p_C - p}{C_4}, \tag{32}$$

where C_3 = 10.8 GPa, C_4 = 2.37 GPa, and p_C = 134 MPa at 110 °C.

The displacement of the transition point under the action of external pressure for the copolymer with the 52.8/47.2 composition can be described by the following relation:[73]

$$T_C = 76\ ^\circ\text{C} + 0.314p. \tag{33}$$

When the VDF content in the copolymer is 64.6 mol.%, two equations are needed to describe these dependences due to the hysteresis phenomena:
for heating,

$$T_C = 80\ ^\circ\text{C} + 0.383p \tag{34}$$

and for cooling,

$$T_C = 60\ ^\circ\text{C} + 0.401p. \tag{35}$$

The influence of pressure on the ferroelectric transition in these two copolymers can be followed from the data presented in Table 7. The experimental coefficients for the displacement of the Curie point as a function of pressure found by dielectric measurements and by the thermal expansion method are in good agreement with one another. The theoretical values of these coefficients were calculated using the Clausius–Clapeyron equation

Table 7. Curie temperatures, experimental and calculated coefficients of the displacement of the Curie temperatures (dT_C/dp /deg MPa), relative volume changes ($\Delta V/V_0$) and enthalpies (ΔH) for VDF/TrFE copolymers.[73, 123]

Regime	T_C / °C	dT_C/dp		$\frac{\Delta V}{V_0} \times 10^2$	$\Delta H \times 10^{-7}$ /J m^{-3}
		experiment	calculation		
Composition 52.8/47.2					
Heating	67	0.314 [a] 0.318 [b]	0.487	1.56	1.09
Composition 64.6/35.4					
Heating	86	0.383 [a] 0.381 [b]	0.206	1.51	2.63
Cooling	60	0.401 [a] 0.394 [b]	0.170	−1.05	−2.06

[a] Dielectric measurements; [b] thermal expansion.

$$\frac{dT_C}{dp} = \frac{T_C(\Delta V/V_0)}{\Delta H}. \quad (36)$$

It can be seen from the Table that the experimental and theoretical coefficients for the transition displacement can differ by a factor of more than two. Comparison of the presented dT_C/dp values with those for a similar copolymer containing 70 mol.% of VDF shows [122] that the previous thermal history of samples can affect substantially the pattern of the influence of pressure on the transition considered.

The effect of pressure on the 54/46 VDF/TrFE copolymer has been studied.[124, 125] This was done using a set of methods including DSC, X-ray diffraction, $D-E$ hysteresis, and ultrasonic studies. The temperature dependences of a number of parameters determined by these methods are shown in Fig. 28. It can be seen that at a pressure of 350 MPa the Curie transition becomes a two-stage process. In fact, according to DSC, two endotherms appear instead of one. The interplanar spacings for the 110 and 200 reflections also change in two stages. Two characteristic points are present in the temperature dependences of the absorbance, the sound velocity and the remanent polarisation.

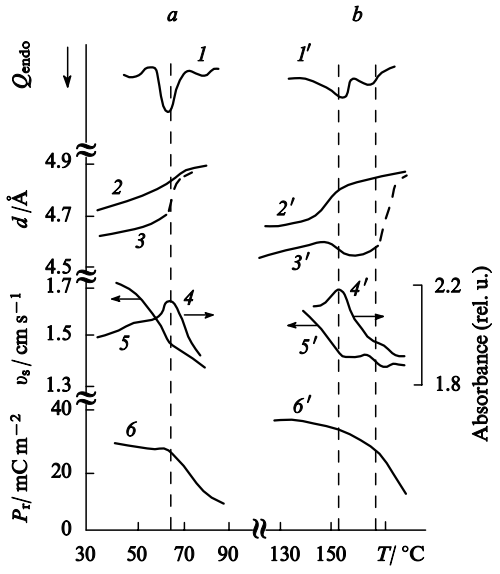


Figure 28. Temperature dependences of heat evolution (*1*, *1′*), interplanar spacing (*2*, *2′*, *3*, *3′*), absorbance (*4*, *4′*), sound velocity (*5*, *5′*) and remanent polarisation (*6*, *6′*) at a pressure of 0.1 (*a*) and 350 MPa (*b*) for the 54/46 VDF/TrFE copolymer.[124]

This unusual phenomenon can be interpreted based on the above hypothesis concerning the formation of two types of ferroelectric phase, LT and QL, in the copolymers considered.[124, 126] It is assumed that under normal pressure, crystallisation proceeds in the QL phase, whereas at the Curie point, the QL phase transforms in one step into the paraelectric phase. As the pressure increases to 350 MPa at room temperature, the QL ferroelectric phase transforms into a more perfect phase, LT. This can be judged from the decrease in the interplanar spacings for the 110 and 200 reflections (see Fig. 28, curves *2*, *2′* and *3*, *3′*). Heating under increased pressure is accompanied by transformation of the LT phase into the less perfect QL phase, which is subsequently transformed into the paraelectric phase. This scheme is consistent with a two-stage mechanism of the Curie transition, which is confirmed experimentally.

The influence of mechanical loading on the characteristics of the ferroelectric transition will be considered separately. Studies have been performed with textured films of VDF/TrFE copolymers to which mechanical stress X has been applied along [125] or across [127] the axis of tension. The Curie transition was monitored based on the characteristics of thermal shrinkage on heating (cooling) of uniaxially stretched films. It was found that the relative decrease in the size of the film (x) is most pronounced near the Curie transition. This characteristic temperature range was found to be well correlated with the range of specific changes in the structural parameters determined by X-ray diffraction and IR spectroscopy.[126]

Figure 29 presents the displacement of the Curie point as a function of external stress. These plots allow one to follow the shift of the Curie transition. (The negative ΔT values imply displacement of T_C to lower temperatures). It can be seen that slight stress both along and across the axis of tension shifts the transition in both the heating and cooling regimes to lower temperatures. Thus, the shifts in the Curie temperature induced in the copolymers studied by an increase in the external stress are opposite to the pressure-induced shifts.

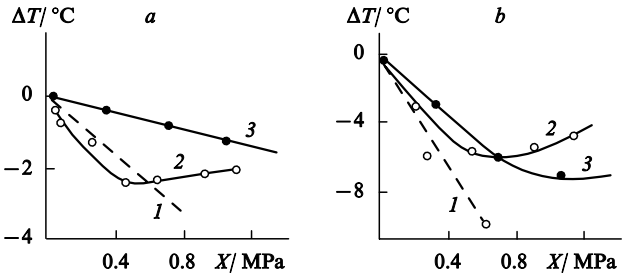


Figure 29. Influence of the external mechanical stress in isotropic (*1*) and uniaxially stretched (*2*, *3*) films of the 65/35 VDF/TrFE copolymer on the displacement of the Curie point during cooling (*a*) and heating (*b*).[127] The stress was applied along (*2*) and across (*3*) the stretching axis.

If we assume that the free energies of the ferroelectric (LT) and paraelectric (HT) phases are equal at the Curie point, then the shift of the Curie point caused by transverse stress X is described by the equation [127]

$$\frac{dT_C}{dX} = -\frac{k'\Delta x_C}{\Delta S}, \quad (37)$$

where k' is a constant, Δx_C is the change in the transverse dimension of the crystallite at the transition point, and ΔS is the difference between the entropies of the LT and HT phases. The sign of dT_C/dX in relation (37) is determined only by the sign of the constant k'. The negative sign is mainly due to high Poisson coefficient ($\mu_P = 4.5$), which is typical of textured crystallisable polymers.

It is very important to find out whether characteristics of the amorphous phase remain invariate during mechanical loading in the above experiments. Unfortunately, this point has been considered only in passing,[125, 127, 128] although it deserves more comprehensive study. In fact, it has been found[28, 129, 130] that loading of textured films of crystallisable polymers may bring about complex conformational transitions in amorphous regions (especially in those adjacent to the crystal).

This is confirmed by a study[131] dealing with the variation of the longitudinal velocity of sound v_s and birefringence upon loading along the axis of tension of textured films of VDF/TFE. The increase in these values (for films with relatively low texturing temperatures T_d) points to conformational rearrangements, $TGTG^- \rightarrow (TT)_n$ and $T_3GT_3G^- \rightarrow (TT)_n$, for chain sections in disordered regions, which are highly pliable. The probability of these rearrangements depends substantially on the temperature of texturing (uniaxial stretching), which influences the number of conformational defects. Indeed, in the case of high T_d, the v_s and birefringence values change only slightly. The data of low-angle X-ray scattering indicate that the structure formed at these T_d is characterised by a greater difference between the densities (in the draw direction) of the crystal and the amorphous phase.[131, 132]

External mechanical stress should apparently influence yet another ferroelectric characteristic of textured films — the time of polarisation switching τ_s in an electric field. For uniaxially stretched films, it would be pertinent to consider the influence of mechanical stress in the film plane applied at an angle normal to the axis of tension. This problem was solved in terms of the 60-degree switching model, according to which the nuclei of the new (switched) phase are formed at the crystal–amorphous phase boundary.[133] This model was substantiated by experimental facts pointing to a special role of the boundaries between the crystal and the amorphous phase and the TTC sections in them, which can act as the nuclei for new domains. Proceeding from this model, Jishi[134] considered the influence of the external stress X on τ_s with allowance for the Gaussian shape of stress distribution at the crystal–amorphous phase interface. By specifying particular values for the characteristic effective stress found from the experimental plots for the piezoelectric constant d_{32} *vs* mechanical stress,[135] the researcher cited showed that τ_s should diminish substantially under the action of stress. For example, at room temperature, the mechanical stress $X = 12$ MPa for a field with a strength of 200 MV m^{-1} should decrease τ_s by more than three orders of magnitude.[134] Unfortunately, this was not confirmed experimentally.

The role of pressure in the switching processes has been studied experimentally.[136] Figure 30 shows the characteristics of the switching process in PVDF with the ferroelectric β-phase as a function of the applied pressure. It can be seen that an increase in pressure increases the average switching time (τ_s) and regularly decreases the maximum current (Fig. 30*a*). The full transpolarisation charge, found by integrating the experimental curves, changes almost linearly starting from 200–300 MPa (Fig. 30*b*). The maximum current and τ_s vary nonlinearly as functions of pressure. To interpret the data obtained, the changes in the volume of the films with various degrees of crystallinity have been studied. This made it possible to estimate the compressibility of the crystalline and amorphous phases in a bulk sample.

The crystal was found to be the least compressible and the disordered phase was the most compressible; the real bulk specimen was found to have a medium compressibility. Since τ_s increases with pressure (when the specific volume decreases), it was assumed that the switching time should depend on the fraction of free volume f. This relationship can be described by an equation of the type of the Doolittle equation,[137] which is often used when studying the relaxation processes in polymers

$$\tau \approx \exp\left(\frac{1}{f}\right). \qquad (38)$$

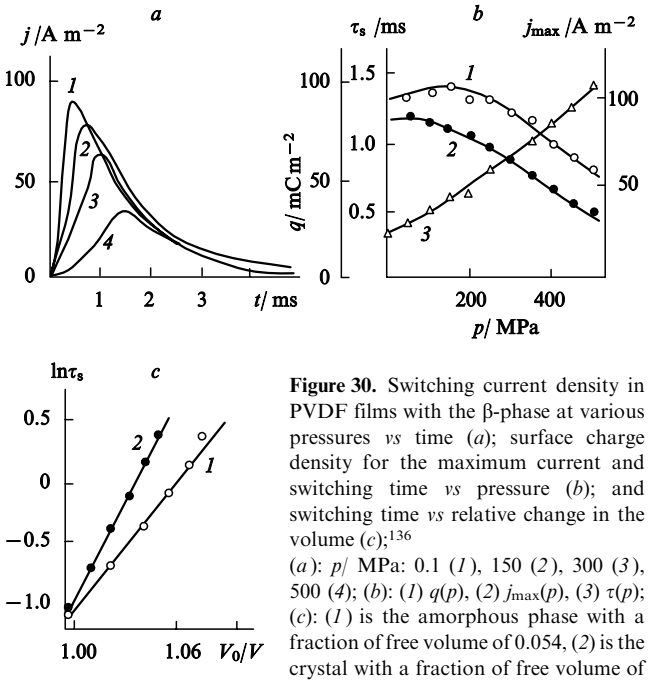


Figure 30. Switching current density in PVDF films with the β-phase at various pressures *vs* time (*a*); surface charge density for the maximum current and switching time *vs* pressure (*b*); and switching time *vs* relative change in the volume (*c*);[136]
(*a*): *p*/ MPa: 0.1 (*1*), 150 (*2*), 300 (*3*), 500 (*4*); (*b*): (*1*) $q(p)$, (*2*) $j_{max}(p)$, (*3*) $\tau(p)$; (*c*): (*1*) is the amorphous phase with a fraction of free volume of 0.054, (*2*) is the crystal with a fraction of free volume of 0.034.

The f value is expressed *via* the relative change of the volume[136]

$$f(p) = \frac{f_0 V(p)}{V_0}, \qquad (39)$$

where f_0 is the relative free volume at atmospheric pressure and room temperature, *i.e.* when $V(p) = V_0$. It follows from relations (38) and (39) that

$$\ln\tau(p) = \frac{A + V_0}{f_0}. \qquad (40)$$

If this concept is valid, the variation of $\tau(p)$ as a function of $V_0/V(p)$ should follow a linear pattern in semilogarithmic coordinates (Fig. 30*c*). The slope of the plots for $\ln\tau_s$ *vs* V_0/V determines the f_0 value. The f_0 values were calculated for both the crystalline and amorphous phases based on the data on compressibility of samples with various crystallinity degrees. It was found that for the amorphous phase, $f_0 = 0.054$, which is close to the values 0.05–0.07, typical of standard amorphous polymers.[138]

Thus, experimental plots for the switching time *vs* pressure imply that the state of the amorphous phase plays a very important role in the mechanism of polarisation switching in crystallites. This is consistent with the above-stated hypothesis that nuclei of new domains can arise in the amorphous phase (or at its boundary with the crystal), TTC sections playing a special role. Evidently, the dynamic characteristics of TTC should be the first to be taken into account, which is confirmed by the parameters of switching in samples with various previous thermal history and in samples exposed to γ-rays.[136]

VII. The influence of the structural features of polymers on their ferroelectric characteristics

As the crystalline phase becomes more perfect, the ferroelectric parameters in crystallisable polymers are improved. An original method for decreasing the imperfection of the crystal lattice has been found.[139] A deuterated PVDF sample with the crystals of the β-phase was compared with a similar non-deuterated sample. The degree of perfection of the crystal lattice was estimated indirectly relying on the parameters of the $D-E$ hysteresis dependences, obtained under the same poling conditions. For the non-deuterated sample (field strength >200 MV m^{-1}), the remanent

polarisation was 56 mC m^{-2}, which is consistent with the results of other researchers. The P_r value for the deuterated film proved to be almost twice as great ($\sim$100 mC m^{-2}), which was explained by a more perfect structure of the ordered regions. The reasons for this phenomenon are still not entirely clear, because a mere increase in the degree of crystallinity α could cause a similar increase in P_r.

The influence of the parameter α on P_r has been specially studied for 80/20 VDF/TFE samples with different previous thermal histories.[140] Three modes of crystallisation from the melt were considered, namely: quenching, crystallisation at 120 °C and a pressure of 0.1 MPa, and crystallisation at 250 °C and a pressure of 500 MPa. The melting points T_m were estimated from DSC data, and the degrees of crystallinity α were calculated from the density (Table 8). The α values varied from 43% to 80%. An increase in α was accompanied by an increase in not only the melting point but also the piezoelectric constant e (upon poling for 30 min in a field of 20 MV m^{-1}). The electrostriction constant k changed especially sharply (by an order of magnitude). The changes in the dielectric constant ε' confirmed the character of the variation of α (the crystalline phase has lower ε').

Table 8. Physical properties of the 80/20 VDF/TFE copolymer samples crystallised under various conditions.[140]

ε' (10 Hz)	k (10 Hz)	$e \times 10^{-3}$/ C m^{-2}	T_m /°C	α (%)
10.3	−0.2	3.7	128	43
9.5	−1.0	4.6	140	60
7.6	−2.0	10.2	142	80

Figure 31*a* shows the curves for the polarisation current in the samples studied. It can be seen that, as α increases, the curve narrows down and shifts to lower fields. This points to a decrease in the coercive field. These curves were used to calculate the remanent polarisation. Both values are presented as functions of the degree of crystallinity in Fig. 31*b*. It can be seen that the plots are linear but variations of the two values are antiparallel; as α increases, P_r increases and E_c decreases. The former finding appears quite natural if ferroelectric properties are considered to originate from the crystalline phase. By extrapolating $P_r(\alpha)$ to $\alpha = 1$, one can find the P_r value for the crystals. It is equal to 84 mC m^{-2}. The relationship between P_r and the spontaneous polarisation P_s for isotropic samples can be represented as [140, 141]

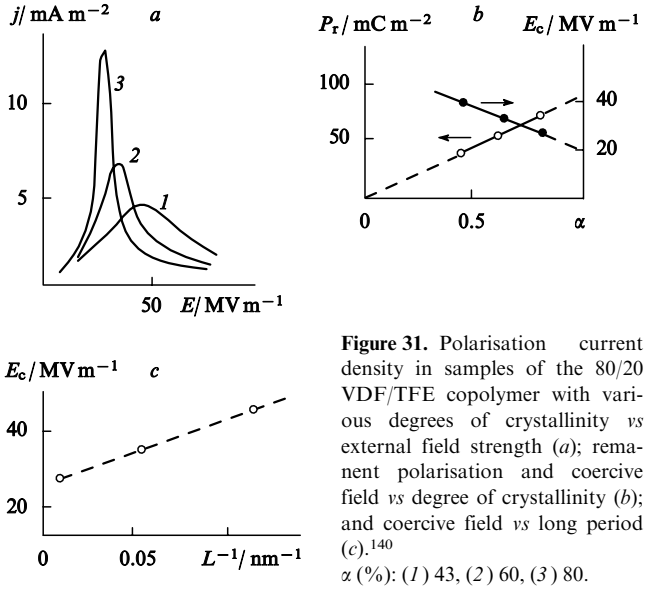


Figure 31. Polarisation current density in samples of the 80/20 VDF/TFE copolymer with various degrees of crystallinity *vs* external field strength (*a*); remanent polarisation and coercive field *vs* degree of crystallinity (*b*); and coercive field *vs* long period (*c*).[140]
α (%): (*1*) 43, (*2*) 60, (*3*) 80.

$$P_r = P_s[1 - \langle \cos^2\theta \rangle], \quad (41)$$

where θ is the angle between the field direction and the chain axis. In this particular case, $\langle \cos^2\theta \rangle = 1/3$; hence, the P_s value for the crystal is 126 mC m^{-2}. This is close to the value (140 mC m^{-2}) calculated from the relation[140]

$$P_s = \left(\frac{\varepsilon + 2}{3}\right) \langle \mu \rangle N \alpha F, \quad (42)$$

where $\varepsilon = 3$ is the dielectric constant of the crystal, $\langle \mu \rangle = 2.1$ D is the dipole moment of the CF_2 group, $N = 1.4 \times 10^{28}$ m^{-3} is the concentration of dipoles calculated based on the lattice parameters, $F = 0.9$ is the fraction of bonds formed in the normal ('head-to-tail'[28]) fashion.

The decrease in the coercive field with an increase in the degree of crystallinity can be accounted for qualitatively by the high dielectric constant of the amorphous phase. This diminishes the field which really acts on the crystals, if they are assumed to be immersed into a disordered phase matrix. As the degree of crystallinity increases, the matrix should be reversed; thus, the crystals become located in an external field, which decreases the observed E_c.

A relationship has been found between the E_c value and some characteristics of the morphology of crystals of the ferroelectric phase.[140] It was found by scanning electron microscopy that in samples crystallised at 500 MPa, 150–250-nm thick lamellae, typical of extended-chain crystals (ECC), are formed. The low-angle X-ray scattering technique showed that the values for the long period L are also correlated with the α values; for samples with $\alpha = 0.43$ and 0.60, the L values are 8–12 and 30 nm, respectively. The variation of E_c as a function of $1/L$ was found to be linear (Fig. 31*c*); therefore, the magnitude of the coercive field for a hypothetical sample with an infinitely thick lamella can be calculated. This correlation can also be helpful in elucidating the role of specific defects of polymeric crystal folds in the mechanism of generation of ferroelectricity. It is assumed that the proportion of the folded areas in the crystal decreases as the large period increases; this creates more favourable conditions for the rearrangement of the dipole structure under the influence of an external field. This assumption is substantiated because near folds, the directions of the bond dipole moments vary continuously. This fact, together with the fact that specific defects of the 'entanglement' type can arise in these regions, hamper cooperative rearrangements in an electric field.

The dependence of the remanent polarisation on the volume fraction of crystals and the details of morphology can be followed by examining the data on the influence of annealing on the structural and ferroelectric characteristics of PVDF films.[142, 143] For this purpose, uniaxially stretched films were used in which crystals occurred in the ferroelectric β-phase. The annealing was carried out under isometric conditions in order to prevent film shrinkage and crystal disorientation. Annealing at a temperature above 100 °C causes substantial changes in the crystal structure. The decrease in the half-width ($\beta_{0.5}$) of the principal intermolecular reflections of the β-phase, 200 and 110, indicates a substantial increase in the transverse dimension of the crystal and/or its perfection. The shift of these reflections to greater angles points to an increased density of packing of the chains in the crystal. The remanent polarisation virtually does not depend on the above structural parameters because it does not change up to $T_0 = 160$ °C. A sharp increase in P_r (from 56 to 85 mC m^{-2}) is observed only upon annealing in the temperature range 170–180 °C, *i.e.* in the range of pre-melting of the PVDF crystals. The appreciable increase in P_r observed under these conditions can be attributed to an increase in the degree of crystallinity (from 45 to 68%).[142] Unfortunately, this has not been verified by direct methods. It can only be noted that the observed increase in P_r does not contradict the hypothesis [140] concerning the role of crystal folds. In fact, high-temperature annealing should be accompanied by melting of small (imperfect)

crystals. Since annealing proceeds under conditions of external stress, recrystallisation processes can be accompanied by the formation of new crystals including extended-chain crystals, *i.e.* the concentration of specific defects of lamellar crystal folds can diminish, which is favourable for the P_r values.

The increase in the perfection of the crystal structure upon annealing at 100–160 °C, established by the X-ray diffraction method,[142] does not influence the P_r value but limits the dynamics of the polarisation switching process. Thus the time of switching τ_s at −20 °C (in a field of 200 MV m^{-1}) amounts to 67.0 μs for the initial sample and becomes 52.4 or 41.3 μs after annealing at 120 or 160 °C, respectively.[143] A more detailed analysis shows that better packing of chains in the crystal results mainly in an increase in the rate of growth of the domain boundaries.[143]

One of the approaches used to modify the polymer structure and molecular dynamics is plasticisation of polymers.[144–146] In the case of crystallisable polymers, the introduced plasticiser (low-molecular-mass compound) is accumulated in amorphous regions, *i.e.* in sites characterised by an increased fraction of the free volume and decreased intermolecular interaction. It is of interest to follow the role of a plasticiser in the variation of the ferroelectricity characteristics. Tricresyl phosphate (TCP) was used as the plasticiser; it was introduced into a finished PVDF film at 130 °C in an amount of 5.5 mass % (see Ref. 145) or 1 mass % (see Ref. 146). The former study was devoted to the influence of the plasticiser on the field-induced α → β transformation in isotropic PVDF films crystallised in a nonpolar α-phase.[28] The proportion of the polar β-modification arising was found to be much higher in the plasticised films under the same poling conditions.[145] The variation of the chain packing density in the ferroelectric phase was followed in relation to textured films with the β-phase oriented after treatment in a strong field. Comparison of the data on plasticised and non-plasticised films showed that in the former case, the polarisation-induced shifts of the principal intermolecular reflections, 200 and 110, of the β-phase to higher angles proved to be greater than those for the non-plasticised film. This was unambiguously attributed to the presence of the plasticiser because an increase in its concentration caused a regular shift of this reflection.[145]

The effect of the same plasticiser on the remanent polarisation has been studied using characteristics of $D-E$ hysteresis and thermodepolarisation currents. Even upon slight doping of PVDF films (the TCP content was 1 mass %), an increase in P_r was noted. This influence was more pronounced at low polarisation fields; at 60 mV m^{-1} and 20 °C, the addition of TCP resulted in an increase in P_r from 1 to 6 mC m^{-2}. The role of the plasticiser at high fields is less significant: at 200 MV m^{-1}, the the P_r value increases upon doping from 57 to 66 mC m^{-2}.[146] These data demonstrate that the disordered phase plays a special role in the mechanism of formation of ferroelectricity in PVDF. The plasticiser most probably affects characteristics of the chain dynamics in the amorphous phase, especially at the boundaries with the crystals. The weakening of the interchain interaction in the sections with TTC should enhance the micro-Brownian mobility of chain segments. In this case, the crystal growth can be completed by some of the chains from the disordered phase; this must occur by an epitaxial mechanism. The increase in the proportion of the crystalline phase results in higher P_r values.

When considering the important role of the degree of crystallinity in the formation of ferroelectric characteristics of PVDF and VDF copolymers, one should not ignore other, equally significant, structural factors. When P_s remains constant, P_r can increase due to variation of $\langle\cos^2\theta\rangle$ [see relation (41)]. An increase in P_s can formally be attained by texturing an isotropic sample ($\langle\cos^2\theta\rangle = 1/3$) by uniaxial or biaxial stretching. According to X-ray diffraction data, the axes of macromolecules are arranged predominantly along the axis of tension within the plane of the film. The field is always directed at a right angle to the film plane, which implies a decrease in $\langle\cos^2\theta\rangle$ and an increase in P_r.

The validity of the foregoing is confirmed, for example, by comparing the characteristics of the $D-E$ hysteresis in isotropic and textured films of VDF/TFE and VDF/TrFE copolymers, which always crystallise from the melt as the ferroelectric β-phase. The transition from the isotropic state to the textured state should be accompanied only by variation of the θ angle and should not be complicated by polymorphic transitions of the α → β type as in the homopolymer.[28] This idea was verified for 94/6 [32] and 71/29 VDF/TFE.[28] It was found that the texturing process is really accompanied by an increase in P_r and also by a decrease in the coercive field.[28] The parameters of the $D-E$ hysteresis in the films of VDF/TrFE copolymers with compositions 52/48, 65/35 and 73/27 have been compared.[147] The films were obtained by extrusion followed by rolling. The extruded films are characterised by slight crystal orientation; therefore, $\langle\cos^2\theta\rangle$ for these films would be close to that for isotropic samples. Rolling of the films between rolls is equivalent to a sort of uniaxial or biaxial stretching and brings about a clear-cut texture, which should substantially change the $\langle\cos^2\theta\rangle$ value. The ferroelectric characteristics of these films are listed in Table 9.

Table 9. Remanent polarisation, coercive field and piezoelectric constant e_{31} in rolled (I) and extruded (II) films of VDF/TrFE copolymers with a crystalline phase fraction of 41%.[147]

Composition	P_r / mC m^{-2} (see [a])		E_c / MV m^{-1}		P_r / mC m^{-2} (see [b])		e_{31} / mC m^{-2} (see [b])	
	I	II	I	II	I	II	I	II
52/48	76	57	32	36	102	66	51	25
65/35	44	81	39	47	–	–	–	–
73/24	25	62	34	43	–	–	–	–

Note. The P_r and E_c values were found from characteristics of the $D-E$ hysteresis.

[a] Poling in the corona discharge at room temperature.

[b] Contact poling at elevated temperatures.

It can be seen that the behaviour of the 52/48 copolymer is qualitatively similar to that of VDF/TFE copolymers, *i.e.* rolling results in higher P_r values and somewhat lower coercive fields compared to those before rolling. This is manifested especially clearly in the case of films prepared by contact poling at elevated temperatures, for which P_r (and, consequently, e_{31}) differ by a factor of ∼2. The data obtained for copolymers with higher VDF contents are contradictory; on passing from an extruded film to a rolled film, E_c changes as in the previous case but the variation of P_r shows an abnormal pattern. Unfortunately, the researchers cited[147] offer no explanation for this finding. This abnormal variation is surprising because the influence of the degree of crystallinity on P_r should not work in this case (the samples had equal proportions of the crystalline phase).

The relationship between the type of texture in the materials in question and the parameters of ferroelectricity has not been adequately studied. This can be illustrated, for example, by the data on $D-E$ hysteresis of biaxially and uniaxially stretched PVDF films.[148] The former film contained crystals of both polar (β) and nonpolar (α) phases and the latter film contained only crystals of the ferroelectric phase. An increase in the number of cycles of $D-E$ hysteresis for the former film was accompanied by an increase in both P_r and P_s, which is observed most frequently for polarisation of PVDF films. This can be caused to some extent by field-induced polymorphic transformations of the α → α_p and α → β types.[28] The P_r and P_s values of the latter film decreased as the number of polarisation cycles increased. This finding was explained [148] by the somewhat speculative assumption that the field induces additional crystallisation of chains of the amorphous phase and this changes the ratio of the characteristic sizes of crystals and, hence, also changes the depolarisation factor.

The previous thermal history of texturing is a very important circumstance influencing the ferroelectric characteristics.[149] An increase in the temperature of uniaxial stretching is accompanied by a regular increase in the large period. The interlamellar layers are packed less densely due to a higher content of defective conformations, $TGTG^-$ and $T_3GT_3G^-$.[28,131,149] The remanent polarisation in these films is several times lower.[33] The important role of the amorphous phase in the generation of ferroelectricity in VDF/TrFE copolymers has been pointed out in a series of studies,[150–153] in which the Curie transition has been studied by Brillouin[150,151] and non-coherent neutron scattering.[152] The attention is focussed on the dynamics of chains in this phase because near the Curie transition, the cooperative mobility with great amplitudes is characterised by reorientation frequencies of more than 10^5 Hz.[28,153] It has been shown in relation to the 65/35 VDF/TrFE copolymers[154] that it is in oriented films that the parameters of several reflections of the ferroelectric crystals change markedly in the switching processes, whereas no changes are observed in isotropic films. Orientation is known to increase substantially the probability of formation of TTC.[155] The dynamics of the latter should be characterised by low relaxation times. As a consequence, the response of polar segments in such chains to an external electric field should initiate switching of the dipole moments of domains in the crystal. Therefore, the microstructure of the amorphous regions, especially at the boundaries with the crystal, should be taken into account in the mechanism of formation of ferroelectricity.

Identification of defects in ferroelectric crystals and elucidation of their influence on the ferroelectric characteristics of the polymers studied is an important problem. Some of the defects are entirely due to the character of macromolecules and generally cannot be eliminated. These defects can be represented, for example, by chain ends, which are located inside the crystal, and folds, typical of lamellar crystals of polymers. Some features of polymerisation of the compounds in question account for the appearance of the chemical defect caused by the 'head-to-head' attachment, which can be incorporated in the crystal bulk.[28] For crystals of the nonpolar α-phase, specific defects are also possible, consisting in different arrangements of chains in the lattice according to the 'up' and 'down' type.[28] In the interchain interactions, this can result in conformational rearrangements according to the $TGTG^- \rightarrow GTG^-T$ pattern. When the temperature increases, the equilibrium between these isomers shifts and, hence, the ordered phase passes into the 'condis' crystal state.[156] This transition is detected in the 47–77 °C range as a weak endothermic peak (with an enthalpy of 150–200 J mol^{-1}) in the heating cycle in DSC experiments.[156] This type of interaction is believed to be also responsible for dielectric relaxation,[28] which occurs in the crystalline phase of PVDF with α-modification.[157] At higher temperatures, this type of defect initiates conformational transitions of the $TGTG^- \rightarrow T_3GT_3G^-$ type and promotes the high-temperature $\alpha \rightarrow \gamma$ phase transition.[28,158,159] On exposure to strong electric fields of PVDF films crystallised as the α-phase, several new reflections were found,[160] which could not be assigned to any of the known polymorphic modifications (α, β, γ or α_p).[28] The appearance of a new superlattice for a conformationally non-commensurate form of PVDF is attributed to the interaction of the field with conformational defects of the type considered above.[160]

Some details of the ferroelectric–paraelectric transition can be followed by comparing X-ray and spectroscopy data. In the case of oriented PVDF crystallised as the ferroelectric β-phase, the appearance of an additional blurred reflection near the identified 001 reflection is interpreted as being due to the conformational defect of the kink-bond type,[161] *i.e.* local bonds in the $TGTG^-$ conformation appear in the crystal, while the majority of chains occur in the planar zigzag conformation.[162] Defects of this type can be found in both VDF/TFE[131,163,164] and VDF/TrFE copolymers.[67] These defects can be especially significant for the Curie transition, which is really confirmed by the temperature dependences shown in Fig. 16 and in Table 10. It can be seen that the transverse dimension of the crystal l_c remains virtually unchanged up to a temperature of 120 °C. However, the decrease in the concentration of bonds occurring in the *trans*-conformation starts well before 120 °C.

Table 10. Values of the long period L, the transverse dimension of the crystal l_c, the size of amorphous layers l_a and the degree of crtystallinity α for 70/30 VDF/TrFE films at various temperatures.[165]

T/ °C	L/ nm	l_c/ nm	l_a/ nm	α (%)
115	26.9	13.4	13.5	50
117	27.2	13.7	13.3	51
120	27.2	14.4	12.8	53
125	29.0	16.0	13.0	55
130	31.0	18.0	13.0	58
135	35.0	20.0	15.0	58

Thus, the lattice rearrangement at the Curie point (~120 °C) is preceded by smooth accumulation of conformational defects, which occurs most likely as a thermally induced fluctuation process. The smooth changes in the microhardness of this copolymer can be due to the same process.[165] The rearrangement of the polar phase lattice into the lattice of the nonpolar phase might take place at a certain critical concentration of kink bonds (conformational defects) in the ferroelectric crystal. Above the Curie point, the crystals of the paraelectric phase start to grow noticeably and, simultaneously, the degree of crystallinity increases (see Table 10). The latter is due to the fact that some chains of the disordered phase are incorporated in the crystal by the mechanism of diffusion movement of defective bonds, which are laid on the surface of a new crystal. This process is expected to be facilitated by the similarity of the conformations in the amorphous phase and in the paraelectric crystal.

The 'memory' effects have been studied in relation to the 75/25 VDF/TrFE copolymer in the vicinity of the Curie transition.[166–168] Analysis of the plots presented in Fig. 32 helps us to understand the essence of this effect. It can be seen that the ferroelectric phase (the reflection on the side of greater angles) and the paraelectric phase (the reflection on the side of smaller angles) coexist near the Curie point.

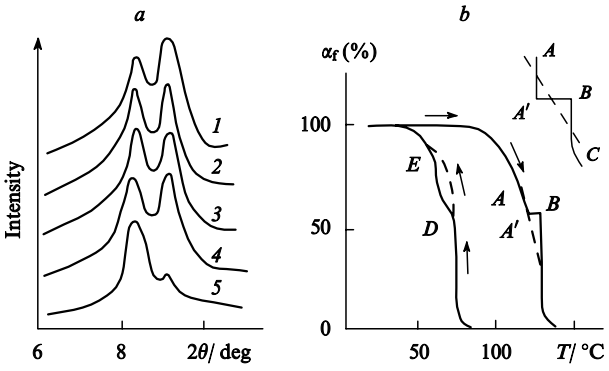


Figure 32. Character of the variation of the diffraction maxima in the vicinity of the Curie transition (*a*) and temperature dependences of the degree of the ferroelectric transition (α_f) (*b*) in 75/25 VDF/TrFE films.[168] T/ °C: (*1*) 120 (point *A*), (*2*) 120 (point *A′*), (*3*) 123, (*4*) 126, (*5*) 129.

Isotropic films prepared by quenching from the melt were studied. The rate of heating in the experiment was 2 K min^{-1}, the isothermal maintenance at each point was 30 min, and the maintenance at 120 °C (annealing) was carried out for 19 h and after that, the X-ray diffraction patterns were recorded. The annealing was accompanied by a marked decrease in the intensity of the reflection for the ferroelectric phase (see Fig. 32*a*). The

fraction of the ferroelectric phase remaining near the transition can be estimated from the intensity ratio of the two reflections (Fig. 32*b*). The change in the content of the ferroelectric phase upon annealing is marked by points A and A'. It can be seen that prolonged storage at 120 °C is accompanied by a change in the shape of the phase diagram curve; point A passes into A' instead of the movement along the trajectory shown by the dashed line. The subsequent temperature variation does not change the fraction of the ferroelectric phase ($A'B$ section). Only at point C, is the character of the phase diagram restored. When the curve is recorded in the cooling regime, in addition to the hysteresis noted previously, the shape of the curve changes at point D (which corresponds to point A' regarding the phase ratio). The initial shape is restored at point E, reflecting the 'memory' effect in the system. Similar effects are also observed in inorganic ferroelectrics with incommensurate crystal structures; they are explained by interaction of mobile defects with the domain walls.[169]

In the case of the polymer systems considered here, the incommensurability is determined by different chain conformations in the two phases; therefore, there are prerequisites for the memory effect. Judging by sections AA' and BC of the phase diagram, some relaxation processes occur in the crystalline phase and ensure transition of the system into an equilibrium state. These processes (which are described, in all probability, by an exponential law[168]) might also be responsible for the unusual influence of the heating rate on the temperature of the Curie transition in VDF/TrFE copolymers.[170, 171] The presence of these processes is confirmed by the study of the longitudinal acoustic mode (LAM), discovered in the crystals of VDF/TrFE copolymers in the frequency region of $10-20$ cm^{-1} (see Ref. 172). The characteristics of the LAM show that, as the proportion of TrFE in its copolymers with VDF increases, the libration frequency in the ferroelectric crystal decreases virtually linearly as a function of the average interchain distance.

The LAM bands for the copolymers considered here are poorly observable compared, for example, to those for polyethylene (PE).[173] This was attributed to the low degree of orientation in the copolymers, where the draw ratio was only 4, whereas in PE it reached 20. The poor orientation accounts for a broad distribution of the lamellae over thicknesses, resulting in appreciably broadened LAM bands.

The LAM characteristics were used to determine the sound velocity and the elastic constant c_{33} for a ferroelectric PVDF crystal. This polymer contains ~ 50 Å-thick lamellae; hence, based on the LAM frequency found and with the assumption of the half-wave resonance, the sound velocity in the crystal of the PVDF β-phase is $v_c = 7500$ m s^{-1}. If we assume that the crystal density $\rho_c = 1.97$ g cm^{-3} (see Ref. 28), then $c_{33} = \rho v_s^2 = 110$ GPa, which is comparable with this constant for the polyethylene crystal.

The elastic constants of the disordered phase have been estimated in terms of the two-phase model.[172] They were 3.6 and 2.6 GPa for temperatures 27 and 87 °C; these values correspond to sound velocities of 1450 (27 °C) and 1250 m s^{-1} (87 °C).

As the Curie point is approached, both phases (crystalline and amorphous) are 'softened' in similar ways: $\Delta v_{s\,cr}/v_{s\,cr} = -22\%$ and $\Delta v_{s\,a}/v_{s\,a} = -14\%$. This can serve as one more piece of evidence supporting the hypothesis of the strong connection between the chain dynamics in the disordered phase and characteristics of the Curie transition in the crystal.

The higher the temperature of crystallisation, the larger and the more perfect the crystals formed. When the crystals are formed in the paraelectric phase, they are less perfect. If crystallisation occurs at temperatures below T_C, the resulting ferroelectric crystals should be smaller and more perfect than those formed in the paraelectric phase. Hence T_C is determined by two factors acting in the opposite directions. A study has been devoted to verification of this hypothesis.[171] It was shown that an increase in the crystallisation temperature is accompanied by an increase in the melting point (indicating the formation of larger crystals) but in this case, the Curie point in the cooling regime decreases abnormally.

Similar conclusions have been drawn from the analysis of the Curie transition characteristics in the heating regime. The DSC curves for two copolymer samples obtained by fast quenching and by slow cooling of the melt were compared. The latter crystallisation mode in polymers is normally accompanied by a decrease in the fraction of the disordered phase and by crystal growth. Simultaneously, the melting point regularly shifts to higher temperatures. However, the Curie transition (in the heating regime) again shifts abnormally to lower temperatures. It was shown[171] that crystals of the ferroelectric phase in samples with different previous thermal history are almost identical in size. This means that displacement of the Curie point in these samples cannot be explained by the change in the crystal geometry alone.

A similar variation of T_C observed for VDF/TrFE films prepared by crystallisation from solutions in solvents having different affinities to the TrFE groups is due to different concentrations of these groups in ferroelectric crystals.[174] The same might be responsible for this phenomenon observerd in the above experiments. The co-monomer TrFE can be regarded as a defect in the PVDF chain. It is known that 'head-to-head' type defects can occur in PVDF crystals;[28] therefore, TrFE sections should also be incorporated in the ferroelectric phase. Since the thermodynamic flexibility of TrFE chains is lower than that of PVDF chains, it takes a long period of time for the former to be incorporated in the crystal. When the cooling rate is high (or the crystallisation temperature is low), it may happen that diffusion processes do not ensure, for kinetic reasons, the equilibrium number of TrFE groups in the crystal. Therefore, their concentration in the crystal may prove to be lower than the average concentration along the chain. Thus, the crystal becomes enriched in the VDF groups, which are responsible for the ferroelectricity. A decrease in the proportion of TrFE in the copolymer is known to result in all cases in higher Curie points. Thus, the Curie transition in the ferroelectric crystals obtained by fast quenching (or by crystallisation at lower temperatures), which are depleted of the TrFE groups, should be shifted to higher temperatures, which is actually observed in the experiments.

To understand the mechanism of ferroelectricity, it is significant to elucidate the role of crystal defectiveness. This problem was considered in relation to the 65/35 VDF/TrFE copolymer.[154] The data listed in Table 11 demonstrate how the transverse dimension and the second-kind defectiveness of the crystal, estimated from known relations (see, for example, Ref. 175), change upon polarisation. An increase in the polarising field leads mainly to an increase in the coherence length of the crystal and to a slight increase in the degree of its perfection.

Table 11. Coherence length of the crystal (l_{110}) in the ferroelectric (LT) and paraelectric (HT) phases and the second-kind defectiveness (g) in the LT phase upon polarisation of 65/35 VDF/TrFE films.[154]

E/ MV m^{-1}	l_{110}/ nm		g
	LT phase	HT phase	
0	13	57	–
60	19	–	0.034
90	33	–	0.032
200	39	–	0.030

These processes are equivalent to an increase in the degree of crystallinity. The mechanism of this phenomenon assumes conformational rearrangements of the $TGTG^- \rightarrow (TT)_n$ and $T_3GT_3G^- \rightarrow (TT)_n$ types in the amorphous phase of the polymer. The additional incorporation in the crystal of sections with the planar zigzag conformation can be responsible for the increase in the coherence length after polarisation noted above.

This is confirmed to a degree by the results of a study by Latour and Moreira, [176] who found that polarisation of similar VDF/TrFE copolymers results in an increase in the intensity of the libration mode (~ 70 cm^{-1}) for the crystal in which the chains occur in a planar zigzag conformation.

Structural changes occurring during polarisation switching have also been studied for non-oriented films of the same copolymers.[154] The researchers noted that the extreme points are located in the regions where electric induction D reaches a virtually equilibrium value rather than in the regions characterised by the maximum rate of its variation. In experiments, an increase in the polarising field shifts the $D(t)$ curve to shorter times. The position of the minimum on the time dependence of the peak intensity varied in a similar way; however, in all cases, the minimum fell within the final stage of the switching process.[28] The resulting correlations were interpreted taking account of various ways of formation of new (switched) domains. If the old and the switched domains are coherent (and the fraction of switched domains is χ), the intensity of a reflection is determined by the expression

$$I = (1-\chi)|F|^2 + \chi|F^*|^2 \simeq |F|^2,$$

where F and F^* are structural factors of the old and new domains, respectively, which should be close because the type of the lattice remains the same. If the domains are non-coherent, then

$$I = |(17w)F + wF^*|^2 \leqslant |F|^2.$$

Thus, the assumption that the originating domain is not coherent with respect to the old one accounts for the decrease in the intensity of the 110 reflection observed experimentally. This decrease takes place if the new domain is rotated with respect to the old one (see Fig. 5). In all probability, the model with 120- or 180-degree rotation of the chain is realised. The latter is preferable because it requires that the boundary between the domains be located at the 100 planes, whereas for the 120-degree rotation, the 310 planes should be involved. [155]

When the chain rotates through 180 °, the hydrogen atoms go into the places of fluorines. The stress arising in the lattice can be diminished if the chain is translated by $c/2$ along the axis. Nevertheless, the 001 and 002 planes are distorted at the site of contact of the old and new domains. If the chains in two adjacent nascent domains are translated by $c/2$ in the opposite directions, the distortions are appreciably diminished. Thus, joining of two domains does not require translational motion of the chain in the arising new lattice with a new position with respect to the field.

It has been noted above that polarisation results in a threefold increase in the transverse dimension of the β-phase crystal in the VDF/TrFE copolymer (see Table 11). For a similar copolymer with the composition 75/25, this fact has also been confirmed by DSC.[177] The intensity of the low-temperature peak, which is attributed to the Curie transition, increases markedly after polarisation. Upon annealing at a temperature above 128 °C after polarisation, the intensity of this peak decreases. The electron diffraction and IR spectroscopy data [178] do not show any changes in the lattice parameters or chain conformations, while changes in the domains do occur. After repeated annealing, a disproportion occurs in the narrow temperature range, 127 – 129 °C, namely the remanent polarisation or electromechanical coupling coefficient (K_t) is already equal to zero,[179] whereas ferroelectric crystals are still present (the enthalpy of the Curie transition, $\Delta H \neq 0$). To eliminate this contradiction, it has been assumed [177] that rearrangements take place in ferroelectric crystals in this narrow temperature range (before transition to the paraelectric phase). As a result of chain rotation, in some domains, sub-domains are formed (without changes in the lattice parameters and chain conformations), in which spontaneous polarisation points to the opposite direction. Generally, this gives a zero remanent polarisation when ferroelectric crystals are still retained.

It has been shown in relation to the VDF/TFE copolymer [140] that crystallisation at elevated pressures is accompanied by the formation of thick (150 – 250 nm) lamellar crystals. These samples are also characterised by high remanent polarisation. Thus, it is clear that the P_r value is correlated with the morphology of the ferroelectric crystals formed. These correlations for VDF/TrFE copolymers have been considered in a series of studies. [180 – 186] In one study, [181] the problem of structurisation in copolymers with high VDF contents, 86.88 mol.% and 94 mol.%, has been considered. These objects are of interest because, on the one hand, high temperatures of the Curie transition should be expected for these VDF proportions (this is important for the practical implementation of energy converters), and, on the other hand, crystallisation as the nonpolar α-phase is possible in this case.[28] This brought about the need to establish the details of the structurisation of the copolymers in question and to identify their role in the variation of ferroelectric characteristics.

The films were prepared from a solution in dimethylformamide and annealed at a temperature (T_h) somewhat below the melting point. The structural characteristics were analysed using X-ray diffraction methods, IR spectroscopy, and electron diffraction. The morphology of the resulting crystals was studied by optical and electron microscopy. The copolymers under study can be described by the general formula $(VDF)_x(TrFE)_{1-x}$; the type of the morphology depends substantially on the x value. For $0.82 \leqslant x \leqslant 0.9$, this preparation technique always yielded thick lamellar crystals with dimensions ~ 0.1 μm, which has been noted previously for copolymers with $0.6 \leqslant x \leqslant 0.82$. [178] In the case of copolymers with $x = 0.94$, thick lamellae are formed only upon high-pressure crystallisation ($\sim 100 - 500$ MPa); crystallisation under standard conditions results in spherulite morphology, typical of the PVDF α-phase.[28] Analysis of X-ray diffraction data shows that thick lamellae are formed by crystals of the α-, β- and, perhaps, even γ-phase. For copolymers with $x \geqslant 0.9$, the

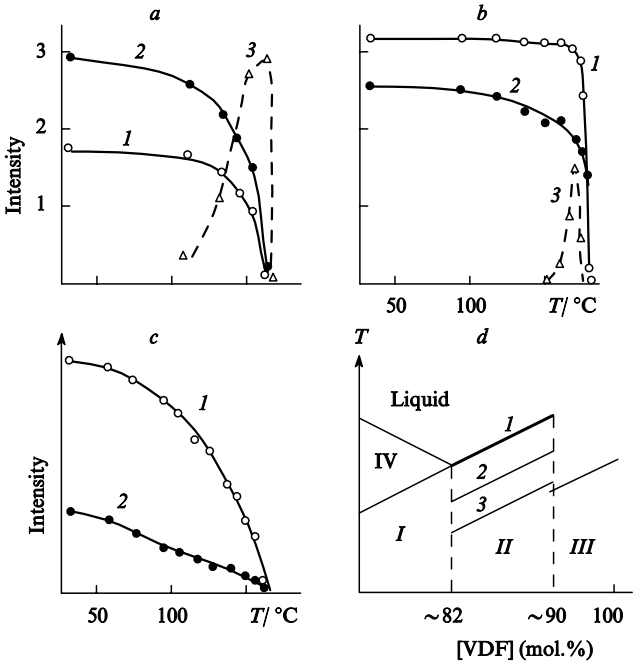


Figure 33. Temperature dependences of the X-ray reflection intensities for isotropic (*a*, *b*) and uniaxially stretched (*c*) films of the 88/12 VDF/TrFE copolymer before (*a*) and after (*b*, *c*) polarisation and the phase diagram for copolymers with high VDF fractions (*d*);[181]
(*a*): (*1*) β-phase, the coinciding 200 and 110 reflections; (*2*) α-phase, the 101 reflection; (*3*) rotator phase; (*b*, *c*): (*1*) β-phase, the 200 and 110 reflections; (*2*) β-phase, 001, 310, 020; (*3*) rotator phase; (*d*): transitions: (*1*) β-phase → liquid, rotator phase → liquid; (*2*) γ-phase → rotator phase; (*3*) α-phase → rotator phase; *I* — β-phase, thick lamellae; *II* — a mixture of α-, β-, and γ-phases, thick lamellae; *III* — α-phase, spherulites; *IV* — rotator phase.

spherulites are formed by the crystals of the α-phase (Fig. 33). The morphology is very significant for the stability of the crystals formed from copolymers of the same composition. This is demonstrated by the comparison of the temperature dependences of the intensities of the X-ray reflections of films incorporating lamellar crystals and thin fibrils, obtained by annealing and uniaxial stretching (Fig. 33*a*, *b*). It can be seen that in the former case, noticeable decrease in the intensity of the principal intermolecular reflections of the β-phase, 200 and 110, starts only at ~100 °C, while in the latter case (oriented films), it starts nearly at room temperature. A special role in this stability is played by film polarisation processes. After polarisation, the intensity of the 200 and 110 reflections does not change up to 150 °C (Fig. 33*b*). Detailed analysis shows that a polymorphic transition of the $\alpha \rightarrow \beta$ type occurs in the polarisation cycles; this was detected relying on the typical change in the intensity ratio of reflections of the α- and β-phases and characteristic absorption bands in the IR spectra.[181]

The presence of a rotator phase is an important feature of thick lamellar crystals, which manifests itself at elevated temperatures (see Fig. 33*a*, *b*). This phase is responsible for a reflection with the angle position $2\theta \simeq 18°$; therefore, it may be a modification of the paraelectric phase. The region in which the rotator phase is displayed depends on the structural features of the sample. This becomes clear upon comparison of the curves shown in Fig. 33*a*, *b*. In the initial sample, the lamellae contain a mixture of crystals of α- and β-modifications, which is confirmed by X-ray diffraction and spectroscopic data. In this case, the rotator phase starts to appear even at 100 °C and is retained up to the melting point. After polarisation, this phase appears only at ~150 °C, the region of its existence being markedly narrower. After polarisation, the α-phase transforms into the polar β-modification and the intensity of bands responsible for the $TGTG^-$ conformation in the IR spectra substantially decreases.[181] Thus, the presence of α-phase regions (mixed with the β-phase) and the presence of conformational defects as sections of a helical conformation, with the planar zigzag being the major conformation, facilitate the appearance of the rotator phase.

High contents of VDF in copolymers with TrFE cause a number of structural features (Fig. 33*d*). If $x \leqslant 0.82$, a standard phase diagram is observed, *i.e.* on heating, the ferroelectric phase is converted into the paraelectric phase and then into the melt. For the $0.82 \leqslant x \leqslant 9.90$ region, in which thick lamellae are formed by crystals of α-, β- and γ-modifications, a multiplet character of transitions should be expected. As the temperature increases, the α-modification crystals are the first to pass into the rotator phase; they are followed by the γ-phase and then by the β-phase. The validity of this scheme is supported by the fact that endotherms for three transitions can be seen in the thermograms of the 88/12 copolymer.[181] Some additional electrophysical data for the copolymers in question are listed in Table 12. It can be seen that all the samples with the morphology of thick lamellae are characterised by very high remanent polarisations, and, correspondingly, the electromechanical coupling coefficient. The increase in the VDF proportion in the copolymer is accompanied by a regular increase in the coercive field, as has been noted above. By comparing the E_c values for samples with $x = 0.81$, one can elucidate the influence of the texturing factor on E_c. Orientation of the film decreases E_c, which has also been noted in analysis of the results of other studies.[28] The piezoelectric constant d_{31} in textured films is, on average, more than twice as high as that for isotropic samples. However, the sound velocity is somewhat greater in the latter case. If the sound velocity is determined from the relation

$$\upsilon_s = \sqrt{\frac{c}{\rho}},$$

(c is the elasticity modulus, ρ is the substance density), it turns out that isotropic samples possess lower compliance ($1/c$) than oriented ones. This circumstance may be reflected in the features of the piezoelectric response of textured films.

Table 12. Electrophysical characteristics of isotropic and oriented films of VDF/TrFE copolymers after annealing at a temperature of T_h and poling in the field E.[181]

[VDF] (mol.%)	T_h / °C	E [a]	K_t	P_r / mC m^{-2}	E_c (see [a])	υ_s / km s^{-1}	d_{31} / pC N^{-1}
Isotropic samples [b]							
81	140	100	0.29	120	39	2.42	9.4
86	156	130	0.25	110	44	2.58	8.5
88	160	110	0.22	100	48	2.48	8.0
94	160	110	0	0	–	–	–
Oriented samples [c]							
81	140	75	0.28	95	31	2.36	8.9
86	154	72	0.16	–	–	2.24	18.0
88	160	80	0.18	–	–	2.13	19.0
94	150	81	0.19	–	–	2.27	20.5
100	170	101	0.20	–	–	2.30	25.0

[a] Expressed in MV m^{-1}. [b] Poling in an alternating field (triangular pulses with a frequency of 10^{-2} Hz) at room temperature. [c] Poling in a static field at 120–140 °C.

Some details of structural transformations in the same copolymers with high proportions of VDF were elucidated in a study,[182] in which crystallisation was carried out at high pressures and thus the morphology of thick lamellar crystals was ensured. The results of studies of ferro- and piezo-electric properties of these copolymers are presented in Table 13. For comparison, data for one copolymer crystallised at normal pressure are also given in the Table. It can be seen that for copolymers with VDF contents of at least 86 mol.%, the Curie point (T_C) proves to be higher than the melting temperature (T_m). On the one hand, this can be interpreted as being due to the large thickness of lamellar crystals. On the other hand, it can be seen that the morphology of ferroelectric crystals has no influence on the pattern of dependence of the coercive field on the copolymer composition. As in the case of other crystallisation methods, an increase in the proportion of TrFE regularly shifts E_c to lower values. However, some facts cannot be explained. For example, the P_r and, hence, the K_t values for all films crystallised at elevated pressures prove to be lower than those for samples crystallised at a pressure of 0.1 MPa. The reason for this fact is not entirely clear. To interpret this abnormal feature, Ohigashi *et al.*[182] assumed, without adequate substantiation, that high-pressure crystallisation affords less perfect crystals. A practically valuable conclusion was drawn in this study, namely, the morphology of thick lamellar crystals can be used to produce energy converters based on the copolymers considered here with an extended temperature range of operation. This was confirmed by the data on the pulse echo signals from the 86/14 copolymer at 165 °C.

Table 13. Ferro- and piezo-electric characteristics of VDF/TrFE crystallised at high pressures.[182]

[VDF] (mol.%)	T_m / °C	T_C / °C	E_c / mV m^{-1}	P_r / mC m^{-2}	K_t	υ_s / km s^{-1}
75	150	124	45	79	0.17	2.41
75 [a]	150	124	40	110	0.29	2.41
86	165	175	54	76	0.19	2.39
94	184	210	62	64	0.12	2.40
100	205	230	75	97	0.13	2.72

[a] Crystallisation at 0.1 MPa and 140 °C.

As noted above, thick lamellae are typical of ECC. Folded-chain crystals (FCC) are more often formed in polymers; however, ECC can also appear under specific conditions. This problem has been studied in detail for crystallisation of PE.[187] It was found that crystallisation from the orthorhombic phase yields FCC and crystallisation from the mobile hexagonal phase affords ECC.[188] For less dense packing of chains in the hexagonal phase, diffusion sliding processes are possible, which underlies the theory of thickening of lamellar crystals.[189,190] In addition to PE, the formation of ECC has been noted for other crystallisable polymers, for example, polychlorotrifluoroethylene (PCTrFE), *trans*-1,4-polybutadiene,[191] and in VDF/TrFE copolymers. If the composition of these copolymers is below the triple point ($x \approx 0.82$) (see Fig. 33*d*), they can crystallise (like PE) as orthorhombic (ferroelectric) and mobile hexagonal (paraelectric) phases. The mobile hexagonal phase can occur even under atmospheric pressure (a similar behaviour has been noted for PCTrFE and *trans*-1,4-polybutadiene); in the case of PE, this phase appears only at elevated pressures.[183]

The first data on the formation of thick lamellae in PVDF were reported for crystallisation at elevated pressures.[28,192,193] Subsequently, the possibility of the formation of ECC under atmospheric pressure has been verified. VDF/TrFE copolymers with VDF proportions (x) of 0.75 and 0.78 were chosen for this purpose. These values are lower than the x value in the triple point (0.82); therefore, in accordance with the phase diagram (see Fig. 33*d*), crystallisation can be carried out as the mobile hexagonal paraelectric HT phase. The data from scanning electron microscopy of samples crystallised at various degrees of supercooling show that the morphology of thick lamellar crystals is actually observed. At early stages of crystallisation, single lamellae were ~0.3-μm thick. At later stages, stacking of lamellae into ~0.8-μm thick stacks was noted. This aggregation in VDF/TrFE copolymers is observed more commonly than in PE, which is attributed to the greater role of screw dislocations in the former case. The particles arising are cigar-shaped and 20–30-μm long. Crystallisation of the same copolymers at high pressures (80 MPa) hardly changes the morphology arising. The thickness of single lamellae remains the same and the particle length is 10–20 μm.[183] For copolymers with a known molecular mass, the full extended length was estimated to be ~0.7 μm. This means that chains fit almost entirely into the lamellae.

The theoretical possibility of the formation of thick lamellae, *i.e.* ECC, in the VDF/TrFE copolymer (see Fig. 33*d*) exists also when x is greater than that corresponding to the triple point. In fact, in the range of $0.82 \leqslant x \leqslant 0.9$, the mobile hexagonal (rotator) phase can exist.[181] This hypothesis has been verified in a study.[185] VDF/TrFE copolymers with VDF proportions of 0.88 and 0.89 were studied. When conducting crystallisation from the melt under atmospheric pressure and with various degrees of supercooling, the researchers found cigar-shaped particles with dimensions approximately equal to those obtained upon crystallisation of copolymers with $x < 0.82$. Thus, it was confirmed experimentally that ECC can form even above the triple point in the phase diagram.

Nevertheless, in the study cited,[185] this finding was explained without assuming the existence of some rotator phase but proceeding from the Ostwald 'threshold' rule. The temperature dependences of the free energy for the three phases were derived, under certain assumptions,[194] as straight lines with different slopes. This results in two melting points, one for the hexagonal phase (T_m^h) and one for the orthorhombic phase (T_m^o). According to this diagram, crystallisation at a certain temperature T_{cr} converts the liquid in the supercooled state.

Specific defects referred to as 'entanglements' occur in the melt between the macromolecules. 'Untangling' of these defects on cooling the melt to T_{cr} takes some time; therefore, the liquid remains in the supercooled state for some period. After it has passed into the hexagonal phase, this phase occurs in the metastable state for some period of time. Its transition into the more equilibrated orthorhombic phase also takes some time, because, in addition to the change in the type of lattice, this requires conformational rearrangements in the copolymer chains. The equilibrium in the hexagonal phase–orthorhombic phase (paraelectric–ferroelectric) system shifts with time towards the latter. Due to the enhanced molecular mobility, some of the crystals remaining in the metastable hexagonal phase form thick lamellar crystals as ECC.

The possibility of formation of thick lamellar crystals in the uniaxially stretched VDF homopolymer crystallised as the β-phase has been verified.[186] Two crystallisation modes were employed (Fig. 34*a*).

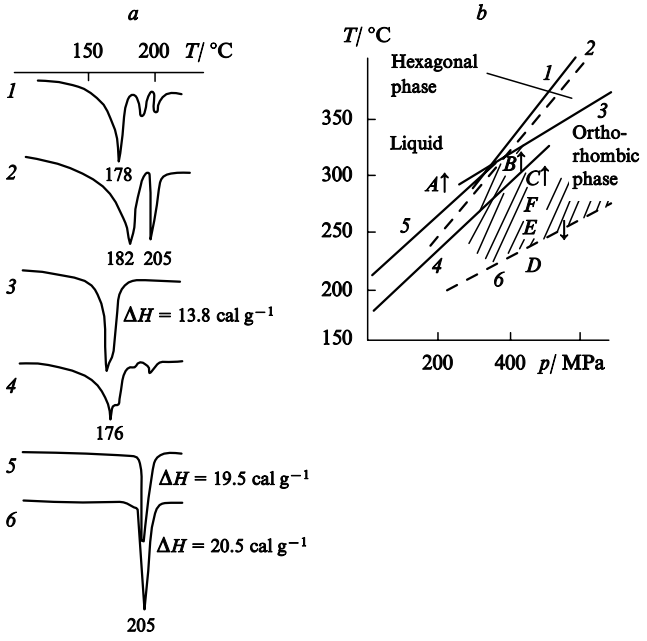


Figure 34. Melting thermograms of stretched PVDF films after high-pressure crystallisation in various regimes (*a*) and the $T-p$ phase diagram (*b*);[186]
(*b*): (*1*) T_m (hexagonal phase); (*2*) T_{cr} (hexagonal phase); (*3*) T_C for the orthorhombic–hexagonal phase transitions; (*4*) T_m for a uniaxially stretched film with the β-phase; (*5*) T_m for the β-phase ECC, (*6*) T_C for the hexagonal–orthorhombic phase transition during cooling. The region of regimes favourable for the formation of ECC is hatched. Points $A-F$ correspond to the conditions of the crystallisation of samples (*1–6*) in (*a*).

Samples *1–3* were crystallised in the constant-pressure mode (200, 400 and 500 MPa, respectively), the temperature being increased to the maximum value (280, 300 and 300 °C, respectively). Samples *4–6* were crystallised under isothermal conditions (217, 262 and 282 °C, respectively), the pressure being increased from the initial value to the maximum value ($100 \rightarrow 500$, $200 \rightarrow 500$, and $200 \rightarrow 500$ MPa, respectively). According to DSC data, the characters of melting endotherms observed for different samples are substantially different. The thermograms of samples *2*, *5* and *6* with intense high-temperature peaks (maximum temperature 205 °C) can be distinguished. Analysis of the data of optical and electron microscopy for crystallised films demonstrated that it is in these samples that thick lamellar crystals are formed, *i.e.* the ECC morphology is realised. The transition enthalpies for samples *5* and *6* are 19.5 and 20.5 cal g^{-1}, respectively. These values are roughly equal to the sum of the enthalpies of the Curie transition and melting in the 74/26 VDF/TrFE copolymer.[179] This means that the Curie and melting points in PVDF films coincide; therefore, only one process is recorded.

The $T-p$ phase diagram for PVDF shown in Fig. 34*b* helps in formulating the conditions for crystallisation yielding the ECC morphology. Since the Curie point in PVDF is very high, its crystallisation as the mobile hexagonal phase can be accompanied by thermal destruction processes. Certainly, they deteriorate the structural characteristics of ECC. Due to the large hysteresis in the Curie transition during heating and cooling, it is better to cool the melt and transform it into the hexagonal phase (metastable state); in this case, crystallisation can be carried out at markedly lower temperatures. Above the hatched region, thermal destruction exerts unfavourable influence, while below straight line *6* the system occurs as the orthorhombic phase, in which thick lamellar crystals do not form. The thickness of these crystals in samples *5* and *6* (see Fig. 34*a*) is 0.1 – 0.2 μm, which is comparable with the crystal thickness in 79/21 and 75/25 VDF/TrFE copolymers, although interplanar spacings of the 110 or 200 reflections (4.25 Å) in the samples under consideration are 5% – 7% lower than those in these copolymers.[178,179]

Analysis of the X-ray diffraction data shows that even in sample *6* the lamellae consist of mixed crystals of the β- and γ-phases. On high-temperature polarisation of the films, the latter is transformed into the pure β-phase. Thus, the assumption that the morphology of thick lamellar crystals improves ferroelectric characteristics was confirmed once again. Comparison of the $D-E$ hysteresis curves for the initial (oriented) film and sample *6* shows that the P_r value is greater in the latter case. More detailed data are presented in Table 14. The Curie point is found above the melting region (as in the case of copolymers with higher VDF contents). The highest sound velocities in these films and the minimum dielectric constants point indirectly to the highest degree of crystallinity in these polymers. However, this conclusion contradicts the reported data,[140] according to which an increase in the degree of crystallinity resulted in a decrease in the coercive field (see Fig. 31*c*), which was then found to be maximum for PVDF with ECC (see Table 14). In the opinion of Hattori *et al.*,[186] this can be attributed to the fact that the latter material does not form a pseudo-hexagonal lattice with $a/b = \sqrt{3}$. For PVDF with ECC, the a and b values are 8.66 and 4.25 Å, respectively, which do not yield this ratio.

The data on the structure of VDF/TrFE copolymers with critical compositions $0.82 \leqslant x \leqslant 0.90$ are the most contradictory. As noted above, thick lamellae have been detected in these copolymers.[181] They should incorporate both ferroelectric β-phase crystals and nonpolar crystals of the α-phase (and, perhaps, even γ-phase) (see Fig. 33*d*). This assumption made it possible to explain why the Curie point and the melting point coincide. Thick lamellae with a size of ~0.1 μm have also been detected[196] on slow cooling of copolymers with the composition 86/14. A low-angle X-ray scattering study showed the presence of thin crystals ($l \simeq 8.5$ nm) apart from thick lamellae. If the hypothetical crystals of the α-, β- and γ-phases are assumed to coexist in both types of lamellae, two melting points and two Curie transitions should be expected, because thin lamellae disappear at 147 – 155 °C, whereas thick ones are retained up to 165 – 170 °C.[196] The α-phase melts more readily;[28] therefore, thin lamellae are likely to be formed by crystals of the α-phase, and thick lamellae are mainly formed by crystals of the β-phase.

In all probability, the morphology of thin lamellae is metastable because their content sharply diminishes at about ~150 °C.[197] The increase in the proportion of thick lamellae indicates that recrystallisation processes in this temperature region can be accompanied by solid-phase transformations of the $\alpha \rightarrow \beta$ type.[28] This assumption is not without reason because such a transition has actually been detected by the X-ray diffraction method in, for instance, the 94/6 VDF/TFE copolymer crystallised in the metastable state,[28,197] and in the case of the 86/14 VDF/TrFE copolymer, a decrease in the degree of crystallinity has been noted well before melting.[197] If the Curie transition occurs in this temperature range, it could be initiated to some extent by the dynamical changes in the disordered regions, as has been noted above.

VIII. Ferroelectricity of ultrathin films

Due to the pronounced influence of the morphology of thick lamellar crystals on the ferroelectric characteristics of PVDF and VDF copolymers, it is of interest to consider the results of studies of these characteristics in thin and ultrathin films. The electrophysical characteristics of the three-layer metal – dielectric – semiconductor system have been analysed.[198] The system contained a 32- or 150-nm thick dielectric film of the 73/27 VDF/TrFE copolymer deposited from a solution onto a silicon substrate with the hole type of conductivity. After the copolymer film had been coated by a protective SiO_2 layer (50 – 70 nm), the breakdown field intensity for this film was 230 MV m^{-1}, which is comparable with the values typical of films with a standard thickness. Analysis of the dependence of the capacity (at a frequency of 1 MHz) on the voltage applied on the metal – dielectric – semiconductor structure made it possible to estimate the remanent polarisation in the copolymer films after poling (~100 MV m^{-1}). For a 32-nm thick film, P_r amounts to 5.9 mC m^{-2}; for a thickness of 150 nm, this value is 4.1 mC m^{-2}. These values are approximately an order of magnitude lower than the P_r values for ordinary films. The reason for this is obscure because the coercive fields in these films, like those in ordinary films, are about 40 – 33 MV m^{-1} (see Ref. 198).

In other studies,[199,200] copolymer films have been deposited by the vacuum vaporisation technique. In the case of 80/20

Table 14. Ferro- and piezo-electric properties of PVDF and VDF copolymers.[186]

Sample	T_m / °C	T_C / °C	K_t	ε' (5 – 10 MHz)	v_s / km s^{-1}	P_r / mC m^{-2}	E_c / MV m^{-1}	Note
VDF/TrFE								
75/25	152	124	0.29	5.3	2.41	111	38	The sample was annealed in the hexagonal phase at 0.1MPa (Ref. 180).
88/12	170	177[a]	0.22	5.3	2.43	100	48	The sample was crystallised in the metastable hexagonal phase at 0.1 MPa and transferred into the β-phase upon polarisation. (Ref. 181).
β-PVDF	175	–	0.20	6.2	2.26	60	50	Data of Ref. 195
β-PVDF (ECC)	205	240[a]	0.27	5.9	2.72	95	70	The sample was polarised in an alternating field, first, at room temperature and then at an elevated temperature

[a] T_C was estimated by extrapolation of the value found from the $T-p$ diagram to a pressure of 0.1 MPa.

VDF/TrFE, a KBr crystal served as the substrate. Study of films of various thicknesses (~10 to 60 nm) by IR spectroscopy resulted in the conclusion that deposition is accompanied by thermal destruction of macromolecules. The destruction yields fragments retaining the initial chain conformation rather than the monomers.

The change in the substrate temperature leads to a changed orientation of chains with respect to the surface. At 35 °C (cold substrate), the axes of macromolecules are arranged at right angles to the surface and at 80 °C (hot substrate) they are parallel to the surface. Similar effects have also been described in other studies,[201,202] which have also noted that the orientation of copolymer chains on the substrate also depends on the film thickness. The temperature effects on the formation of films on the substrates can be regarded as general because they are also manifested for the same films deposited by epitaxial growth from solutions.[28]

It seems attractive to combine polarisation with deposition of thin films on the substrate. This attempt was made in a study,[200] in which the 54/46 and 73/27 VDF/TrFE copolymers were sprayed onto quartz at a rate of 0.02 nm s^{-1} in a field of up to 30 MV m^{-1}. The 400-nm thick films of the copolymer with 54 mol.% of VDF displayed dielectric anomalies in the Curie transition region only in those cases where spraying was carried out in a field (30 MV m^{-1}); when deposition was performed without a field, no dielectric anomalies were observed. As in ordinary films, the Curie transition had signs of a second-order phase transition (without hysteresis). These facts confirm the significant role of electric field in the formation of a ferroelectric structure. The fact that no ferroelectricity was found in films that had not been exposed to an external electric field points indirectly to the occurrence of irregular sections, most probably, of a chemical nature, which hamper the formation of the ferroelectric phase.

This assumption is supported by the data obtained by the same researchers for 73/27 VDF/TrFE. Films prepared by spraying in a field displayed no dielectric anomalies near the Curie transition (~120 °C) because the sample melted at 105 °C. Melting could be due to chain rupture reactions, which efficiently proceed during deposition; they should markedly decrease the average molecular mass of the chain and, hence, the melting point. Thermal destruction should increase the concentration (and mobility) of ionic impurities. Indeed, the shape of the $D-E$ hysteresis curves implies an enhanced role of free charge carriers.[200] This can increase the probability of electric break-down of the films. The coercive fields were found to be lower (by two orders of magnitude). This can be explained qualitatively by assuming that the films thus obtained possess higher degrees of crystallinity (see Fig. 31). This situation can be a consequence of the substantial decrease in the average molecular mass upon thermal destruction, which apparently gives a low-molecular-mass product.

Thus, thin films deposited by spraying exhibit ferroelectric properties; however, the chain structure in these materials is transformed in such a way that ferroelectric characteristics prove most often to be poorer than those for thick films. The formation of thin films from solutions, which allows one to control the conformational characteristics of the chain and the phase state of the crystals formed due to the specific influence of a particular solvent, appears more promising.[28] This method brought the studies at a new level after Russian scientists had proved the possibility of producing monomolecular films of the polymers in question using the Langmuir–Blodgett technique.[45,203–210]

These films are promising for the use in optical memory cells provided that ferroelectric switching has been detected in them. Films of the 70/30 VDF/TrFE copolymer, deposited from solutions in dimethyl sulfoxide with a copolymer concentration of 0.01 mass % have been studied.[45,203–210] The Langmuir–Blodgett films were formed on the surface of doubly distilled water using a setup described in the literature.[211] After the films had been transferred onto a metallic substrate and the upper electrode had been deposited, it was possible to study electrophysical characteristics of the films. Analysis of surface tension isotherms showed that the thickness of a monomolecular film is ~0.5 nm.[45] Films composed of 5 to 40 monolayers were mostly used. Ferroelectric characteristics, in particular, spontaneous polarisation, were measured using the pyroeffect, namely, by recording the current arising on exposure of the film to a 100-μs pulse of the Nd-laser radiation (λ = 1.06 μm). Figure 35 shows the field dependences of the pyroelectric response and the transpolarisation current density in a Langmuir–Blodgett film composed of 30 monolayers. The presence of pyroactivity in the initial (non-polarised) film points to a non-zero residual (spontaneous) polarisation, which may be due to the specific conditions of the film formation.

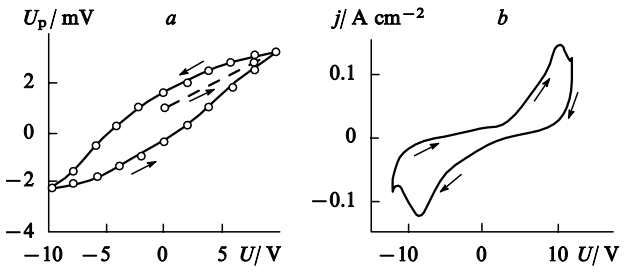


Figure 35. Pyroelectric response (*a*) and transpolarisation current density (*b*) *vs* electric voltage in a 15-nm thick Langmuir–Blodgett film of the 70/30 VDF/TrFE copolymer.[206]

The presence of switching effects indicates unambiguously that these films possess ferroelectricity, which is manifested in a special way. Firstly, the coercive field strengths, E_c = 300 MV m^{-1}, are almost an order of magnitude greater than those observed in ordinary films (see Fig. 35 and Table 9). Secondly, analysis of the scanning tunnelling microscopy data (STM) shows a two-dimensional lattice with two identity periods on the film surface. One of the periods (2.6 Å) is virtually constant for all samples and is related to the lattice constant c = 2.56 Å (see Table 4) along the macromolecule axis. The other identity period varies from sample to sample from 2.2 to 4 Å and characterises the intermolecular packing. Langmuir–Blodgett films are expected to have very high break-down fields (at least, 600 MV m^{-1}). These films are characterised by higher pyroelectric coefficients than ordinary films — 400 μC m^{-2} K^{-1} against ~30 μC m^{-2} K^{-1}.

If a denser, on the average, packing of chains is assumed for Langmuir–Blodgett films, the Curie point in these films may be expected to shift to higher temperatures relative to that in thick (block) films. It can be seen from Fig. 36 that the Curie transition in the Langmuir–Blodgett films is displaced to lower temperatures relative to that for ordinary films (~15 μm).

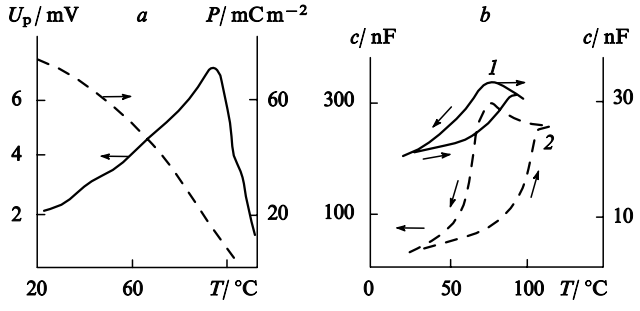


Figure 36. Temperature dependences of the pyroelectric voltage, polarisation (*a*) and capacity (*b*) in the Langmuir–Blodgett films (*1*) and ordinary films (*2*) of the 70/30 VDF/TrFE copolymer.[206,212]

Thus, the shift of the Curie point observed experimentally is opposite to that suggested beforehand. In all probability, the reason for this anomaly is the same as for the unusual behaviour of the spontaneous polarisation, which starts to diminish well before the Curie point. These abnormal features are apparently due to different energy states of macromolecules on the film surface and in its bulk. Macroscopic ferroelectric characteristics in thick films should be determined by parameters of chains in the bulk, whereas in the case of Langmuir – Blodgett films, the chains located on the surface can contribute more significantly to the properties.

The appearance of ferroelectricity in 100 – 200 Å thick films implies that this layer permits the formation of a three-dimensional crystal of the ferroelectric phase. Chains in the planar zigzag conformation are packed in such a way that polar axis *b* becomes the predominant direction. The polarisation component directed at right angles to the film surface is usually measured; therefore, the transverse dimension of the crystal should be not less than the film thickness. The transverse dimension of the crystal can be estimated based on the width of the 200 and 110 intermolecular reflections of the ferroelectric phase. In the case of the thin lamellar morphology, this dimension for block films is ~100 – 200 Å (see, for example, Table 11). This means that only one crystal is formed in the perpendicular direction in a Langmuir – Blodgett film consisting of 30 monolayers, *i.e.* in this direction, the degree of crystallinity is 100%. This is confirmed indirectly by values of spontaneous polarisation equal to 0.1 – 0.15 C m^{-2},[206] which are comparable with the values calculated for the crystal of the β-phase (0.13 C m^{-2}).

More evidence for the advanced hypothesis could be provided by the magnitude of the component of the dielectric constant ε' along the perpendicular to the film. By using the dependences presented in Fig. 36, Palto *et al.*[212] found that for room temperature, $\varepsilon' = 4$, which is substantially lower than this value for a 15-μm film ($\varepsilon' = 12$). The high ε' value for ordinary films is due to the contribution of amorphous areas with developed cooperative mobility, in which the dielectric constant is much greater than in the crystal.[28] Therefore, the low ε values may point to the formation of single lamellar crystals across the Langmuir – Blodgett films. This assumption appears more natural than, for example, the hypothesis of Zhong *et al.*[213] concerning thin ferroelectric inorganic films.

The formation of the threshold thickness of the crystal (~150 Å) in the case of Langmuir – Blodgett films is an important point. Indeed, the electric resistance of these films containing 12 or 7 layers is markedly lower than that of ordinary films.[203] Moreover, the coercitive field was found to increase regularly upon a decrease in the number of monomolecular layers in the film; for a film with 30 monolayers, $E_c \simeq 300$, for a 12-monolayer film it is 400 – 700, and for a 7-monolayer films it is 1000 – 1200 MV m^{-1}.

Conduction by the tunnelling mechanism may arise in the Langmuir – Blodgett films under the action of a strong electric field. This phenomenon was actually observed in a study,[203] in which the curves of pyroelectric hysteresis were measured (Fig. 37*a*). In addition to recording of the pyroelectric response, the conductance of the Langmuir – Blodgett films was estimated. Upon pyroelectric switching, the conductance changed by more than three orders of magnitude (from 10^{-6} to 10^{-9} Ω^{-1}).

One more difference between the characteristics of the Curie transition in ordinary films and in Langmuir – Blodgett films can be noted. It can be seen from Fig. 36*b* that in the latter case, the maximum capacity is only 1.6 times as high as that at room temperature. In the former case, it increases more than fivefold. The dielectric constants of the Langmuir – Blodgett film at room temperature is 4 (that for an ordinary film is ~12), and its maximum value is ~8.5 (that for an ordinary film is ~60). Assuming that one crystallite fits across the Langmuir – Blodgett film, this pronounced differences of the maximum ε' values for block films should be attributed to the presence of sections of the disordered phase. This proves once again the non-trivial role of this phase in the transition, although according to the classical views, it is expected to be associated with the crystalline phase.

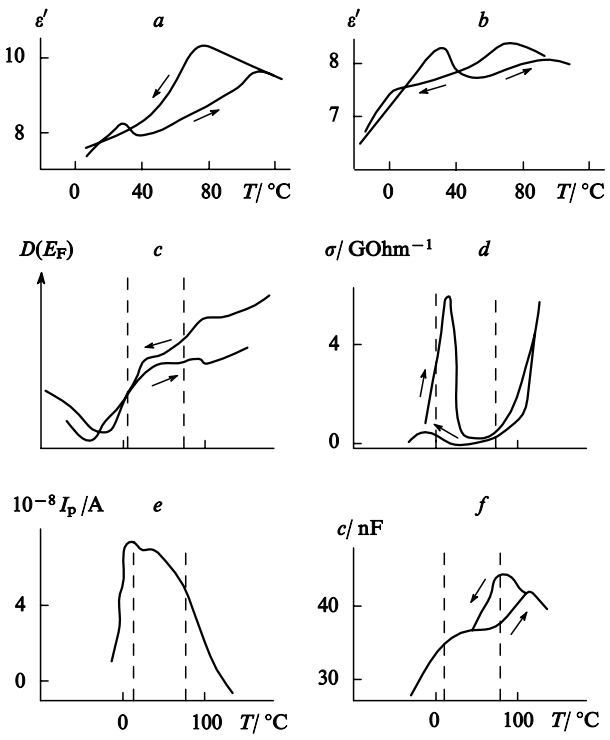


Figure 37. Temperature dependences of the dielectric constant (*a*, *b*), density of states at the Fermi level (*c*), conductivity (*d*), pyroelectric current (*e*) and capacity (*f*) in the Langmuir – Blodgett films of the 70/30 VDF/TrFE copolymer with a number of monolayers of 30 (*a*), 2 (*b*) and 5 (*c*–*f*).

The presence of amorphous regions with excess free space in ordinary films permits one to estimate the local field of ferroelectric crystals. This can be done by doping ferroelectric copolymers by particular dyes, which create admixture colour centres. The molecules of the doping additive are located in the regions with more free space, *i.e.* in the disordered phase. Dye molecules are usually characterised by high dipole moments; therefore, they should be captured by polar planes adjacent to amorphous areas. Thus, the dye molecules would be located in the ferroelectric crystal field and their optical characteristics would carry information about local crystal fields. This fact underlies the method for the estimation of these characteristics developed by Blinov *et al.*[208].

The local field E_{loc} at some point of a dielectric polarised in external field E can be represented as the sum [208]

$$E_{loc} = E + E_1 + E_2 + E_3, \tag{43}$$

where E_1 is the depolarising field caused by the bound surface charge; E_2 is the Lorentzian field induced by the charge of the internal surface of the imaginary spherical cavity about the chosen point, and E_3 is the field of the charges inside this cavity. The last term is equal to zero for isotropic media and for crystals with cubic symmetry. In the short-circuited state after polarisation $E + E_1 = 0$; therefore, in the case of isotropic distribution of atoms

$$E_{loc} = E_2 = \frac{P}{3\varepsilon_0}, \tag{44}$$

where P is the sum of the induced P_i and spontaneous P_s polarisations. Since for ferroelectrics $P_s > 100$ mC m^{-2} and $P_s \gg P_i$,

$$E_{loc} = \frac{P_s}{3\varepsilon_0}. \quad (45)$$

If one proceeds from the value $P_s = 100$ mC m^{-2}, in conformity with Eqn (45), $E_{loc} \approx 4$ GV m^{-1}. To verify this value experimentally, three dyes, rhodamine 6G (R6G), 4-diethylamino-4′-nitroazobenzene (DEANAB) and 4-diethylamino-4′-nitrostilbene (DEANS), parameters of the excited states for which are well known, were introduced into the VDF/TrFE copolymer.[214–217] Absorption of a light quantum by a dye molecule is accompanied by a change in its static dipole moment μ and polarisability α.[217,218] Therefore, the electric field E decreases the energies of the ground (denoted by subscript g) and excited (denoted by e) states to different extents

$$\Delta W_g = -\mu_g E - \frac{\alpha_g E^2}{2}, \quad (46)$$

and

$$\Delta W_e = -\mu_e E - \frac{\alpha_e E^2}{2}. \quad (47)$$

As a consequence, under the action of an electric field, the optical transition frequency (ν) shifts by [219]

$$\Delta\nu = \frac{1}{hc}\left(\Delta\mu E + \frac{1}{2}\Delta\alpha E^2\right), \quad (48)$$

where $\Delta\mu = \mu_e - \mu_0$ and $\Delta\alpha = \alpha_e - \alpha_0$ are the changes in the dipole moment and the average polarisability in the excited state.

The frequency shift consists of two components, linear and quadratic with respect to the field [see Eqn (48)]. The validity of this equation for doped VDF/TrFE copolymers was verified for the copolymer containing DEANAB in a concentration of 0.5 mass %. The films were not polarised; therefore, only the local field for the initial ferroelectric crystal E_l should be considered. In accordance with Eqn (45), below the Curie point $E_l \neq 0$, and in the paraelectric phase $E_l = 0$ because $P_s = 0$. Thus, on passing through the Curie point ($\sim$370–380 K), the absorption band should shift, which is actually observed by experiment.[208] The absorption bands of the dyes DEANAB and R6G change in different ways near the Curie transition; in the former case, they shift to shorter wavelengths, and in the latter case, conversely, they shift to longer wavelengths. In addition, the magnitudes of these shifts for these dyes are also substantially different.[208] These facts can also be explained in terms of the proposed model. In fact, it has been reported [216,220] that for DEANAB, $\Delta\mu = 8$–10 D and $\Delta\alpha = +45$ Å^3, and for R6G these values are markedly lower — $\Delta\mu = 1.5$ D and $\Delta\alpha = -1.2$ Å^3. According to Eqn (48), this should result in a smaller shift of the band for R6G, which was actually observed in the experiments.

The model considered here makes it possible to estimate the local field after poling of a doped film. As noted above, polarisation can be accompanied by substantial structural changes, which influence E_l. Polarisation is attained using high-strength fields; therefore, charge carriers are injected from the electrode into the film and they also influence E_l. The local field can be calculated from the frequency shift of the absorption band after polarisation. This calculation was performed [46,47] in relation to mixtures of PVDF with PMMA doped with a dye. Other researches tackled this problem more rigorously.[208] They believed that direct recording of the shift of the bands is complicated because the bands are broad. Therefore, they proposed recording the degree of light modulation by an alternating field applied to the sample.[218,220–222] Practically, the task was to measure the gain in the optical density ΔD at frequency ν corresponding to the chosen band following the imposition of an electric field on the sample. This value should be proportional to the first and second derivatives of the optical density with respect to frequency [218]

$$\Delta D(\nu) = A_1 \nu \frac{\partial D(\nu)}{\partial \nu} + A_2 \frac{\partial^2 D(\nu)}{\partial \nu^2}. \quad (49)$$

Assuming a particular symmetry of the molecular distribution over the factors A_1 and A_2 for measurements at the first and second harmonics of the modulating field, one can find E_l.

Poling of a Langmuir–Blodgett film of PVDF in a $\pm$40 MV m^{-1} field induces a substantial Stark effect, proportional to the first derivative $\partial D/\partial\nu$. When the direction of the polarising field changes, the sign of the linear Stark effect changes. This means that the dipole moments of the dye are also re-oriented in the opposite direction. If a constant field E_n is applied together with the modulating field, variation of the former induces the variation of the amplitude of the linear Stark effect in accordance with a pattern having a hysteresis. The hysteresis may arise due to the interaction of the dye dipoles with the internal field of the ferroelectric. The E_l value was found to be 300 MV m^{-1}. Thus, as in the studies cited above, [46,47] the internal field was found to be much more intense than the polarising field.

The structures of Langmuir–Blodgett films have been considered [223] in relation to the homopolymer PVDF, which usually crystallises as a nonpolar α-phase.[28] Primary attention was devoted to conformational characteristics of films prepared from a solution in DMSO.[223] Analysis of the IR spectra showed that crystallisation in the thickest film (30 monolayers) gives a ferroelectric β-phase with planar zigzag conformations of chains.[28] This is confirmed by the presence of specific absorption bands at 470, 509, 840 and 1275 cm^{-1}. The formation of this conformation is apparently facilitated by the substrate on which the film is formed. This substrate is water, the molecules of which have a high dipole moment. Under these conditions, the minimum free energy can be attained by decreasing electrostatic interactions. The decrease is most pronounced if a chain in the planar zigzag conformation is parallel to the water surface.[223]

This role of water in the establishment of the conformation of PVDF chains is supported by the fact that polymerisation of VDF in aqueous media always results in a polymer crystallised as the polar β-phase.[224] In addition, if the foregoing is true, the Langmuir–Blodgett film being formed (provided that the transfer on a solid substrate does not change the situation) should possess a non-zero spontaneous polarisation P_s. Indeed, a finite value of pyroelectric response has been noted experimentally for a non-polarised film.[223]

As the number of monomolecular layers n in the Langmuir–Blodgett films decreases, the conformations of macromolecules may change, due to the enhancement of the role of surface states differing in energy characteristics from those in the bulk. In order to verify this hypothesis, the IR spectra of films containing different numbers of monomolecular layers have been compared.[223]

A decrease in the number of monolayers in a Langmuir–Blodgett film (n = 15 and 10) brings about the appearance of conformational defects as the TGTG$^-$ and T$_3$GT$_3$G$^-$ isomers, which can be detected from the increase in the intensity of the absorption bands corresponding to them (Table 15). Apparently, these changes occur as accumulation of conformational defects as the above-mentioned isomers in the ferroelectric β-phase. The defects originate within long sequences of planar zigzag conformations (see Table 15). This is confirmed by the character of variation of the intensities of bands at 1275 and 840 cm^{-1}, sensitive to these sequences.[28,225] The longest sequences are the first to be affected because the decrease in n from 30 to 10 results in the intensity of the band at 1275 cm^{-1} decreasing by 30% and that of the band at 840 cm^{-1} decreasing by only 10%.

The structural changes following a decrease in the thickness of a Langmuir–Blodgett film deteriorate the three-dimensional ordering in the ferroelectric crystal. This is indicated by the increase in the intensities of the two bands associated with the amorphous structure, 600 and 905 cm^{-1}. This conclusion is also supported by the variation of the intensity of the band at 470 cm^{-1}, which is attributed to *trans*-isomers in disordered areas in PVDF.[28] The increase in the intensity of this band

Table 15. Relative variation of the normalised intensities of several bands in the IR spectra of the Langmuir–Blodgett films of PVDF with various numbers of monolayers.[223]

Bands	Conformation	Phase [a]	*n*		
			30	15	10
470	TT	a	0.29	0.28	0.53
509	TT	a, c	0.21	0.18	0.19
530	$TGTG^-$	–	0.04	0.16	0.28
600	–	a	0.09	0.74	1.14
612	$TGTG^-$	–	0.06	0.40	0.43
770	$T_3GT_3G^-$	–	< 0.05	0.20	0.31
795	$TGTG^-$	–	< 0.01	0.08	0.14
813	$T_3GT_3G^-$	–	0.05	–	0.14
840	$(TT)_n$ $(n \geqslant 3)$	–	1.09	1.02	0.97
905	–	a	0.06	0.36	0.22
F(β)	–	–	0.85	0.58	0.45
1275	$(TT)_n$ $(n \geqslant 4)$	–	2.2	1.7	1.5
1235	$T_3GT_3G^-$	c	0.37	0.67	0.29
1142	–	–	0.67	0.62	0.32
1115	–	–	0.27	0.52	0.73
1097	–	–	0.18	0.062	0.11
1035	–	–	1.09	1.19	1.33
1011	–	–	0.12	0.26	0.22

[a] Amorphous (a) and crystalline (c) phases.

following a decrease in *n*, points to the tendency for disordering of chains in the planar zigzag conformation.

The above structural changes in the studied films can also influence their electrophysical characteristics. If the structural changes in the Langmuir–Blodgett films of PVDF and VDF/TrFE copolymer are assumed to be similar, then regular features can be found for the latter, for example, in the parameters of the Curie transition.

The dielectric anomalies (the maximum of the dielectric constant) near the Curie transition in the Langmuir–Blodgett films of the 70/30 VDF/TrFE copolymer have been considered. [226] Two anomalous regions (a low-temperature and a high-temperature region), were found in all films (*n* varied from 30 to 2). Since the first anomaly becomes more pronounced as *n* decreases (see Fig. 37*a*,*b*), it was regarded as being due to the surface ferroelectric transition. The assumption that the structural changes in very thin Langmuir–Blodgett films formed from the copolymer and the homopolymer are similar entails an interesting conclusion. The low-temperature Curie transition can be ascribed to the crystals of the ferroelectric β-phase with high concentration of conformational defects and with the tendency for disruption of the three-dimensional ordering in the bulk.

The pyroelectric response curves for the switching of polarisation in the Langmuir–Blodgett films based on PVDF [223] exhibit hysteresis similar to that observed in the Langmuir–Blodgett films based on the VDF/TrFE copolymer (see Fig. 35).[223] For a PVDF film with $n = 30$, the calculated coercive field strength was 500 MV m^{-1}. This coincides in order of magnitude with that for the film based on the VDF/TrFE copolymer. Tentative experiments with the Langmuir–Blodgett films having $n = 15$ show that the switching voltage remains the same (8–10 V), *i.e.* the coercive field is enhanced by a factor of nearly two. As noted above, similar results have been observed for VDF/TrFE copolymer films. Thus, a decrease in the number of monomolecular layers in the Langmuir–Blodgett films of the polymers in question increases the coercive field. This fact together with the data on the structural changes in the PVDF film entail the following interesting conclusion. The increase in the intensity of the band at 600 cm^{-1} following the decrease in the number of monolayers formally implies a decrease in the degree of crystallinity; therefore, the enhancement of the coercive field is due to an increase in the proportion of the disordered phase. This conclusion is confirmed by the results obtained for block PVDF films, in which a decrease in the degree of crystallinity also results in a linear increase in the coercive field, although these fields in block films are substantially lower in magnitude.[140]

Analysis of the hysteresis curves for the pyroelectric response (see Fig. 35) displayed yet another specific feature of the Langmuir–Blodgett films. Judging by the voltage applied for measurement of the pyroelectric response, the intensity of the break-down field should be at least 1 GV m^{-1}. This value is much greater than the corresponding values for block films. The above-noted specific structural features of the Langmuir–Blodgett films may be responsible for this. This film can be regarded as a material with 100% degree of crystallinity in the direction perpendicular to its surface. The mobility of free charge carriers in this material is much lower than that in a material containing the amorphous phase, in which chains execute cooperative motions with large amplitudes.[28] The break-down in the Langmuir–Blodgett films under study is limited most likely by a thermal mechanism, which requires a particular free path length of the carriers. The free path length can happen to be longer than the film thickness. In this case, there are no prerequisites for an avalanche-like movement of charge carriers, which limits the currents for the thermal breakdown mechanism.

The local fields created by ferroelectric crystals have been studied in detail [227] by Stark spectroscopy. The optical probe used was a multilayer of the anthraquinone dye KD-78, having a principal absorption band at about 15700 cm^{-1}. The ferroelectric moiety of the film contained 70 monomolecular layers of PVDF and the probing moiety incorporated six bimolecular layers of KD-78. A symmetrical set of aluminium electrodes was used in the experiments. The change in the absorbance (ΔA) was measured at the principal frequency (f) and the second harmonic ($2f$). The relations derived by Palto [227] were used to calculate two characteristics, namely, the amplitude of the local alternating field (E_l) and the static local field (E_{dc}). Figure 38 presents the experimental Stark spectra for the PVDF Langmuir–Blodgett

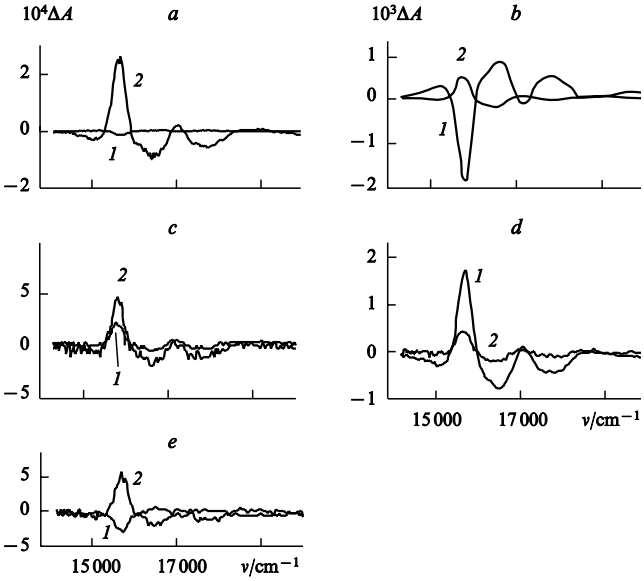


Figure 38. Spectra of the Stark effect at the first (*1*) and second (*2*) harmonics demonstrating bistable switching of the static local field in the initial nonpolarised (*a*) and polarised (*b*–*e*) Langmuir–Blodgett PVDF films;[226]
(*b*) a bias voltage, $U_{dc} = +10$ V, was applied to the sample; (*c*) $U_{dc} = 0$ after poling by a voltage of +10 V; (*d*) a bias voltage, $U_{dc} = -10$ V, was applied to the sample; (*e*) $U_{dc} = 0$ after poling by a voltage of −10 V. The spectra were measured at the alternating voltage amplitude $U = 5$ V, basic frequency $f = 1000$ Hz.

films; it is using this spectra that these characteristics were calculated. A clear-cut quadratic Stark effect of the probing layer measured at the second harmonic is observed in the initial non-polarised film. With allowance for the electroopical constant for KD-78, $C_b = 5.7 \times 10^{-22}$ m^2, and the amplitude ΔA of the quadratic Stark effect, the local field was found to be 270 MV m^{-1}.

The Stark effect at the first harmonics for the initial sample is 20 times weaker ($\Delta A_1 \simeq 1.2 \times 10^{-5}$); this corresponds to a static local field strength of -13 MV m^{-1} (see Ref. 227), which is due to the remanent polarisation in the initial film. After a constant bias voltage ($+10$ V with respect to the electrode) has been imposed on the substrate, the remanent polarisation sharply increases because the amplitude of the Stark effect at the first harmonics increases by more than two orders of magnitude (see Fig. 38*b*). The ΔA_2 also increases approximately twofold, and the above-mentioned local fields become $E_l \simeq 380$ MV m^{-1} and $E_{dc} \simeq -1.4$ GV m^{-1}. The ratio $E_{dc}/E_l \approx -3.7$, which is much greater in magnitude than the ratio of the constant voltage to the alternating voltage amplitude, which is equal to two. Thus, the local field factor at zero frequencies is ~ 1.9 times greater that at a modulation frequency, equal to 1 kHz, *i.e.* dispersion of the local field factor is observed.

An unusual result was obtained after removal of the $+10$ V voltage (see Fig. 38*c*). It can be seen that the sign of the effect at the first harmonic changes, which indicates unambiguously the change in the local field direction with respect to that in the initial (non-polarised) sample. The static local field becomes $+170$ MV m^{-1}, *i.e.* it is higher than that in the initial film by more than an order of magnitude. This may be due to substantial structural rearrangements (for instance, a sharp decrease in the number of conformational defects) in the Langmuir–Blodgett film after polarisation. A voltage with the opposite sign (-10 V, see Fig. 38*d*) does not change the Stark effect at the second harmonic, *i.e.* E_l remains unchanged. However, the effect at the first harmonic does change. If the electric displacement is subsequently diminished to zero, the static field would be retained but its sign would be reversed, -170 MV m^{-1}. This field does not relax over a plausible period of time but it can be switched to the opposite one.

Thus, two directions of the local static field correspond to the two directions of the polarisation vector in the ferroelectric crystal. However, one contradiction has been noted.[227] In fact, the direction of the local static field should coincide with the direction of the remanent polarisation. The opposite situation occurs in the experiment: the sign of the Stark effect at the first harmonic in the presence of a polarising field is opposite to the sign of the Stark effect after the removal of the bias field (see Fig. 38*d*, *e*).

A model has been developed[227] which assumed full symmetry of the near-electrode areas with identical space charge distribution. Analysis of the situation in the absence of this symmetry shows that the direction of the local static field can be opposite to that of the polarisation. In this case, the question arises of whether the assumption of the asymmetry of the space charge on the sides of near-cathode and near-anode regions is physically substantiated.[228] This question can be answered by using the results of some studies dealing with the behaviour of PVDF in strong electric fields. The pyroelectric characteristics of polarised samples on application of thermal pulses on the sides of the cathode and the anode has been studied.[229] The pyroelectric effect was found to be higher in the latter case. This was interpreted as being indicative of an asymmetry of the space charge on the sides of the cathode and the anode.

Another independent group of experiments included elucidation of the possibility of the appearance of a bending moment in polarised films upon imposing an electric field.[230] It was shown that in the case of a non-shielded electrode (*i.e.* when there were prerequisites for the injection of charge carriers from the electrode in the polymer) and not very high polarisation fields, bending actually arose in the film when working in the mode of the inverse piezoelectric effect. This fact was unambiguously ascribed to the asymmetry of the arising space charge on the cathode and anode sides.[230] This asymmetry can appear if the conditions for the injection of electrons and holes into the polymer are non-equivalent. Analysis of the voltammetric characteristics of PVDF films obtained in studies of the conduction in strong electric fields also confirms this assumption.[231] The authors of two studies cited[229,230] arrived at the same conclusion, namely, that in the case of contact poling of PVDF, the injection of holes into the material is preferred over the injection of electrons. Thus, the interpretation of the abnormal behaviour of the local field direction after removal of the polarising voltage proposed by Palto[227] is confirmed by independent experiments.

Apart from the electrophysical characteristics of thin Langmuir–Blodgett films ($n = 5$), the change in the direct and inverse photoemission spectra (DPES and IPES, respectively) was considered to be additional substantiation of the presence of surface ferroelectricity.[232] The methods of electronic spectroscopy, which are extremely sensitive to the state of the surface, can provide useful and independent information on this problem. Analysis of the temperature dependences of these spectra shows substantial changes in the electronic structure of the films near the low-temperature transition (20 °C) (Fig. 37*a*, *b*, *f*), similar to those found in the surface layers of germanium[233,234] and silicon.[235] The density of states at the Fermi level in the low-temperature transition region changes markedly (see Fig. 37). This was interpreted as pointing to strong electron–phonon interactions near this transition. Assuming that the copolymer compositions at the surface and in the bulk are identical, Choi *et al.*[232] concluded that the difference between the electronic structures in the bulk and near the surface may be due to the lower coordination of atoms in the latter case. The presence of characteristic points on the temperature dependences of the conductivity, pyroelectric current, dielectric permittivity or electric capacity was also interpreted as being due to the presence of two types of transition — those on the surface and in the bulk.

The whole set of these data makes it possible to elucidate the mechanism of formation of the ferroelectric phase following a decrease in the thickness of Langmuir–Blodgett films somewhat more precisely. Indeed, the interpretation of experimental data[226,232] does not account for some details of the experimental curves. For example, two dielectric anomalies of the temperature dependences of the dielectric permittivity are observed as well for the block films of the 65/35 VDF/TrFE copolymer (see Fig. 18 and 27). According to X-ray diffraction data, two types of ferroelectric phase, QL and LT, should be present in these compounds.[28] The less perfect QL phase may be responsible for the low-temperature transition.

Some indirect data supporting the interpretation of the anomalies observed[226,232] which assumes the existence of ferroelectric QL and LT phases can also be found in earlier publications by the same authors. Indeed, no low-temperature transition was noted in a similar Langmuir–Blodgett film (see Fig. 36), *i.e.* this transition is not always reproducible. The low-temperature 'anomaly' of the dielectric permittivity is more clear-cut in the heating regime, whereas in the cooling regime it is weak and the high-temperature anomaly is more pronounced (see Fig. 37). Since this film is formed by only two copolymer monolayers (*i.e.* there is actually no bulk), it can be assumed that the film structures in the heating and cooling regimes should be different. A similar behaviour is also typical of thicker films ($n = 5$). Thus the conduction 'anomaly' observed in the region of the low-temperature transition is also more pronounced during heating (see Fig. 37*d*). Moreover, the electronic spectroscopy data indicate that the transition ascribed to the bulk is observed only in the cooling regime (see Fig. 37*c*).

These facts can be interpreted more simply taking into account the existence of the QL and LT phases. In this case, the different ratios of the 'anomalies' at 20 and 80 °C are obviously

due to interconversion of these phases. In particular, during heating (to fairly high temperatures), annealing can occur, which is always accompanied by enhancement of the lattice ordering for crystallisable polymers. In this particular case, this is the QL → LT type transition. Apparently, an increase in the proportion of the latter (more perfect) phase accounts for the 'anomalies' noted for several characteristics of the transition in the heating–cooling cycles.

According to STM, Langmuir–Blodgett films of the copolymer [226] contain chains with bent skeleton, which is consistent with one of the models of the QL phase structure (see Fig. 21*a*).[28] STM studies show [227] that the identity period across the chain ranges from 2.7 to 5 Å for different regions of the film. This may be because areas of either phase differing in packing density across the chain can be present in the scanning area.[28, 67]

Thus, it can be assumed that Langmuir–Blodgett films incorporate two types of ferroelectric phase with different degrees of perfection. The ratio of these phases can change upon a decrease in the film thickness towards a higher content of the less perfect ferroelectric phase. This is confirmed by IR spectroscopy (see Table 15).

The concept assuming the existence of two types of ferroelectric phase in PVDF and VDF copolymers can also help in the interpretation of yet another phenomenon observed in the Langmuir–Blodgett films of the VDF/TrFE copolymer. Ducharme *et al.* [236] verified the hypothesis of Devonshire [237] about the presence of a critical temperature (T_{cr}) and a critical electric field (E_{cr}) in ferroelectrics with a first-order phase transition (at the Curie point). Practically, the task was to follow the hysteresis curves of the dielectric permittivity ε' upon application of an alternating electric field on the Langmuir–Blodgett film. It was found that below 70 °C the field dependences of ε' display a single peak (although it is asymmetrical) falling on the region of the coercive field. In the temperature range from 90 to 140 °C, the $\varepsilon'(E)$ curves have two maxima, the positions of which depend on the temperature.[236] It was suggested to represent the $E-T$ phase diagram for this temperature range (at 1 atm) as the linear plot for the Curie point *vs* the field strength (see Fig. 39*b*) similar to the plot that can be obtained for the block films of the 52/48 VDF/TrFE copolymer (see, *e.g.*, Fig. 25).[95] By processing the experimental data,[236] critical parameters of the films were determined. Data for these films and for other ferroelectrics are listed in Table 16. It can be seen that the critical field for the Langmuir–Blodgett film is higher by several orders of magnitude than the fields for other ferroelectrics. This fact is predictable for VDF copolymers because the coercive fields for them are also much higher. The difference between the T_C values for the Langmuir–Blodgett film and a block copolymer film raises more questions. Some of them can be answered upon examination of Fig. 39. When measurements are performed during heating in the absence of a field (curve *1*), two types of transition

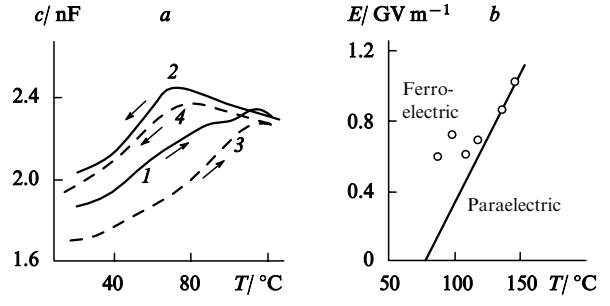


Figure 39. Temperature dependences of the capacity in the heating–cooling cycles in the absence of a field and with a bias field (*a*) and the $E-T$ phase diagram (p = 1 atm) for the Langmuir–Blodgett films of the 70/30 VDF/TrFE copolymer with n = 30;[236]
(*1*, *2*) without a bias field; (*3*, *4*) with a bias field, U = 5 V.

Table 16. Parameters of the ferroelectric phase transitions in the Langmuir–Blodgett (n = 30) [236] and block [238] films of the 70/30 VDF/TrFE copolymer, in $BaTiO_3$ (see [239]), in the crystals of deuterated potassium dihydrogen phosphate (DPDP) [240] and in a liquid-crystal ferroelectric (LCF).[241]

Parameter	Langmuir–Blodgett–film	Block film	$BaTiO_3$	DPDP	LCF
T_C / °C	80 ± 10	102	108	−61	55.0
T_{cr} / °C	145.5	–	116	−60	55.8
$10^6 E_{cr}$ / V m^{-1}	$(0.93 \pm 0.1) \times \times 10^3$	–	0.6	0.83	5.0
$\frac{dT_c}{dE}$ / m (°C) V^{-1}	$(7 \pm 2) \times 10^{-8}$	12×10^{-8}	6.5×10^{-4}	1.25×10^{-6}	1.6×10^{-7}

with temperatures of ~80 and ~110 °C are recorded, while in the cooling regime (curve *2*) only one transition is detected taking into account the temperature hysteresis. This points to the presence of two types of ferroelectric phases, the ratio of which changes on passing from the heating regime to the cooling regime due to the QT → LT transition on annealing (heating). This transition can also be induced by an electric bias field because only one transition is observed in this case even during heating (see curve *3*).

One circumstance which has not received adequate attention [236] should be noted, namely, the exceptionally broad temperature range in which the double hysteresis loops of ε' are observed. For Langmuir–Blodgett films, this range is 65 °C, whereas for $BaTiO_3$ it covers only 8 °C (and even less for other ferroelectrics). This can also be interpreted with the aid of the assumed existence of two types of ferroelectric phase, QL and LT. If these phases differ in the degree of lattice perfection, their coercive fields should also differ, which is reflected as twin hysteresis loops on the $\varepsilon'(E)$ curves. [236] If this assumption is used to explain the broad range of critical temperatures (see Table 16, Fig. 39), an equally broad temperature range of coexistence of these phases should be expected. In fact, in the VDF/TrFE copolymer with the composition 65/35 (*i.e.* approximately the same as that of the copolymer studied in the publication under discussion [236]), the QL and LT phases coexist in a temperature range of not less than 70 °C (see Fig. 20). This value is close to that indicated by Fig. 39, which confirms once again the validity of this hypothesis.

Evidence that the ferroelectric QL phase can occur not only in VDF/TrFE copolymers but in the homopolymer and in other copolymers (for example, with TFE) can be found in the literature. If the low-temperature transition is assumed to be due to the QL → paraelectric transformation, it should also be expected in the Langmuir–Blodgett films based on PVDF. Tentative results show that this is actually the case.

In all probability, the QL phase reflects the existence of so-called quasi-domains, characterised by a particular type of long-range order, in the disordered phase of the objects considered. The presence of quasi-domains was judged relying on the 'anomalies' of the low-temperature dielectric relaxation processes in PVDF.[242] These processes are attributed to the mobility in the disordered phase.[28] The static dielectric permittivity in the temperature range studied has been found to increase with temperature, which is an atypical type of behaviour for most polymers. The general thermodynamic expression for the entropy of a dielectric in field E has the form [243]

$$S = S_0 + \frac{\partial \varepsilon_0}{\partial T} \frac{E^2}{8\pi},$$

where S_0 is the entropy without a field. When a field is applied, the entropy increases. This can be interpreted only as an indication of

existence of correlated chain sections with a definite long-range order in the disordered areas.[243]

The quasi-domains in question (like classical domains) should undergo a transition into a disordered (paraelectric) state. This is indicated by the dielectric anomalies (in particular, a maximum of the dielectric absorption $\Delta\varepsilon$) found for the β-relaxation in PVDF.[244] In the homopolymer, this maximum is often masked by the α_c-relaxation region.[28] The intensity of α_c-relaxation substantially decreases with a decrease in the degree of crystallinity. Therefore, the dielectric anomalies in the region of the hypothetical transition should be detected more easily in amorphised polymers of this class.

An efficient way of amorphisation of PVDF is its copolymerisation with comonomers having bulky substituents. In particular, hexafluoropropylene (HFP) can be used for these purpose. Indeed, the crystallinity of the 86/14 VDF/HFP copolymer proves to be markedly lower.[245] The temperature dependences of the dielectric permittivity in the region of 40–50 °C has an anomaly, which was attributed to a smeared transition of quasi-domains into a disordered state.

The low-temperature dielectric anomaly in the Langmuir–Blodgett film of the 70/30 VDF/TrFE copolymer[226] can be identified by a more detailed comparison of the dielectric data for samples obtained by the standard method (block films) and by the Langmuir–Blodgett method. It has been noted above that two transitions are detected for both types of films (see Fig. 18*a* and 37*a*, *b*, *f*). Some researchers separated the contributions of the dielectric constant components by the amorphous and crystalline phases to the overall curves.[246] It was found that the amorphous phase in all the VDF/TrFE copolymers considered (73/27, 65/35 and 54/46) is characterised by a blurred maximum in the 0–40 °C range. The maxima of the dielectric constant of the Langmuir–Blodgett films derived from the VDF/TrFE copolymer,[226] PVDF[242,244] and the VDF/HFP copolymer[245] are located in about the same temperature range. Thus, these maxima can be considered to be of the same origin; in the case of block films, this is the transition of quasi-domains occurring in the disordered regions into the disordered state and for the Langmuir–Blodgett films, this is a similar transition occurring in the near-surface macromolecules, the conformational state of which is close to that in the amorphous phase of block films.[223]

Evidently, the reason for the formation of the quasi-domains (in other words, the QL phase) lies in the fact that the chains of the amorphous phase in the vicinity of the crystals of the ferroelectric β-phase occur under the influence of strong local fields. According to theoretical estimates,[247] they can be as high as 9.28 GV m^{-1} in PVDF (with crystals of the β-form) at room temperature. They are of the same order of magnitude (4 GV m^{-1}) for 70/30 VDF/TrFE copolymer, although the experimental values are somewhat lower. Such high fields in the area of localisation of chains of the disordered phase create conditions for them to be arranged in quasi-domains. In fact, in such a field, the potential energy of the CF_2 bond dipole in PVDF at room temperature is very high (11.7 kcal mol^{-1}).[247] However, the formation of quasi-domains (QL phase) in the disordered phase is possible in this case only when the fluctuations are high-amplitude cooperative motions in this phase. A peculiar feature of PVDF and VDF copolymers is that, due to the low glass transition temperature, these motions really occur in the amorphous phase at room temperature (with relaxation times of $\sim 10^{-7}$ s);[28,242] therefore, it is quite likely that prerequisites for the formation of sections with an intermediate form of ordering would arise in the areas adjacent to the crystals.

Once the above-described nature of the formation of quasi-domains (QL phase) has been accepted, one reason for the transition of these fluctuation structures into the disordered state (low-temperature transition) can be explained as follows. The allowance made for the contribution of dipole oscillations in the ferroelectric crystal of the β-phase[247] shows that an increase in the temperature diminishes the spontaneous polarisation and, correspondingly, the local field at the boundaries with the disordered phase. Therefore, at a particular temperature, the quasi-domains would be destroyed, which is actually detected as the presence of the low-temperature dielectric anomaly.

One more piece of evidence for the existence of quasi-domains in the amorphous phase can be derived from the chain dynamics characteristics found by NMR. For example, the spin–lattice relaxation times T_1 for the amorphous (T_{1a}) and crystalline (T_{1c}) phases of VDF/TrFE copolymer have been compared.[100] These characteristics were found to differ by more than an order of magnitude below the Curie point and by a factor of only two above this point. Thus, the chain dynamics in the disordered phase is characterised by approximately the same parameters as that in the paraelectric phase. This fact can be regarded as indirect evidence for the existence in the amorphous phase of these quasi-domains with imperfect long-range order similar to that occurring in the paraelectric phase.

The results obtained by the broad-line technique, a modification of the NMR method, also point to the presence of quasi-domains in the amorphous phase. If the quasi-domains actually do exist, the dynamics in them should differ from the dynamics in the proper disordered (isotropic) phase and in the crystal. Information on this point can be derived by strict analysis of the line contours in the NMR spectra of the compounds in question. This was demonstrated in relation to the VDF/TrFE copolymers.[110] In particular, if the composition is 70/30, the free induction signal (for ^1H nuclei) at 15–60 °C is described by three components. The widest component refers to the ferroelectric phase, and the narrowest one corresponds to the isotropic amorphous phase. The intermediate component is attributed to so-called stressed amorphous phase. This might imply the quasi-domains mentioned above, in which the dynamics should be more hindered than that in the isotropic amorphous phase due to the presence of a certain long-range order. Furthermore, the reported[110] data on the temperature dependence of the intensity of the intermediate component can be interpreted in a different way. In the region of 60–120 °C (below the Curie point), the intensity of the intermediate component increases appreciably. This was attributed to partial transition of the ferroelectric phase into the paraelectric phase. However, this hypothesis provokes serious objections. The researchers cited noted themselves that the experimental value of the second moment ΔH_2^2 for this component is 2.5 G^2, which is substantially lower than the value calculated for the lattice of the paraelectric phase (11.6 G^2).

To explain this contradiction, a definite type of motion in the paraelectric lattice, namely, rotation of the chains about their axes, had to be assumed. If the intermediate component is related to quasi-domains, this fact can be explained. In the 60–120 °C region, some of the domains (in small crystals with less perfect packing) can pass into a state with higher symmetry (quasi-domains). The packing in them is less perfect than in the paraelectric phase; therefore, the dynamics is less hindered, which accounts for the low experimental value of ΔH_2^2.

The assumption that the ferroelectric QL phase is identical to the quasi-domains, found in the amorphous phase in some experiments, is supported to some extent by the temperature dependences of the X-ray diffraction parameters for isotropic and textured samples of the 94/6 VDF/TrFE copolymer.[196] At a temperature of 160 °C (below the melting point), two reflections are observed, one of them corresponding to the β-phase and the other diffuse halo reflection being due to the paraelectric phase (Fig. 40). This can be judged relying on the interplanar spacings, which coincide with those in the same phase of the VDF/TrFE copolymer (see Fig. 20).

In the 170–180 °C temperature range, the interplanar spacing in the paraelectric phase sharply increases (see Fig. 40*b*). This may imply that the ferroelectric and paraelectric phases coexist up to the melting point. If the Curie point is considered to overlap with the melting region (due to the very high proportion of VDF in the copolymer), melting should be accompanied by the ferroelectric–paraelectric transition. Actually, melting of paraelectric

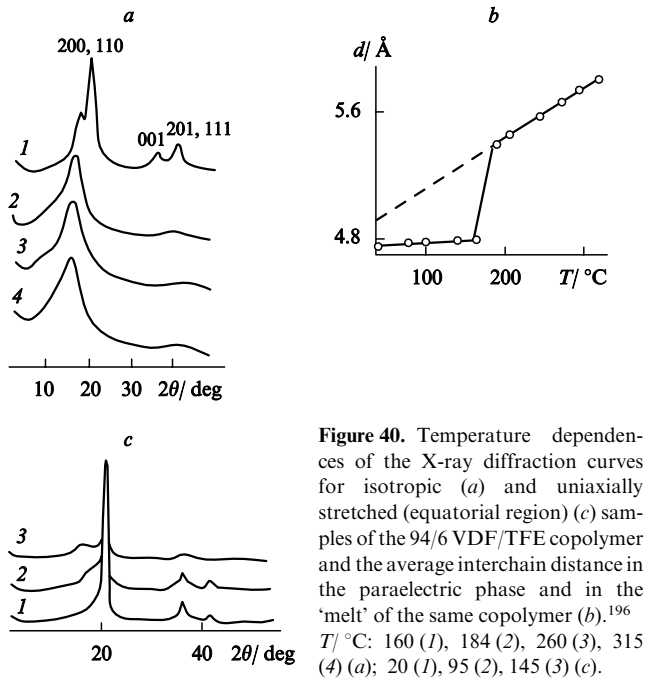


Figure 40. Temperature dependences of the X-ray diffraction curves for isotropic (*a*) and uniaxially stretched (equatorial region) (*c*) samples of the 94/6 VDF/TFE copolymer and the average interchain distance in the paraelectric phase and in the 'melt' of the same copolymer (*b*).[196] *T*/ °C: 160 (*1*), 184 (*2*), 260 (*3*), 315 (*4*) (*a*); 20 (*1*), 95 (*2*), 145 (*3*) (*c*).

crystals can also be involved because the interplanar spacing in the lattice of the paraelectric phase sharply changes (see Fig. 40*b*). The halo reflection remaining for the melt ($T > 184$ °C) has a complex structure, *i.e.* in addition to the principal line, its asymmetry on the low-angle side is clearly observed. It can be seen that the half-width of the reflection (see Fig. 40*a*) is fairly small, which is unusual for isotropic systems with short-range order. Therefore, it was assumed [196] that the amorphous phase of the melt consists of two components. One component corresponds to the isotropic constituent, matched by the low-angle asymmetry of the halo reflection in the melt. The principal line characterises the presence of regions with anisotropic distribution of polymer segments. These regions can be characterised by a certain long-range order similar to that observed in the nematic phase of liquid crystals. These structures should be fairly stable to heating because the halo reflex is retained up to 315 °C (Fig. 40*a*).

If the energy of interatomic interaction is estimated based on the average interchain distance, this conclusion is also confirmed by Fig. 40*b*; extrapolation of the high-temperature straight line to room temperature gives $d = 4.92$ Å, whereas for the paraelectric phase $d = 4.76$ Å.

Upon texturing the copolymer samples (for example, by uniaxial stretching), the two components of the amorphous phase can be readily separated from one another. The isotropic component would be manifested as an azimuth-independent halo, and the anisotropic component would cause scattering only in the equatorial region.[196] The interaction energy in the areas described by the anisotropic component should be much lower than that in the ferroelectric crystal (see Fig. 40*c*). This can be judged by the temperature dependences of the average interchain distance for both phases. When measurements are carried out under isometric conditions (when disorientation of the β-phase crystallites is excluded), the anisotropic component of the X-ray diffraction patterns in the equatorial direction (see Fig. 40*c*) is better resolved from the principal intermolecular reflection of the ferroelectric phase at high temperatures.

Thus, analysis of the data listed above provides general characteristics of the nuances of the phase states of VDF-based polymeric ferroelectrics. The densest packing is found in the ferroelectric crystal lattices. If the density is characterised by the average interchain distance, it can be estimated based on the identity period *d* for the 200, 110 planes of the β-phase. In the 94/6 VDF/TFE copolymer at room temperature, this *d* value is 4.30 Å.[196] Transition from the ferroelectric phase to the paraelectric phase is accompanied by a substantial decrease in the packing density in the crystal — at room temperature *d* increases from 4.30 to 4.76 Å (see Fig. 40*b*). It is significant that in VDF/TrFE copolymers with high contents of the former component, the two phases can coexist up to the melting point. The Curie transition, in which the crystals in the ferroelectric phase pass into a non-polar forms, occurs in the same region.

The amorphous phase of these polymers should incorporate two types of structure, one of them being typical of isotropic liquids. The anisotropic constituent of the amorphous phase should contain areas with a particular type of long-range order. The chain segments can be packed in these areas in such a way that the directions of their moments in particular regions are identical. Thus, so-called quasi-domains localised in the amorphous phase are formed; they can be classified as the imperfect ferroelectric QL phase. As noted above in analysing the NMR data, the energy of interaction in these quasi-domains should be close to that in the paraelectric phase.[110]

Thus, in quasi-domains, chains are packed more loosely than in the domains of the proper crystal phase (for the 94/6 VDF/TFE copolymer this difference is ~15%). Therefore, two Curie transitions should occur in these compounds; they have been detected in both block films and Langmuir–Blodgett films. The specifics of the latter is that a decrease in the number of monolayers results in a higher proportion of chains in which three-dimensional order is lost and conformational defects are accumulated. Thus, the equilibrium in a domain–quasi-domain mixture (or a mixture of LT and QL phases) shifts towards higher contents of the latter component. Experimentally, this manifests itself as enhancement of the low-temperature transition.

IX. Conclusion

The analysis of the published data on the ferroelectricity in PVDF and VDF-based copolymers carried out in this review leads to the following main conclusions.

In the crystallisable polymers considered here, the amorphous phase is more than merely an inert matrix. The cooperative mobility in the disordered phase contributes to the switching of ferroelectric domains.

Polarisation is accompanied by an irreversible increase in the degree of crystallinity. This can be attained *via* an increase in the transverse dimension of crystallites of the β-phase due to incorporation of some chains of the disordered phase.

Unfreezing of the cooperative mobility in the amorphous phase facilitates field-induced structural rearrangements in it. The type and the degree of mobility in the disordered regions surrounding the ferroelectric crystals has a substantial effect on the coercive field.

The high dynamic heterogeneity of PVDF at room temperature can account for the stability of the ferroelectric characteristics, in particular, remanent polarisation. On exposure to a strong field, the new position of domains is stabilised upon 'shielding' by the space charge. The effective mobility of charge carriers is limited by the relaxation times of segments in the disordered phase, which are ~100 ns at room temperature. Under these conditions, a new equilibrium state of the space charge is attained over short periods, thus ensuring the above-noted stability of the switched domains.

The type of supermolecular structure was found to influence some ferroelectric characteristics. Specifically, the morphology of thick lamellar crystals proves to promote high spontaneous polarisation. If there are conditions for crystallisation of the chains in textured PVDF as ECC, the Curie point becomes markedly higher.

Two types of ferroelectric phase differing in the degree of perfection are characteristic of PVDF and VDF copolymers. The dielectric anomalies observed in the relaxation region ascribed to

glass transition imply that the QL phase can be localised in disordered regions of the polymer.

The Langmuir – Blodgett films derived from PVDF and VDF/TrFE copolymer possess single crystal textures because they display finite values of the pyroelectric response in the nonpolarised state. As the number of monolayers in these films decreases, conformational defects are accumulated and the crystallographic order tends to be violated.

References

1. H Kawai *Jpn. J. Appl. Phys.* **8** 975 (1969)
2. V V Kochervinskii *Usp. Khim.* **63** 383 (1994) [*Russ. Chem. Rev.* **63** 367 (1994)]
3. T T Wang, J M Herbert, A M Glass (Eds) *The Application of Ferroelectric Polymers* (London, New York: Chapman and Hall, 1988)
4. Y S Jo, M Sakurai, Y Inoue, R Chujo, S Tasaka, S Miyata *Polymer* **28** 1583 (1987)
5. T T Wang, Y Takase *J. Appl. Phys.* **62** 3466 (1987)
6. Y S Jo, Y Maruyama, Y Inoue, R Chujo, S Tasaka, S Miyata *J. Polym. Sci., Part B, Polym. Phys.* **26** 463 (1988)
7. S Tasaka, N Inagaki, T Okutani, S Miyata *Polymer* **30** 1639 (1989)
8. D Zou, S Iwasaki, T Tsutsui, S Saito, M Kishimoto, I Seo *Polymer* **31** 1888 (1990)
9. S Ikeda, H Kiba, M Kutani, Y Wada *Jpn. J. Appl. Phys.* **28** 1870 (1989)
10. D Zou, S Iwasaki, T Tsutsui, S Saito, M Kishimoto, I Seo *Rep. Progr. Polym. Phys. Jpn.* **32** 383 (1989)
11. Y Ohta, Y Inoue, R Chujo, M Kishimoto, Y Seo *Polymer* **31** 1581 (1990)
12. Y Inoue, Y Maruyama, M Sakurai, Y S Jo, R Chujo *Polymer* **31** 1594 (1990)
13. Y Inoue, Y Maruyama, M Sakurai, Y S Jo, R Chujo *Polymer* **31** 850 (1990)
14. S C Mathur, B A Newman, J I Scheinbeim *J. Polym. Sci., Part B, Polym. Phys.,* **26** 447 (1988)
15. B A Newman, K G Kim, J I Scheinbeim *J. Mater. Sci.* **25** 1779 (1990)
16. J I Scheinbeim, J W Lee, B A Newman *Macromolecules* **25** 3729 (1992)
17. H Ueda, S U Carr *Polym. J.* **16** 661 (1984)
18. H Von Berlepsch, W Kunstler, A Wedel, R Danz, D Geib *IEEE Trans. Electr. Insul.* **24** 357 (1989)
19. S Tasaka, T Shouko, N Inugaki *Jpn. J. Appl. Phys., Part 2* **31** L1086 (1992)
20. Y Takahashi, S Ukashima, M Ijima, E Fukada *J. Appl. Phys.* **70** 6983 (1991)
21. A Prieto, R Perez, J A Sabirana *J. Appl. Phys.* **66** 803 (1989)
22. K Sato, K Otsuka, M Matsumoto *Makromol. Chem. Rapid Commun.* **9** 631 (1988)
23. W Meier, H Finkelman *Makromol. Chem. Rapid Commun.* **11** 599 (1990)
24. H R Brand, H Pleiner *Makromol. Chem. Rapid Commun.* **11** 607 (1990)
25. Y Kita, T Manai, T Sato *Bull. Inst. Chem. Res. Kyoto Univ.* **69** 444 (1991)
26. H Maeda *J. Appl. Polym. Sci.* **42** 3013 (1991)
27. E Fukada *Progr. Polym. Sci.* **2** 329 (1971)
28. V V Kochervinskii *Usp. Khim.* **65** 936 (1996) [*Russ. Chem. Rev.* **65** 865 (1996)]
29. T Furukawa, M Date, E Fukada *J. Appl. Phys.* **51** 1135 (1980)
30. M Tamura, S Hagiwara, S Matsumoto, N Ono *J. Appl. Phys.* **48** 513 (1977)
31. V V Kochervinskii *Vysokomol. Soedin., Ser. A* **33** 2106 (1991) [a]
32. V V Kochervinskii, V G Sokolov V M Zubkov *Vysokomol. Soedin., Ser. A* **33** 530 (1991) [a]
33. V V Kochervinskii, V G Sokolov *Vysokomol. Soedin., Ser. A* **33** 1625 (1991) [a]
34. N Koizumi, Y Murata, H Tsunashima *IEEE Trans. Electr. Insul.* **EI-21** 543 (1986)
35. D Geiss, C Rusher *Progr. Colloid Polym. Sci.* **80** 119 (1989)
36. I L Guy, D K Das-Gupta *J. Appl. Phys.* **70** 5691 (1991)
37. J C Hicks, T E Jones, J C Logan *J. Appl. Phys.* **49** 6092 (1978)
38. M Date, T Furukawa, E Fukada *J. Appl. Phys.* **51** 3830 (1980)
39. D Naegele, D Y Yoon *Appl. Phys. Lett.* **33** 132 (1978)
40. I L Guy, J Unsworth *Appl. Phys. Lett.* **52** 532 (1988)
41. K Nakamura, Y Teramoto, N Murayama *Ferroelectrics* **57** 139 (1984)
42. R G Kepler, R A Andersen *J. Appl. Phys.* **49** 1232 (1978)
43. A J Bur, J D Barnes, K J Wahlstrand *J. Appl. Phys.* **59** 2345 (1986)
44. H Dvey-Aharon, T J Sluckin, P L Taylor, A J Hopfinger *Phys. Rev. B, Condens. Matter* **21** 3700 (1980)
45. S Palto, L Blinov, A Bune, E Dubovik, V Fridkin, N Petukhova, K Verkhovskaya, S Yudin *Ferroelectr. Lett.* **19** 665 (1995)
46. N Tsutsumi, G T Davis, A S De Reggi *Macromolecules* **24** 6392 (1991)
47. N Tsutsumi, Y Ueda, T Kiyatsukuri *Polymer* **33** 3305 (1992)
48. E E Havinga, P van Pelt *Ber. Bunsenges. Phys. Chem.* **83** 816 (1979)
49. A S DeReggi, C M Guttman, F I Mopsik, G T Davis, M G Broadhurst *Phys. Rev. Lett.* **40** 413 (1987)
50. F I Mopsik, A S DeReggi *J. Appl. Phys.* **53** 4333 (1982)
51. M Jimbo, S Kobayashi, K Horino, S Ikeda, Y Wada *J. Polym. Sci., Polym. Phys. Ed.* **22** 2139 (1984)
52. S Ikeda, M Jimbo, S Kobayashi, Y Wada *J. Polym. Sci., Polym. Phys. Ed.* **23** 1781 (1985)
53. T Furukawa, M Date, G E Johnson *J. Appl. Phys.* **54** 1540 (1983)
54. T Furukawa, G E Johnson *Appl. Phys. Lett.* **38** 1027 (1981)
55. K Matsushige, S Imada, T Takemura *Polym. J.* **13** 493 (1981)
56. Y Tajitsu, T Masuda, T Furukawa *Jpn. J. Appl. Phys.* **26** 1749 (1987)
57. S Ikeda, E Fukada, M Jimbo, K Koyama, Y Wada *Jpn. J. Appl. Phys., Suppl.* **24-2** 865 (1985)
58. G F Leal Ferreira, R A Moreno *J. Appl. Phys.* **75** 472 (1994)
59. S Ikeda, E Fukada, Y Wada *J. Appl. Phys.* **64** 2026 (1988)
60. M Womes, E Bihler, W Eisenmenger *IEEE Trans. Electr. Insul.* **24** 461 (1989)
61. G Eberle, E Bihler, W Eisenmenger *IEEE Trans. Electr. Insul.* **26** 69 (1991)
62. A Odajima, T T Wang, Y Takase *Ferroelectrics* **62** 39 1985
63. J D Clark, P L Taylor *Lett. Phys. Rev.* **49** 1532 (1982)
64. N A Pertsev, A G Zembil'gotov *Fiz. Tv. Tela* **32** 287 (1991)
65. S Ikeda, H Kominami, K Koyama Y Wada *J. Appl. Phys.* **62** 3339 (1987)
66. A J Lovinger, D D Davis, R E Cais, J M Kometani *Macromolecules* **21** 78(1988)
67. K Tashiro, K Takano, M Kobayashi, Y Chatani, H Tadokoro *Ferroelectrics* **57** 297 (1984)
68. K Tashiro, H Kato, M Kobayashi *Polymer* **33** 2915 (1992)
69. V V Kochervinskii, E M Murasheva *Vysokomol. Soedin., Ser. A* **33** 2096 (1991)
70. A J Lovinger, D D Davis, R E Cais, J M Kometani *Macromolecules* **19** 1491 (1986)
71. T Yagi, N Tatemoto, J-I Sako *Polym. J.* **12** 209 (1980)
72. Y Kubouchi, Y Kumetani, T Yagi, T Masuda, A Nakajima *Pure Appl. Chem.* **61** 83 (1989)
73. N Koizumi, N Haikawa, H Habuka *Ferroelectrics* **57** 99 (1984)
74. R M Faria, J M G Neto, O N Oliveira *J. Phys. D, Appl. Phys.* **27** 611 (1994)
75. Y Murata *Polym. J.* **20** 771 (1988)
76. H Ogura, S Tohriyama, A Hanaki, S Sasaki, K Kase, A Chiba *Jpn. J. Appl. Phys., Part 1* **30** 2819 (1991)
77. T Furukawa, G E Johnson, H E Bair, Y Tajitsu, A Chiba, E Fukada *Ferroelectrics* **32** 61 (1981)
78. T Furukawa, G E Johnson *J. Appl. Phys.* **52** 940 (1981)
79. V J McBrierty, D C Douglass, T Furukawa *Macromolecules* **15** 1063 (1982)
80. F Ishii, A Odajima, H Ohigashi *Polym. Prepr. Jpn.* **31** 2325 (1982); **32** 814 (1983)
81. Y Oka, N Koizumi, Y Murata *J. Polym. Sci., Polym. Phys. Ed.* **24** 2059 (1986)
82. T Yamada, T Ueda, T Kitayama *J. Appl. Phys.* **52** 948 (1981)
83. Z Lin, V H Schmidt *Appl. Phys. Lett.* **57** 2196 (1990)
84. F J Balta-Calleja, C Santa Cruz, A Gonzales-Arche, E Lopez-Cabarcos *J. Mater. Sci.* **27** 2124 (1992)
85. Y Takahashi, A Odajima, K Nakamura, N Murayama *Rep. Progr. Polym. Phys. Jpn.* **22** 151 (1979)

86. K Tashiro, M Nakamura, M Kobayashi, Y Chatani, H Tadokoro *Macromolecules* **17** 1452 (1984)
87. A Odajima *Ferroelectrics* **57** 159 (1984)
88. J Ziman *Models of Disorder* (London: Cambridge University Press, 1997) p. 460
89. N Haikawa, N Koizumi *Polym. Prepr. Jpn.* **31** 2903 (1982)
90. M Ohushi, A Chiba, T Furukawa, M Date *Polym. Prepr. Jpn.* **31** 2907 (1982)
91. L Benguigui *Solid State Commun.* **14** 669 (1974)
92. K Tashiro, K Takano, M Kobayashi, Y Chatani, H Tadokoro *Polym. Prepr. Jpn.,* **30** 1882 (1981)
93. T Muto, Y Takagi *Solid State Physics* Vol. 1 (Eds F Seitz, D Turnbull) (New York: Academic Press, 1955) p. 207
94. C P Bem, D C Rodbell *Phys. Rev.* **126** 104 (1962)
95. M Date *IEEE Trans. Electr. Insul.* **EI-21** 539 (1986)
96. K A Verkhovskaya, Zh A Krasnaya, A V Bune *Fiz. Tv. Tela* **34** 2157 (1992)
97. K A Verkhovskaya *Kristallografiya* **39** 939 (1994) [b]
98. K A Verkhovskaya, V M Fridkin, A V Bune, A S Tatikov, J F Legrand *J. Appl. Phys.* **75** 663 (1994)
99. E Lopez-Cabarcos, A Gonzales-Arche, F Batallan, B Frick *Physica* **156A** 423 (1989)
100. J F Legrand, P J Schuele, V H Schmidt, M Minier *Polymer* **26** 1683 (1985)
101. V J McBrierty, D C Douglass, T H Weber *J. Polym. Sci., Polym. Phys. Ed.* **14** 271 (1976)
102. V H Schmidt *Ferroelectrics* **73** 333 (1987)
103. F H Ishii, A Odajima *Jpn. J. Appl. Phys.* **26** 1641 (1987)
104. I Tatsuzaki, K Sakata, I Todo, M Takunaga *J. Phys. Soc. Jpn.* **33** 438 (1971)
105. I Tatsuzaki, M Takunaga *Pure Appl. Chem.* **40** 115 (1974)
106. F H Ishii, A Tsutsumi, A Odajima *Jpn. J. Appl. Phys., Part 1* **27** 917 (1988)
107. F H Ishii, A Odajima, H Ohigashi *Polym. J.* **15** 875 (1983)
108. F H Ishii, A Odajima *Rep. Progr. Polym. Phys. Jpn.* **32** 433 (1989)
109. F H Ishii, A Odajima *Polym. J.* **23** 999 (1991)
110. J Hershinger, B Meurer, G Weill *Polymer* **28** 721 (1987)
111. A J Lovinger, G T Davis, T Furukawa, M Broadhurst *Macromolecules* **15** 323 (1982)
112. Y Murata, N Koizumi *Polym. J.* **17** 385 (1985)
113. H Tanaka, H Yukawa, T Nishi *J. Chem. Phys.* **90** 6730 (1989)
114. H Tanaka, H Yukawa, T Nishi *J. Chem. Phys.* **90** 6740 (1989)
115. H Tanaka, H Yukawa, T Nishi *Macromolecules* **21** 2469 (1989)
116. K Tashiro, K Takano, M Kobayashi, Y Chatani, H Tadokoro *Polymer* **22** 1312 (1981)
117. K Tashiro, M Kobayashi *Jpn. J. Appl. Phys., Suppl.* **24-2** 873 (1985)
118. A Rigamonti *Adv. Phys.* **3** 115 (1984)
119. G T Davis, T Furukawa, A J Lovinger, M Broadhurst *Macromolecules* **15** 329 (1982)
120. J Hirschinger, B Meurer, G Weill *J. Phys. Fr.* **50** 563 (1989)
121. J Hirschinger, B Meurer, G Weill *J. Phys. Fr.* **50** 583 (1989)
122. G Samara *J. Polym. Sci., Part B, Polym. Phys.* **27** 39 (1989)
123. N Koizumi, Y Murata, N Haikawa *Jpn. J. Appl. Phys., Suppl.* **24-2** 862 (1985)
124. K Matsushige, K Tagashira, T Horiuchi, S Taki, T Takemura *Jpn. J. Appl. Phys., Suppl.* **24-2** 868 (1985)
125. K Tashiro, S Nishimura, M Kobayashi *Macromolecules* **21** 2463 (1988)
126. K Matsushige, T Horiuchi, S Taki, T Takemura *Jpn. J. Appl. Phys.* **24** L203 (1985)
127. K Tashiro, S Nishimura, M Kobayashi *Macromolecules* **23** 2802 (1990)
128. K Tashiro, K Takano, M Kobayashi, Y Chatani, H Tadokoro *Polymer* **25** 195 (1984)
129. V V Kochervinskii, V A Glukhov, V G Sokolov, L Ya Madorskaya, B V Lokshin *Vysokomol. Soedin., Ser. A* **31** 2590 (1989) [a]
130. V V Kochervinskii, V A Glukhov, V F Romadin, V G Sokolov, B V Lokshin *Vysokomol. Soedin., Ser. A* **30** 1916 (1988) [a]
131. V V Kochervinskii, V F Romadin, V A Glukhov, V G Sokolov, M A Saidakhmetov *Vysokomol. Soedin., Ser. A* **31** 1382 (1989) [a]
132. V V Kochervinskii, V A Glukhov, S Yu Kuznetsova *Vysokomol. Soedin., Ser. A* **29** 1530 (1987) [a]
133. R Al-Jishi, P L Taylor *Ferroelectrics* **73** 343 (1987)
134. R Al-Jishi *Ferroelectrics Lett* **9** 165 (1989)
135. B R Hahn *J. Appl. Phys.,* **57** 1294 (1985)
136. K Matsushige, T Takemura, in *Structure – Properties Relationships of Polymer Solids. Proceedings of the 55th Meeting of the American Chemical Society, Atlanta, GA, 1983* p. 115
137. A K Doolittle *J. Appl. Phys.* **22** 1571 (1951)
138. J D Ferry *Viscoelastic Properties of Polymers* (New York: Wiley, 1970)
139. Y Takase, H Tanaka, T T Wang, R E Cais, J M Kometani *Macromolecules* **20** 2318 (1987)
140. S Tasaka, S Miyata *J. Appl. Phys* **57** 906 (1985)
141. W Holzmuller, Wo Ilberg *Rheolog. Acta* **5** 1 (1966)
142. Y Takase, J I Scheinbeim, B A Newman *J. Polym. Sci., Part B, Polym. Phys.* **27** 2347 (1989)
143. Y Takase, J I Scheinbeim, B A Newman *J. Polym. Sci., Part B, Polym. Phys.* **28** 1599 (1990)
144. J I Scheinbeim *J. Appl. Phys.* **51** 5156 (1980)
145. A Sen, J I Scheinbeim, B A Newman *J. Appl. Phys.* **56** 2432 (1984)
146. Y Takase, J I Scheinbeim, B A Newman *Macromolecules* **23** 642 (1990)
147. T Yagi, Y Higashihata, K Fukuyama, J Sako *Ferroelectrics* **57** 327 (1984)
148. I L Gay, J Unsworth *Annual Reports of Conference on Electrical Insulation and Dielectrical Phenomena, Ottawa, 1988* p. 16
149. V V Kochervinskii, V F Romadin, V A Glukhov, V G Sokolov, B I Ostrovskii *Vysokomol. Soedin., Ser. A* **31** 2311 (1989) [a]
150. J K Kruger, J Petzelt, J F Legrand *Colloid Polym. Sci.* **264** 791 (1986)
151. J F Legrand, J Lajzerowicz, B Berge, P Delzenne, P Macchi, C Bourgaux-Leonard, A Wicher, J K Kruger *Ferroelectrics* **78** 151 (1988)
152. J F Legrand, P Delzenne, A J Dianoux, M Bee, C Poinsignon, D Broussoux, V H Schmidt *Polymer Motion in Condensed Systems. Proceedings of Workshop Grenoble, 1985* p. 59
153. J F Legrand *IEEE Trans Electr. Insul.* **EI-28** 336 (1993)
154. Y Takahashi *Jpn. J. Appl. Phys., Part 1* **33** 202 (1994)
155. S N Chvalun, A N Ozerin, V I Selikhova, Yu A Zubov, N F Bakeev *Vysokomol. Soedin., Ser. A* **27** 1385 (1985) [a]
156. K Loufukis, B Wunderlich *Macromolecules* **20** 2474 (1987)
157. Y Miyamoto, H Miyaji, K Asai *J. Polym. Sci., Polym. Phys. Ed.* **18** 597 (1980)
158. Y Takahashi, Y Matsubara, H Tadokoro *Macromolecules* **15** 334 (1982)
159. Y Takahashi *Polym. J.* **15** 733 (1983)
160. Y Takahashi *J. Appl. Phys.* **67** 4060 (1990)
161. Y Takahashi, H Tadokoro, A Odajima *Macromolecules* **13** 1320 (1980)
162. Y Takahashi, H Tadokoro *Ferroelectrics* **57** 187 (1984)
163. V V Kochervinskii, V A Glukhov, V G Sokolov, Yu A Ovchinnikov, N A Trofimov, B V Lokshin *Vysokomol. Soedin., Ser. A* **31** 1829 (1989) [a]
164. V V Kochervinskii, V A Glukhov, V G Sokolov, B V Lokshin *Vysokomol. Soedin., Ser. A* **31** 282 (1989) [a]
165. J Martinez-Salazar, J C C Camara, E Lopez-Cabarcos, F J Balta-Calleja *Colloid Polym. Sci.* **266** 41 (1988)
166. R L Moreira, R Almairac, M Latour, in *The 6th International Symposium on Electrets (Abstracts of Reports), Oxford, 1988* p. 160
167. R L Moreira, R Almairac, M Latour *J. Phys., Condens. Matter.* **1** 4273 (1989)
168. M Latour, R Almairac, R L Moreira *IEEE Trans. Electr. Insul.* **24** 443 (1989)
169. P Sant-Gregoire, F J Schafer, W Kleeman, J Durand, A Goiffon *J. Phys. Solid State Phys.* **17** 1375 (1984)
170. G M Stack, R Y Ting *Polym. Prepr.* **27** 161 (1986)
171. G M Stack, R Y Ting *J. Polym. Sci. B, Polym. Phys.* **26** 55 (1988)
172. J Petzelt, J F Legrand, S Pacesova, S Kamba, G V Kozlov, A A Volkov *Phase Trans.* **12** 305 (1988)
173. R G Snyder, J R Scherer, A Peterlin *Macromolecules* **14** 77 (1981)
174. J S Green, B L Farmer, L F Rabolt *J. Appl. Phys.* **60** 2690 (1986)
175. D R Buchman, R L McCulough, R L Miller *Acta Crystallogr.* **20** 922 (1966)
176. M Latour, R L Moreira *J. Polym. Sci., B, Polym. Phys.* **25** 1717 (1987)
177. H Ohigashi, N Kagani, G R Li *J. Appl. Phys.* **71** 506. (1992)

178. H Ohigashi, S Akama, K Koga *Jpn. J. Appl. Phys.* **27** 2144 (1988)
179. K Koga, H Ohigashi *J. Appl. Phys.* **59** 2142 (1986)
180. H Ohigashi, K Koga *Jpn. J. Appl. Phys.* **21** L455 (1982)
181. K Koga, N Nakano, T Hattori, H Ohigashi *J. Appl. Phys.* **67** 965 (1990)
182. H Ohigashi, T Watanabe, G R Li, T Hattori, Y Takahashi *Jpn. J. Appl. Phys.* **30** 111 (1991)
183. M Hikosaka, K Sakurai, H Ohigashi, T Koizumi *Jpn. J. Appl. Phys., Part 1* **32** 2029 (1993)
184. M Hikosaka, K Sakurai, H Ohigashi, T Koizumi *Jpn. J. Appl. Phys., Part 1* **32** 2780 (1993)
185. M Hikosaka, K Sakurai, H Ohigashi, A Keller *Jpn. J. Appl. Phys., Part 1* **33** 214 (1994)
186. T Hattori, M Kanaoka, H Ohigashi *J. Appl. Phys.* **79** 2016 (1996)
187. B Wunderlich, L Milillo *Makromol. Chem.* **118** 250 (1968)
188. D C Basset, S Block, G Piermarini *J. Appl. Phys.* **45** 4146 (1974)
189. M Hikosaka *Polymer* **28** 1257 (1987)
190. M Hikosaka *Polymer* **31** 458 (1990)
191. M Hikosaka, T Kasahara, S Rastogi, A Keller, H Kawabara, T Komazawa *Polym. Prepr. Jpn.* **30** 307 (1989)
192. K Matsushige, T Takemura *J. Polym. Sci., Polym. Phys. Ed.* **16** 921 (1978)
193. K Matsushige, T Takemura *J. Cryst. Growth* **48** 343 (1980)
194. D C Basset *Developments in Crystalline Polymers-I* (Ed. D C Basset) (London: Appl. Sci., 1982) p. 115
195. H Ohigashi *J. Appl. Phys.* **47** 949 (1976)
196. V V Kochervinskii, N N Kuz'min *Neorg. Mater.* **31** 859 (1995) [c]
197. S Sasaki, K Kubo, A Funato, A Chiba *Jpn. J. Appl. Phys., Part 1* **35** 3496 (1996)
198. N Yamauchi, K Kato, T Wada *Jpn. J. Appl. Phys., Part 2* **23** L671 (1984)
199. T Okajima, K Maki *Jpn. J. Appl. Phys.* **30** L2055 (1991)
200. T Nagamori, T Horiuchi, K Hara, K Matsushige *Jpn. J. Appl. Phys., Part. 1* **31** 1407 (1992)
201. K Tashiro, K Yamamoto, M Kobayashi, O Phaovibul *Rep. Progr. Polym. Phys. Jpn.* **30** 123 (1987)
202. K Tashiro, M Kobayashi *Rep. Progr. Polym. Phys. Jpn.* **31** 183 (1988)
203. A Sorokin, S Palto, L Blinov, V Fridkin, S Yudin *Mol. Mater.* **6** 61 (1996)
204. L M Blinov, V M Fridkin, S P Palto, A Sorokin, S Yudin *Thin Solid Films* **284**–**285** 469 (1996)
205. L M Blinov, V M Fridkin, S P Palto, A Sorokin, S Yudin *Thin Solid Films* **284**–**285** 474 (1996)
206. S P Palto, L M Blinov, E Dubovik, V M Fridkin, N Petukhova, A Sorokin, K Verkhovskaya, S G Yudin, A Zlatkin *Euro-Phys. Lett.* **34** 465 (1996)
207. L M Blinov, K A Verkhovskaya, S P Palto, A V Sorokin *Appl. Phys. Lett.*, **66** 2369 (1996)
208. L M Blinov, K A Verkhovskaya, S P Palto, A V Sorokin, A A Tevosov *Kristallografiya* **41** 328 (1996) [b]
209. L M Blinov, K A Verkhovskaya, S P Palto, A V Sorokin, A A Tevosov *Izv. Akad. Nauk, Ser. Fiz.* **60** 180 (1996)
210. L M Blinov, K A Verkhovskaya, S P Palto, A V Sorokin, A A Tevosov *Crystallogr. Rep.* **41** 310 (1996)
211. S G Yudin, S P Palto, V A Khavrichev, S V Mirinenko, M I Barnik *Thin Solid Films* **210/211** 46 (1992)
212. S P Palto, L M Blinov, A Bune, E Dubovik, V M Fridkin, N Petukhova, K Verkhovskaya, S Yudin *Ferroelectrics* **184** 127 (1996)
213. W Zhong, P Zhang, Y Wang, T Ren *Ferroelectrics* **160** 55 (1994)
214. O Valdes-Ajuilera, D C Neekers *Acc. Chem. Res.* **22** 171 (1989)
215. N V Dubinin, L M Blinov, S V Yablonskii *Opt. Spektrosk.* **44** 807 (1978)
216. M I Barnik, L M Blinov, S P Palto, A A Tevosov, Th Veyrauch *Mol. Mater.* **3** 319 (1994)
217. L M Blinov *Usp. Fiz. Nauk* **155** 443 (1988) [d]
218. L M Blinov, S P Palto, S Yudin *Mol. Mater.* **1** 183 (1992)
219. W Liptay *Advances in Electronic Exitation and Relaxation* (New York: Academic Press, 1974) p. 1
220. M I Barnik, L M Blinov, Th Veyrauch, S P Palto, A Tevosov, W Haase *Chem. Phys. Lett.* **231** 246 (1994)
221. L M Blinov, S P Palto, S G Yudin *Metrologiya* (11) 27 (1986)
222. L M Blinov, S P Palto, G Ruani, C Taliani, A Tevosov, W Haase *Chem. Phys. Lett.* **232** 401 (1995)
223. V V Kochervinskii, B V Lokshin, S P Palto, G N Andreev, L M Blinov, N N Petukhova *Vysokomol. Soedin., Ser. A* **41** 1290 (1999) [a]
224. E L Gal'perin, B P Kosmynin, V F Mindrul, V K Smirnov *Vysokomol. Soedin., Ser. B* **12** 594 (1970) [a]
225. L N Pirozhnaya , O B Zubkova , L A Gribov *Zh. Prikl. Spektrosk.* **48** 65 (1988)
226. A V Bune, V M Fridkin, S Ducharme, L M Blinov, S P Palto, A V Sorokin, S G Yudin, A Zlatkin *Nature (London)* **391/26** 874 (1998)
227. S P Palto, Doctoral Thesis in Physicomathematical Sciences, Institute of Crystallography, Russian Academy of Sciences, Moscow, 1998
228. J Fuhrmann, R Hofmann, H Streibel, U Jahn *IEEE Trans. Electr. Insul.* **EI-21** 529 (1986)
229. R J Phelan, R L Peterson, C A Hamilton , G W Day *Ferroelectrics* **7** 375 (1974)
230. M A Markus *J. Appl. Phys.* **52** 6273 (1981)
231. K Takahashi, H Lee, R E Salomon, M M Labes *J. Appl. Phys.* **48** 4694 (1977)
232. J Choi, P A Dowben, S Pebley, A V Bune, S Ducharme, V M Fridkin, S P Palto, N Petukhova *Phys. Rev. Lett.* **80** 1328 (1998)
233. S D Kevan, N G Stoffel *Phys. Rev. Lett.* **53** 702 (1984)
234. S D Kevan *Phys. Rev. B, Condens. Matter* **32** 2344 (1985)
235. L Gravioli, M G Betti, C Mariani *Phys. Rev. Lett.* **77** 3869 (1996)
236. S Ducharme, A V Bune, L M Blinov, V M Fridkin, S P Palto, A V Sorokin, S G Yudin *Phys. Rev. B, Condens. Matter* **57** 25 (1998)
237. A F Devonshire *Adv. Phys.* **3** 85 (1954)
238. T Furukawa *Phase Trans.* **18** 143 (1989)
239. W J Merz *Phys. Rev.* **91** 513 (1953)
240. K Okada, H Sugie *Phys. Lett.* **37A** 337 (1971)
241. C Bahr, G Heppke *Phys. Rev. A, Gen. Phys., Ser. 3* **39** 5459 (1989)
242. N D Gavrilova, V V Kochervinskii, I A Malyshkina, A M Lotonov, N I Kuznetsova *Vysokomol. Soedin., Ser. A* **41** (1999)
243. H Fröhlikh *Theory of Dielectrics. Dielectric Constant and Dielectric Loss* (Oxford: Claredon Press, 1958)
244. K Nakagawa, Y Ishida *J. Polym. Sci., Polym. Phys. Ed.* **11** 1509 (1973)
245. V V Kochervinskii *Vysokomol. Soedin., Ser.* **40A** 1636 (1998)
246. S Ikeda, M Kutani *Jpn. J. Appl. Phys. Part 1* **30** 2456 (1991)
247. J D Carbeck, D J Lacks, G C Rutledge *J. Chem. Phys.* **103** 10347 (1995)

[a] — *Polym. Sci. (Engl. Transl.)*
[b] — *Russ. Crystallogr. (Engl. Transl.)*
[c] — *Inorg. Matter. (Engl. Transl.)*
[d] — *Physics-Uspekhi (Engl. Transl.)*